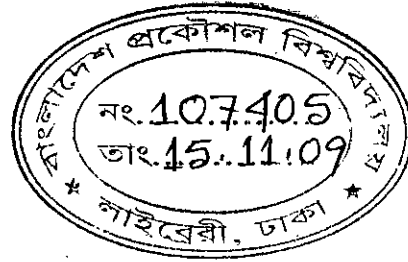# Enhancement of Power Transmission Capability of East-West Interconnector Using Controlled Series Compensation

A Thesis Submitted to the Department of Electrical and Electronic Engineering in Partial Fulfillment of the Requirement for the Degree of
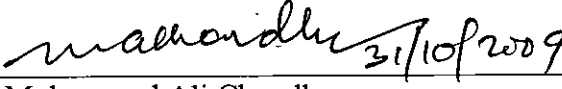
Master of Science in Engineering
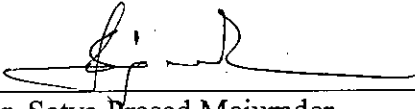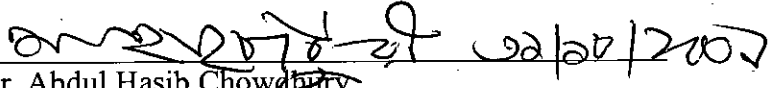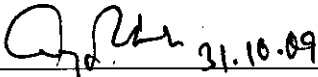
By

Md. Jan-E-Alam

Department of Electrical and Electronic Engineering

BANGLADESH UNIVERSITY OF ENGINEERING AND TECHNOLOGY

October, 2009

The thesis titled **"Enhancement of Power Transmission Capability of East-West Interconnector Using Controlled Series Compensation"**, submitted by **Md. Jan-E-Alam**, Roll: 100506104P, Session: October 2005, has been accepted as satisfactory in partial fulfillment of the requirement for the degree of Master of Science in Engineering on October 31, 2009.

BOARD OF EXAMINERS
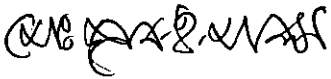
1. _____ 31/10/2009   Chairman
   Dr. Mohammad Ali Choudhury
   Professor, Department of EEE, BUET

2. _____   Member
   Dr. Satya Prasad Majumder   (Ex-Officio)
   Professor, Department of EEE, BUET

3. _____ 02/08/2007   Member
   Dr. Abdul Hasib Chowdhury
   Associate Professor, Department of EEE, BUET

4. _____ 31.10.09   Member
   Dr. Abdur Rahim Mollah   (External)
   Professor, Department of EEE
   American International University – Bangladesh

Declaration

It is hereby declared that this thesis or any part of it has not been submitted elsewhere for the award of any degree or diploma.

Signature of the Candidate

Md. Jan-E-Alam

Acknowledgements

Abstract

Series inductive reactance of a given transmission line is a significant governing factor for the power transmission capability of that line and as the length of line increases beyond a certain range, this reactance may impose considerable limitations on the amount power that can be transferred without violating the prudent operational constraints. Transfer beyond that level can make the system significantly stressed and may even drive into the region of instability. In many practical cases this transfer limit has been observed to be noticeably lower than the thermal capability of conductors physically used to construct the line and hence creates a scope for finding ways to exploit this otherwise unused capacity. In the cases, where the transmission lines in discussion are interconnections among utilities, urge for maximum capacity utilization is much stronger due the constraints related to additional line construction.

This dissertation deals with enhancement of power transmission capability of interconnections using series capacitive compensation. In most of the real world cases, tie-lines among utilities are medium to long high voltage lines, which are usually more susceptible to the power transfer limitations imposed by series inductive reactance. Introducing series capacitive compensation provides with a negative reactance, resulting in a reduced net transfer reactance between two ends of a transmission line and hence the electrical length of the line becomes shorter to facilitate loading towards thermal limit.

The Two-Area system and an approximate model of the Western Grid of Bangladesh Power System network have been used as case study; both old and new East West Interconnection has been considered. Controlled series compensation has been applied through Thyristor Controlled Series Capacitor. Improvement of steady state, dynamic and transient performance by applying series compensation has been presented based on the results obtain by standard static and dynamic analyses, i.e., Load Flow, Continuation Power Flow, Modal Analysis and Transient Analysis. Comparison of loading margins, corresponding to Saddle-Node and Hopf Bifurcation of the system, with and without compensation has been performed to reveal the effect of series compensation on transmission capability. Financial feasibility of series compensation project for these interconnections has been performed in a simplified manner and findings are presented in the thesis.

Contents

List of Figures

List of Tables

List of Abbreviations

ASC   Advanced Series Compensation

ATC   Available Transfer Capacity

BPDB   Bangladesh Power Development Board

BPS   Bangladesh Power System

DAE   Differential Algebraic

DLM   Dynamic Loading Margin

EWI   East West Interconnector

EWIS   East West Interconnected System

FACTS   Flexible AC Transmission System

LM   Loading Margin

LF   Loading Factor

kV   Kilo Volt

MVA   Mega Volt Ampere

MW   Mega Watt

MVAR   Mega Volt Ampere Reactive

PGCB   Power Grid Company of Bangladesh Ltd.

PSMP   Power System Master Plan

PST   Power System Toolbox

SLM   Static Loading Margin

SVC   Static VAR Compensator

TCR   Thyristor Controlled Reactor

TCSC   Thyristior Controlled Series Capacitor

UWPFLOW University of Waterloo Power Flow
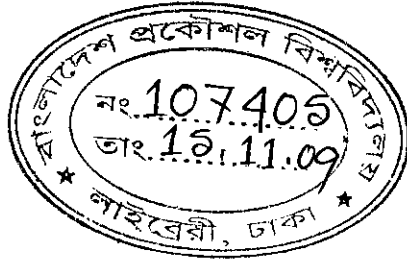
Introduction

1.1 Introduction

Necessity of exploiting maximum capacity of power transmission infrastructures is increasing day by day due to simultaneous effect of demand growth and limitations of constructing new transmission infrastructures. Evolution of different commercial schemes for the electric power industry, specially deregulation of the market, has made this necessity even stronger. As a result, utility planners and operators are in constant search for effective ways to utilize full capacity of their existing resources and infrastructures.

Tie lines or interconnections, being the corridor for inter-area bulk power transactions, are of great importance – both technically and commercially. Considering the construction time, cost, right-of-way and environmental issues in the construction of interconnections, it is usually preferred to find ways to maximize the capacity of existing tie lines.

Theoretically, a transmission line can be loaded up to its thermal limit. But in real life, this is practical only in case of short transmission lines (less than 80 km). Longer lines face the constraints of voltage drop and steady state stability limits before reaching the thermal limit. In medium lines (from 80 km to 250 km), voltage drop limits the loadability, whereas, in long lines (greater than 250 km) loadability depends on the steady state stability limit [1].

Conventionally, power handling capability of a transmission system can be directly influenced by series and shunt compensation [2]. Application of Flexible AC Transmission System (FACTS), capable of providing controlled shunt and series compensation in a dynamic environment, can enhance the power transfer capacity of transmission lines. This is accomplished at the same time with improvement of system stability [3-4]. A number of utilities in the world have applied this solution in their systems and are enjoying the benefits [3, 5].

Possibility of power transmission capability enhancement by series compensation has been studied in this work; controlled series compensation has been implemented by Thyristor Controlled Series Capacitor (TCSC).

1.2 Literature Review

Utilizing full thermal capacity of installed transmission lines has long been an issue in the electric utility industry and development of techniques and schemes for accomplishing this has always been insisted on by utility owners and other entities related to commercial operations. At the initial stage of electric industry evolution, voltage drop across distribution circuits used to be a limiting factor in power delivery and series capacitive compensation was in application to minimize this problem. Marbury et. al. defines series capacitor [6] as an element which is connected in series with a circuit and improves the voltage regulation by inserting a negative reactance. Although many of the first generation installations of series capacitors in the US, since early 1930s, were intended to improve voltage regulation of radial distribution circuits [7], growing requirements for long distance bulk power transmission, mainly attributed to utilization of cheaper generation resources in the distant places pursued to consider the application of series capacitors to enhance power transfer capability of those "long" transmission circuits.

Several early age literatures discussed the requirements of applying series compensation on transmission circuits and discussed the practical difficulties experienced with their operation. In [8], Starr and Evans reviewed the fundamental limitation of a transmission system arising from transfer reactance between the sending and receiving end. Amount of power transfer is an inverse function of the transfer reactance and reducing it enhances the transfer capability of the line. High voltage operation of the lines was proposed as a solution. This seems justified and apparently attractive as, even if line resistances are neglected, both of the ends are modeled as infinite buses and voltage at those buses are kept constant to rated values, still the maximum synchronous capacity of the transmission system increases to 100 times for a 10 times step-up in voltage at both ends. But cost of high voltage equipment and engineering considerations such as high voltage transformer reactance, stability considerations of long lines and requirements of reactive power hinders the worthiness of this option to be a unique one. Multiple circuit operation can be another option, where cost of multiple high voltage lines is again detrimental and makes the project economics less attractive. Operation with reduced system frequency may be an option which is limited by larger size and higher cost of induction equipment and requirement for frequency changers. DC operation has been reported to be economical over the AC operation if the line lengths are in the order of 500 miles and also provides with additional advantages such as no synchronous stability limit exists and lines can be loaded up to economic limit, but basic limitation with DC operation

2

has been identified as lack of flexibility to supply power in the intervening area. Among all the methods discussed in this publication for reducing transfer reactance, series compensation was identified as the "most important alternative or supplement" among the available options.

A. A. Johnson [9] discussed introductory ideas on the effect of applying series compensation on radial and tie feeders. For interconnecting lines among utilities, main application of series compensation is to enhance the transmission capability and system stability rather than to improve voltage regulation which is usually the case for radial feeders. For a given phase angle difference between voltage at the two ends, amount of power transferred is greater with series compensation and this in turn enhances the stability of the system by interchanging more synchronizing power during transient conditions.

Several operating difficulties with the use of initial stage series capacitors have been reported and analyzed in the literature [7, 9], such as ferro-resonance in transformers causing extremely high exciting current which may sustain even at the steady-state, hunting of synchronous machines due to increased resistance-to-reactance ratio and self-excitation of induction motors at sub-synchronous frequency; solutions to mitigate these problems have also been discussed. Voltage drop across and current through series capacitors is several times of that during normal operating condition. For a fixed reactance, cost of series compensation is approximately proportional to the square of current magnitude and hence, based on economic considerations, it was necessary to develop protection systems which allows the capacitors to be rated by nominal operating current [7, 9]. Protective gaps have been used for low-voltage application of series capacitors; magnetic contactors were in use to put back the capacitor when the circuit becomes normal. In high-voltage interconnections, special type of gap was used for by-passing the capacitor; system stability being the major concern with tie-line applications, high speed breakers were used for reinsertion of capacitor units within half cycle to one cycle after fault clearing [9].

With advancement of commercially available capacitor units and to meet ever increasing need for distant and bulk transmission of electrical energy, analyses had been carried out in the industry to realize series compensation of longer and higher voltage lines for enhancement of stable power transfer limit in consideration with practical implementation factors. Long distance lines are usually designed with intermediate switching stations. In [10], Crary et. al. discussed different configurations for locating series capacitors on lines in the range of 300 to 600 miles with several switching stations, on the basis of economic and

stability benefits. Application of series capacitors in intermediate switching stations has been proved to be a highly economical and practical means of long distance power transmission.

Theoretically, magnitude of transfer reactance of a series compensated line should be equal to the difference between magnitudes of series inductive reactance of the line and capacitor reactance; but in practice this is true for comparatively shorter lines and hence, in longer series compensated lines, the term "compensation efficiency" has been used to reflect higher transfer reactance than the theoretical value [11]. It is defined as the ratio of net reduction in transfer reactance to the actual capacitive reactance used. In [11], Kumar et. al. analyzed the effectiveness of series compensation on 500 kV lines of length up to 1000 km. If single capacitor bank is used, best compensation efficiency is achieved by locating the capacitors at the mid-point, and in this case efficiency does not depend on degree of compensation; it is only a function of position and line length; efficiency is higher with lower line length. But, for applications where series compensation is implemented in several parts along the line due to maximum permissible voltage ratings, fault conditions and protective requirements, compensation efficiency is additionally a proportional function of the degree of compensation.

The first commercial installation of 500 kV series capacitors was realized in California, USA – on the Pacific Inter-Tie. Reference [12] provided engineering considerations related to design, installation and operation of the units and serves as a source of practical information for series capacitor installation projects. Degree of compensation is 70% for each of the line sections, applied in two parts and located at both ends of the sections, which is exceptional to the previously discussed midpoint location. From economic point of view, installation and operating cost can influence the position of capacitor banks and hence, construction costs related to additional substation for mid-point location of series capacitors may not always be appreciated. Some of the line sections of the Pacific Inter-Tie was not series compensated as those are of moderate lengths and remains overloaded at normal operation. Hence, series capacitors for these sections will require a higher MVAR rating and obviously the project cost will be higher than the achievable benefits.

Whenever faults occur in long series compensated lines with more than one section, and faulted section is isolated subsequently, the overall line reactance is increased and threatens the system stability. Kimbark [13] proposed a switched-capacitor scheme that increased the amount of compensation upon occurrence of a fault by an amount equal to the increase caused by isolation of faulted line-section. Example calculations for a 360 mile, 525 kV

double circuit transmission line with two sections showed that application of the scheme can enhance the transient stability limit from 2.22 to 2.98 GW, which indicates an increase of 34%.

An electric power system is rarely found to stay in any equilibrium state for a long time; it is rather continuously changing due to natural load behaviors, faults, outage of network elements and so on. Compensation systems installed in a power system should be capable to cope with this characteristic. Until the invention of Thyristor by GE in the early 1960s, compensation schemes have been fixed in nature. The first commercially available controlled compensation system was of shunt type, i.e., a shunt connected Static VAR Compensator (SVC) installed by GE in 1974, whereas the first controllable series compensation appeared a decade later, in 1984. It was a scheme for oscillation damping invented by N. Hingorani and was demonstrated by Siemens on Southern California Edison's Mohave – Lugo 500 kV line [14, 15].

Theory and techniques for analyzing performance of compensation systems on the dynamic behaviors of a power system is different than those for steady state analysis. In [16], Rauth reviewed the typical dynamic behaviors of a power system upon occurrence of a disturbance. The first few cycles upon the disturbance occurred is referred to as "Subtransient Period" where rapid decay of AC and DC components of fault current takes place. If the disturbance occurred is severe and rotor angle excursion is large, then the duration of first half-cycle of rotor angle oscillation is called the "First Swing Period", which usually lasts for 0.5 – 1 sec. This period is highly significant as this is the span of time where transient stability may be lost. Series capacitor enhances the peak synchronizing power capability and hence for a fixed initial power, first-swing stability is higher with series compensation. Rauth [16] also identified the effects of controllable or adjustable reactive compensation on system dynamic and transient stability. Voltage control by reactive compensation aids to stabilize the rotor angle excursion during system disturbances. Adjustable compensation is also required to maintain the voltage within acceptable limits as the system loading or network configuration changes and to minimize the unnecessary flow of reactive power by keeping the transmission losses at a reasonably minimum value.

In [17], Miller et. al. provided a comprehensive analysis of Thyristor Controlled Reactor (TCR) based static compensators including control strategies; though these analyses are focused on shunt applications, yet can be used as reference for analyzing series applications, because of the fact that the TCR scheme analyzed is the main source of variable susceptance

5

in many of the continuously controllable compensation systems. In a TCR, two oppositely poled thyristors are connected in parallel and this combination is connected in series with a reactor. For a fixed amount of physical reactance, available susceptance of the TCR branch is a function of the conduction angle [17].

Concept of "FACTS" was first introduced to the power system community by N. Hingorani in April 1988 and was defined as "thyristor-assisted ac power system" [14], though other power electronic devices and static controllers have been included in the latter definitions. The ever first Thyristor Controlled Series Capacitor (TCSC) scheme for increasing power transmission capability appeared in1992 by Siemens on WAPA's Shriprock-Glen Canyion transmission line. Before installation of this new FACTS device, a joint publication by researchers from WAPA and Siemens [18] provided with theory of operation of the controlled compensation scheme, which was termed as Advanced Series Compensation (ASC). The scheme consisted of a TCR in parallel with a fixed series capacitor. In this paper, authors provided an analytical expression of the resultant reactance available from the ASC as thyristor firing angle is varied and discussed some of the important design considerations for operating the device.

The scheme is electrically a parallel combination of an L-C circuit, where value of inductive reactance is a function of the firing angle, as discussed before. Based on conduction angle of thyristors, the device can be operated both in inductive and capacitive mode, though natural application requires the capacitive one. At firing angle of 180°, thyristor switches are non-conducting and equivalent reactance is equal to the physical reactance of the capacitor; as the firing angle is decreased, equivalent capacitive reactance starts to increase. As the scheme is in series with the transmission line reactance, limits of the firing angle is to be chosen so that series resonance is avoided to save the controller from probable damage due to high voltage drop and internal current. Reference [18] also provides with an expression for percentage harmonic content in ASC voltage and shows that harmonic pollution increases with decrease of firing angle and hence puts another limitation in selecting the firing angle range.

Slow response time of the ASC scheme, influenced by initial firing angle, amount of change in firing angle and amount of net series reactance resulting from change in firing angle, has also been reported in [18]. Given this inherent slow response of the ASC system, capability of this device to respond appropriately to damp power oscillations has been examined; simulation results showed that reactance can be satisfactorily modulated at 2 Hz to damp power swings of less than 2 Hz, which was stated as a reasonable limit considering the real-

world experiences from interconnected system operations. At that time, different local and remote signals were under investigation for using as modulation control input [18].

Since the first generation installations of controlled series compensation systems as mentioned above, considerable amount of research work have been deployed in the industry to develop more accurate models to be able to capture system dynamics with Thyristor Controlled Series Capacitor (TCSC) and to prepare engineering specifications with higher degree of precision for future installations. TCSC being a variable reactance system, limits or constraints of achievable reactance from this system has been an important consideration in modeling approaches. In [19], Paserba et. al. reviewed voltage and reactance characteristics of TCSC and identified it's reactance limit based on firing angle, voltage across TCSC and line current; the final limit to be chosen was proposed as the minimum of these individual limits. The authors here proposed a "voltage-limited" model of TCSC for typical transient and oscillatory stability studies, where magnitude of variable reactance is limited by voltage rating of the TCSC. Simulation results presented show that this model produces more accurate transient performance than the "fixed reactance limit" model.

Several references including [19] and power system analysis tools such as PSS/E and ETMSP initially have been using similar type of model which approximated TCSC dynamics by variable reactance [20]. As reviewed and discussed by Jalai et. al. in [20], these models assumed the controller as an "ideal" one i.e., lacking considerations for controller response time and included the control as an integral part of the TCSC design, lacking flexibility in incorporating external control. Here [20] the authors proposed a new model which represents the inherent slow response of TCSC and keeps provision for external control. For transient analysis, this model replaces the reactance of TCSC with a parallel combination of a capacitor with similar reactance and a current source representing the thyristor current. As the line current is modulated in both magnitude and phase, this model provides a lagged response based on the inherent time-delay whereas the output from traditional models tracked the magnitude of line current without any delay.

In [21], the authors provided a theoretical derivation of the relation of TCSC equivalent reactance with thyristor conduction angle and discussed the limiting factors affecting the range of controllable reactance. Ratio of physical reactance of capacitor and inductor influences the number of resonating points and to obtain only a single resonating point the ratio should be limited to a certain value. This paper also discussed relationship of this ratio to TCSC specifications such as rating of capacitor and inductor, thyristor peak current and

7

peak reverse voltage. Impedance Sensitivity Factor (ISF) has been defined as rate of change of TCSC equivalent reactance with respect to thyristor conduction angle and explains the limitation of TCSC operation near resonance point based on this concept; magnitude of ISF becomes very large near resonance point, i.e., a small change in conduction angle results in a large change in equivalent reactance and severely affects stable operation of the system.

As observed in [18-20], integration of a control loop in the TCSC control function to modulate the equivalent reactance provides satisfactory damping to power oscillations in the post-disturbance scenario and thus enhance power transfer limits caused by transient stability problems. Gronquist et. al. [22] proposed damping control strategies for FACTS controllers based on locally measurable variables and concluded that structural variations of power system does not impact the control laws. Though the analyses presented in this publication are based on energy function method, which is expected to be valid for a larger region of applications than that with linearized system models [22], many of the literatures used linearization technique for this purpose [23-25]. Damping controller used in these references, and also in this work, is the traditional "lead-lag" compensator. Design of the controller involves determination of appropriate control signal and parameters of the controller based on linear analysis. In [23], Fouad et. al. reviewed the controller design approach based on mode controllability and observability analysis and calculation method for determining controller parameters.

Rouco and Pagola [26] discussed controller design approach based on eigenvalue sensitivity, specifically for series compensation devices. For controllers used in series connected FACTS devices, there is a direct dependence of the output on the input if a branch variable is applied as an input signal to the controller and the eigenvalue sensitivity is simply the product of controllability and observability, which is termed as residue. Phase of residue indicates amount of phase compensation required for stabilizing and based on this controller parameters are determined.

In [24], Canizares et. al. discuss the characteristics of a proper input signal for TCSC damping control functions and demonstrate the stability improvement and transfer capability augmentation achieved by application of TCSC on Argentinean HV grid. The same test system has been used in [25] to show the effects of controller gain variation with change in TCSC set point and variable post-contingency set point – both the strategies showed improved transient performance.

Deregulation of the electricity market around the world compels transmission systems to be loaded up to highest possible limit, which is mostly governed by network stability problems, especially the Voltage Stability. A joint taskforce of IEEE/CIGRE [27] defines this as the ability of a power system to maintain steady voltage upon encountering a disturbance from an initial operating condition; physical appearance of "voltage collapse" has been explained as a phenomenon of "blackout" or abnormally low voltage in network resulting from a collection of events accompanying voltage instability. Since several major blackouts around the world have been directly associated with this incident [28], it is of high importance in the industry. Voltage collapse point is mathematically associated with Saddle-Node Bifurcation when one of the eigenvalues of the state matrix becomes zero [29]. Another local bifurcation, termed Hopf Bifurcation, is of adequate importance to the power system community and is identified when a pair of complex conjugate eigenvalue crosses the imaginary axis in course of changing the system load. This phenomenon brings in oscillatory instability to the system.

The term Available Transfer Capacity (ATC) of a transmission utility has achieved considerable attention due to commercial and contractual scenario prevailing in typical deregulated environment. A report by Dobson et. al. [30] serves as an informative source for transfer capacity related issues and provides methodologies for determining different types of transfer capacity. In this reference, ATC has been defined as "the amount by which inter-area bulk power transmission can be increased without compromising system security".

In [2], Canizares et. al. reviewed voltage collapse problems, defined ATC as the maximum possible power transfer before appearance of the collapse point and discussed application of TCSC to enhance ATC of transmission systems. A practical example of Italian transmission grid has been presented; both constant PQ and voltage dependent loads have been considered. Similarly, [28] refers voltage collapse point as the maximum loadability point and analyzes effects of TCSC on voltage collapse phenomenon; a real European system model has been used. Both of the publications conclude that application of TCSC improves the ATC, i.e., increase the distance of collapse point and hence increase the loading margin of the system.

Discussions presented above provide a literature based idea on the limitations imposed by line inductive reactance on transmission capability, possible enhancement by applying series compensation and also motivates to study the effect of this compensation technique for transmission capability enhancement of a tie-line in Bangladesh Power System.

1.3 Problem Identification

Power System in Bangladesh is geographically divided into two main regions by the river Jamuna – namely the Eastern and Western Region. These regions were being operated independently until they were interconnected by the first East-West Interconnector (EWI) between Ghorasal and Ishurdi 230 kV substations in the early 1980s. To facilitate higher transfer of electricity to Western Grid, another interconnection has been constructed and commissioned in March 2009. Main motivation of this work originated from the power transfer limitations experienced in the past, with single interconnection.

The first EWI is a medium length (179 km) double circuit transmission line, rated at 230 kV; actual operation suffers from low voltage problem. Based on actual operating voltage and ampacity of the conductor used (Mallard) as per American Aluminum Company data provided in reference [1], thermal limit of this line is more than 300 MW per circuit at unity power factor. But in practice, transfer of power to Western Grid is usually limited to 200MW per circuit (in terms of injection into Ishurdi bus) by load shedding and hence, a significant portion of thermal capacity remains unused. No study or analysis has been found from Bangladesh Power Development Board (BPDB) or Power Grid Company of Bangladesh (PGCB), during this work, in support of 200 MW transfer limitation; verbal discussion with System Planning Directorate of BPDB uncovered that non-convergence of load flow equations have been found beyond 200 MW injection into Ishurdi bus.

This thesis investigates the possibility of applying series compensation for higher utilization of thermal capacity of East-West Interconnector; and additionally analyzes the effect of controlled series compensation on power transmission capability and stability of the system with both of the tie-lines.

1.4 Organization of the Thesis

This dissertation has been organized into Five Chapters and Two Appendices. **Chapter 1** contains brief literature review on fixed and controlled series compensation with focus on the specific goals of this work, i.e., transmission capability enhancement. **Chapter 2** deals with the tests systems, describes the dynamic models in brief, and discusses briefly the analytical techniques and simulation tools used in this work. Results of analyses have been presented and discussed in **Chapter 3**. **Chapter 4** provides a simplistic financial analysis of the series compensation project. Conclusions and scope for future research work are provided in **Chapter 5**. Appendices are provided to supplement the study and analysis presented herein.

Test Systems, Analytical Techniques & Tools

This chapter deals with the test systems for used for studying the effect of series compensation on power transmission capability of tie lines; provides brief theoretical background on the analytical techniques; and presents a short description of the simulation tools used.

2.1 Test Systems

Two test systems have been used in this work to show the effect of series compensation in transmission capability enhancement. The first one is the well-known Two Area System [31], chosen for demonstrative purposes and the second one is an approximate model of the Western Grid of Bangladesh Power System (BPS) network, which is the main concern of the objective of this thesis.

2.1.1 Two Area System

Two Area Test System [31] and it's modified versions have been in application for years in studying inter-area phenomena of power system operations, specially the stability related issues. The test case comprises of two simple power systems of similar configuration, designated as Area-1 and Area-2, interconnected by a double-circuit tie line. Each of the areas consists of two generators with similar capacity feeding the load centers of that area. The tie line is a medium length transmission line, divided into two sections of identical span. Two capacitive shunts are also connected with the load buses to facilitate reactive support.

According to the base case configuration, Area-2 has a generation shortfall of 367 MW and is covered by surplus generation from Area-1 through the tie-line. Series compensation has been applied at the middle point of the line by additional bus adjacent to the existing sectioning bus. Detailed modeling data of the system is provided in Appendix B.
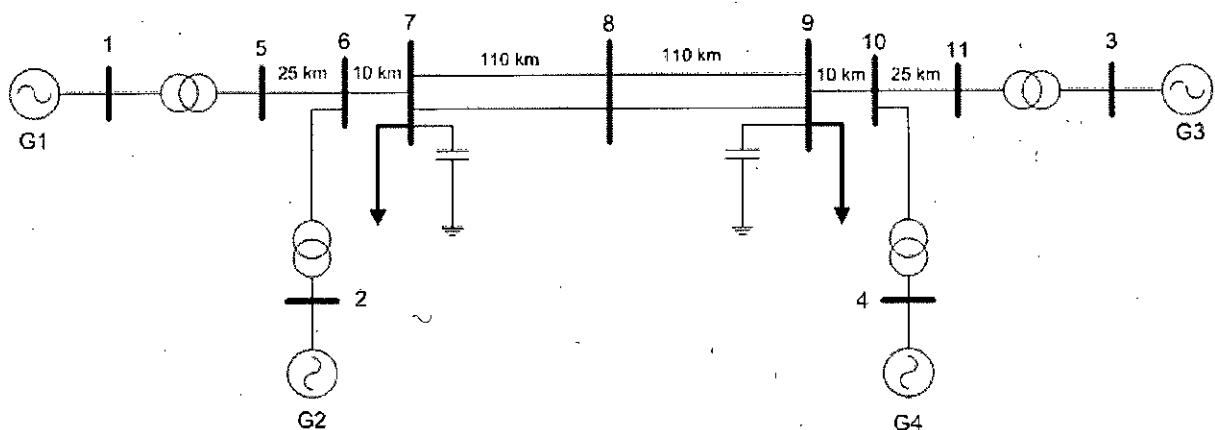
Figure 2.1: Two Area System

2.1.2 East-West Interconnected System

Topology of this system has been derived from the actual network configuration of the western part of BPS network, that can be approximated as a radial one, divided into 5 operational regions, namely – Dhaka, Central, Southern, Northern and Western region. Dhaka region has the largest bulk of generation and exports power to the western part. Dhaka, Central and Southern – these three regions together form the greater Eastern Grid, whereas, the Northern (Rajshahi-Rangpur) and Western (Khulna-Barisal) region form the Western Grid of the system. A single line diagram of the proposed approximation of EWIS is shown in Figure 2.2.

Until March 2009, these two grids have been interconnected by only a single tie-line between Ghorasal (east) to Ishurdi (west). Along with the new interconnection between Ashuganj (east) to Sirajganj (west), several 230 kV lines have been constructed to enhance the power handling capability of the west grid itself. Two scenarios of the EWIS have been considered. One is with single interconnection and without the newly constructed 230 kV lines (Scenario-1) and the other is with two interconnections and those new 230 kV lines (Scenario-2).

In the prevailing time period of Scenario-1, Ishurdi substation was the gateway to receive power from eastern grid and to deliver it over the western grid through several tapped branches from this node extending up to districts of Northern and Western region. Line between Natore and Bogra creates a meshed configuration at the mid part of the western grid. In Scenario-2, Sirajganj substation has been turned into as another flow-gate to facilitate further import to western grid through the new EWI. New 230 kV tapped extensions from Sirajganj into Northern Region (Barapukuria) and into Western Region (Khulna South) forms the 230kV backbone of western grid and uplifts the power handling capability of western

part. Considering the scope of study, modeling of the eastern grid was not required and hence was represented by a single standalone bus, which has been used as the reference or slack bus for power flow model.
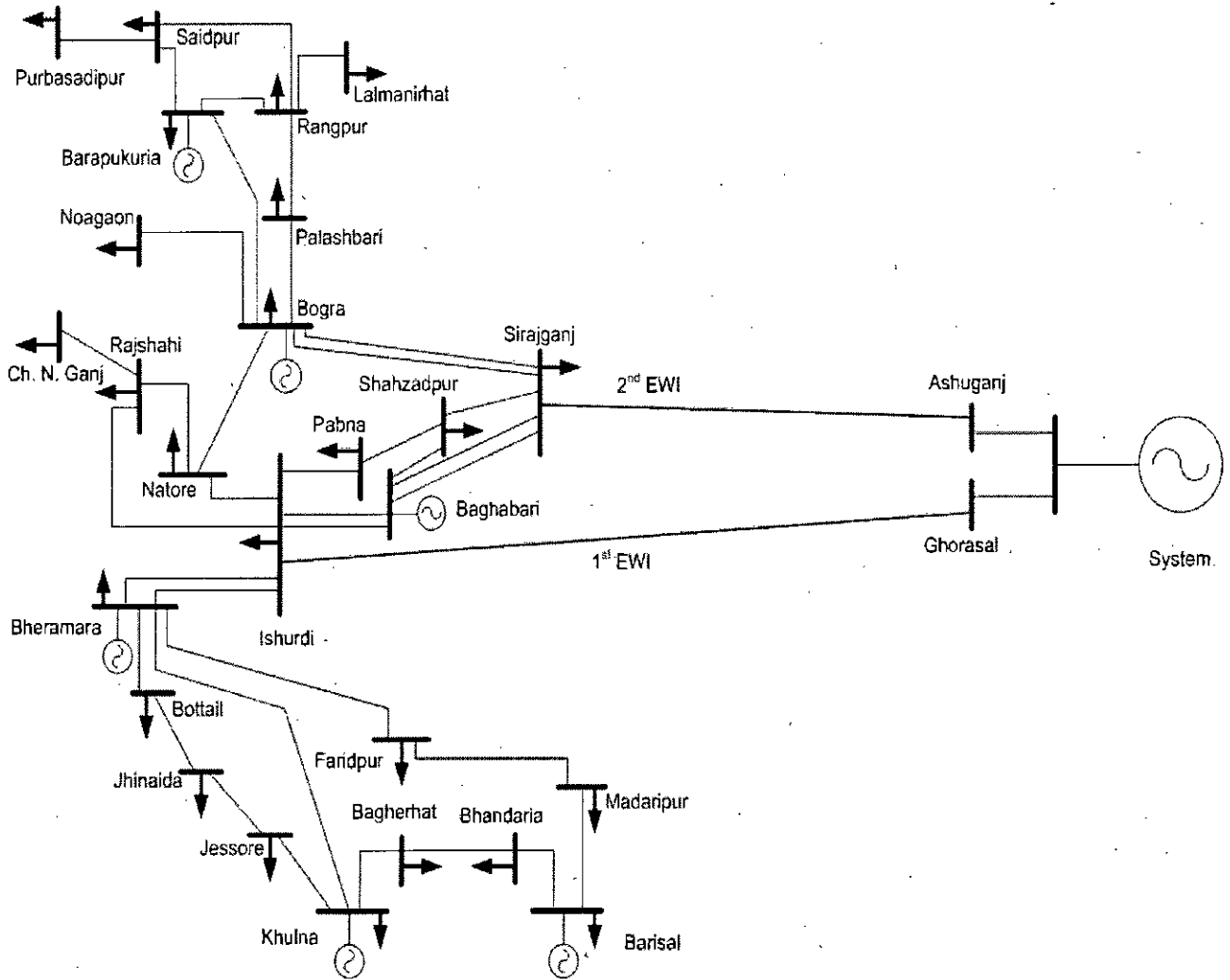
Fig. 2.2: Single Line Diagram of East-West Interconnected System

Scenario-1 of the EWIS has been set up as the base case and specified as such, that real power injection into Ishurdi 230 kV node is approximately 200 MW, which has been considered to be the highest possible import through the 1st EWI. System operation in PGCB is accustomed to keep the transfer to western grid up to this limit by means of load-shedding and as a consequence, practical operating data shows that this transfer scenario usually appears due to loss of generating units in the west-grid. Since this work intends to find out transmission capability enhancement for healthy system operation (without contingency), highest transfer in this work is simulated by increasing the West Grid loading and keeping all the generating units of this region in-service.

13

2.2 System Modeling

The Two Area interconnected system, being a standard test-bed, has been used 'as available' from the reference except for the exciter and turbine governor. Emphasis has been given to discuss detailed modeling of the EWIS.

2.2.1 Generating Units and Synchronous Machines

In the greater western grid, the largest amount of generation takes place in the mid-part of the grid, which comprises of units at Baghabari and Bheramara. Generation in the Northern region has been aggregated in Barapukuria, the largest unit in this region; other small units in Rangpur, Saidpur and Thakurgaon have not been considered due to lower availability, rather generation in Barapukuria has been considered higher than the actual generation available to represent the total generation in this region. In the Western part, generations both in Khulna and Barisal have been considered. Other new rental power plants are expected to come online soon, which have not been considered in this work.

For dynamic modeling of synchronous generators, sub-transient model available from the simulation package has been used. Block diagrams of the Direct and Quadrature-Axis flux linkage model are shown in Figures 2.3 (a) and (b).
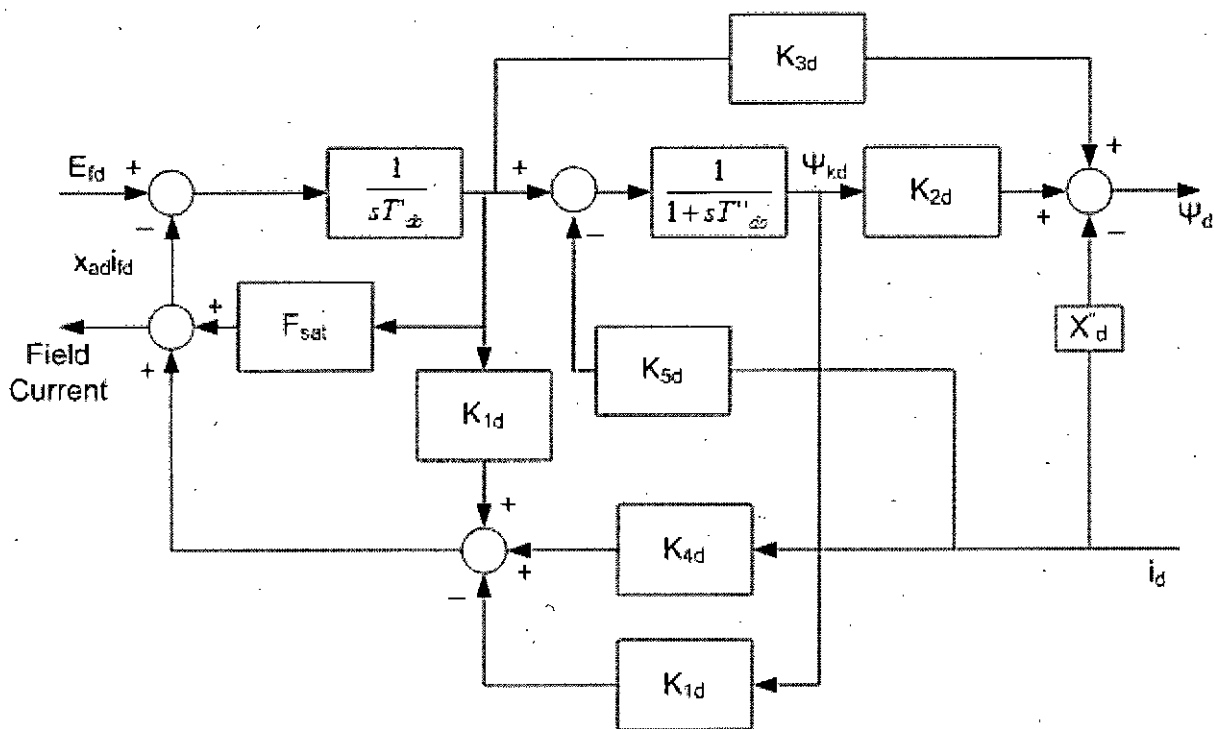
Fig. 2.3 (a): Block Diagram of Direct Axis Sub-Transient Model

Where,

$$K_{1d} = \frac{\left(X_d^{'} - X_d^{''}\right)\left(X_d - X_d^{'}\right)}{\left(X_d^{'} - X_l\right)^2} \text{ [Eqn. 2.1(a)]}, \quad K_{2d} = \frac{\left(X_d^{'} - X_d^{''}\right)}{\left(X_d^{'} - X_l\right)} \text{ [Eqn. 2.1(b)]},$$

$$K_{3d} = \frac{\left(X_d^{''} - X_l\right)}{\left(X_d^{'} - X_l\right)} \text{ [Eqn. 2.1(c)]}, \quad K_{4d} = \frac{\left(X_d^{'} - X_d^{''}\right)\left(X_d - X_d^{'}\right)}{\left(X_d^{'} - X_l\right)} \text{ [Eqn. 2.1(d)]},$$

$$K_{5d} = X_d^{'} - X_l \text{ [Eqn. 2.1(e)]}$$

X_l =   Leakage Reactance
$X_d^{'}$ =   Direct-Axis Transient Reactance
$X_d^{''}$ =   Direct-Axis Sub-Transient Reactance
$T_{do}^{'}$ =   Direct-Axis Open Circuit Time Constant
$T_{do}^{''}$ =   Direct-Axis Open Circuit Sub-Transient Time Constant
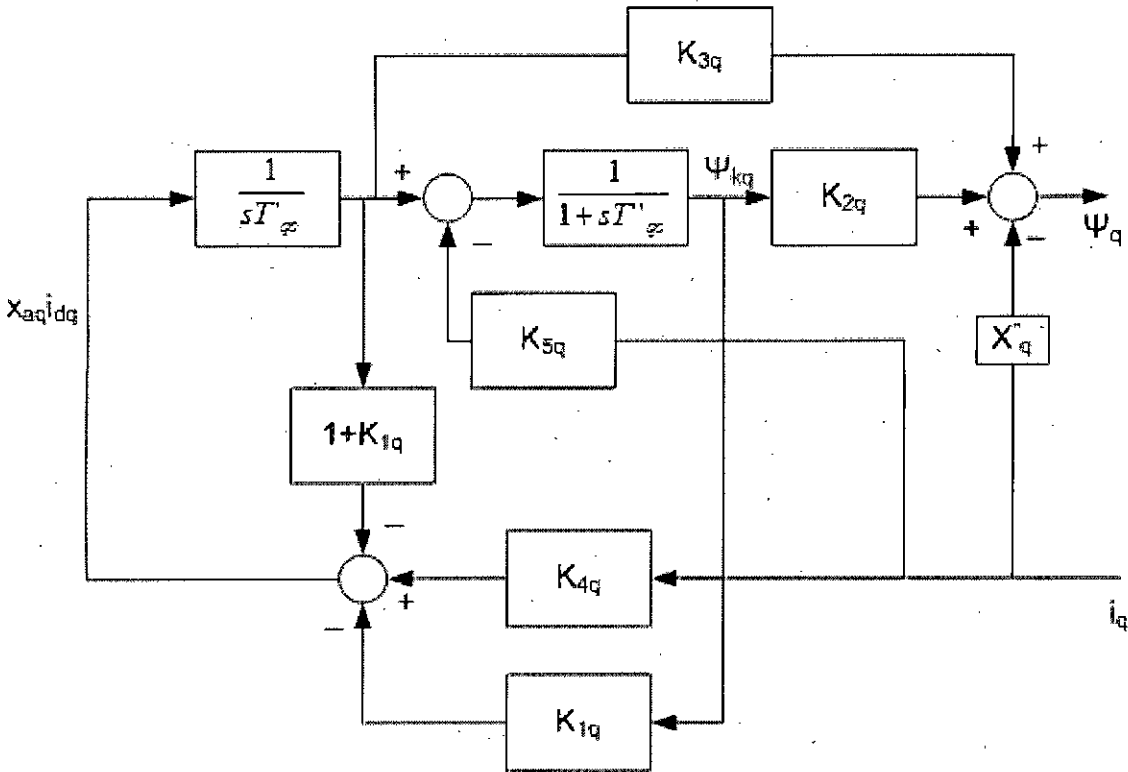
Fig. 2.3 (b): Block Diagram of Quadrature Axis Sub-Transient Model

Where,

$$K_{1q} = \frac{\left(X_q^{'} - X_q^{''}\right)\left(X_q - X_q^{'}\right)}{\left(X_q^{'} - X_l\right)^2} \text{ [Eqn. 2.2(a)]}, \quad K_{2q} = \frac{\left(X_q^{'} - X_q^{''}\right)}{\left(X_q^{'} - X_l\right)} \text{ [Eqn. 2.2(b)]},$$

$$K_{3q} = \frac{\left(X_q^{''} - X_l\right)}{\left(X_q^{'} - X_l\right)} \text{ [Eqn. 2.2(c)]}, \quad K_{4q} = \frac{\left(X_q^{'} - X_q^{''}\right)\left(X_q - X_q^{'}\right)}{\left(X_q^{'} - X_l\right)} \text{ [Eqn. 2.2(d)]},$$

$$K_{5q} = X_q^{'} - X_l \text{ [Eqn. 2.2(e)]}$$

$X_l, X_q^{'}, X_q^{''}, T_{qo}^{'}, T_{qo}^{''}$ have the same meaning as before, as applicable for quadrature axis. Due to constraints in the simulation package, same value of $X_d^{''}$ and $X_q^{''}$ has been used. Complete dynamics of the machine is modeled by the following inertial equations [32]:

$$s\delta = \omega - 1$$
$$\left(D + \tau_j s\right)\omega = T_m - \left(E_q^{''} I_q + E_d^{''} I_d\right) \quad \text{[Eqn. 2.3]}$$

Here, δ and ω represents Rotor Angle and Speed respectively;

D and τ_j represents Damping Constant and Inertia Time Constant, respectively;

T_m represents Mechanical Torque Input;

$E_d^{''}$ and $E_q^{''}$ represents direct and quadrature axis component of sub-transient EMF or generator internal voltage, respectively, determined from flux linkage;

and, I_d and I_q represents direct and quadrature axis component of armature current, respectively, determined from load equations;

Machine data for EWIS have been chosen based on sample data of nearest MVA size machine, as provided in [32].

2.2.2 Exciter

Considering the fact that most of the units in the EWIS are of older type, IEEE Type-1 self excited DC exciter has been used to capture the dynamic behavior of excitation systems; as per IEEE Recommended Practice [33], newer units are modeled with AC or Static type exciters.
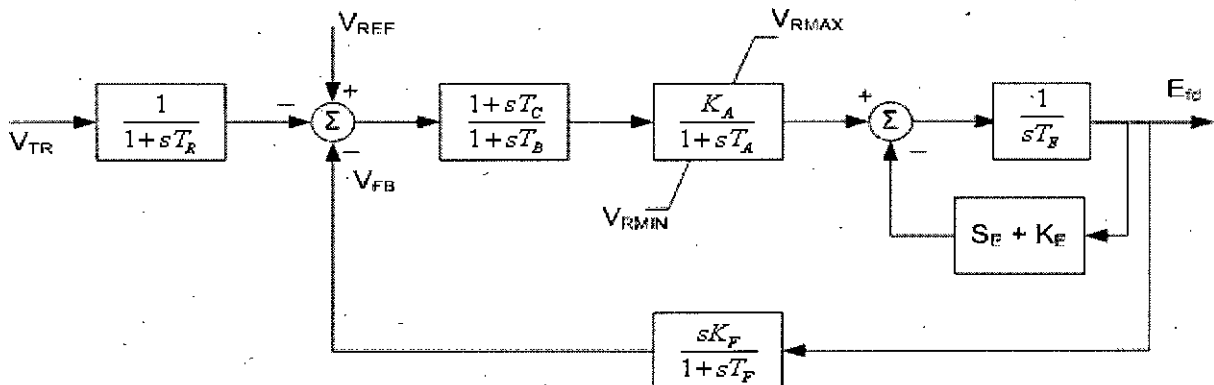
Fig. 2.4: IEEE Type-1 DC Exciter

The process starts with smoothing of the input terminal voltage through a first order filter with time constant T_R. Filtered terminal voltage and stabilizing feedback V_{FB} is subtracted from reference input V_{REF} and the output is then amplified with an amplifier of gain K_A and time constant T_A. Inherent time constants of the voltage regulator is modeled using T_B and T_C, which is usually set to zero for many applications [33] and also in this work. The regulator incorporates a non-windup limit of V_{RMAX} and V_{RMIN} to represent saturation or power supply limitation. Voltage regulator output controls the exciter. Value of K_E is used to model the shunt field rheostat setting; in this work K_E is entered zero and the simulation program calculates the appropriate value so that initially the value of V_R is zero [33]. Effect of saturation is modeled by a non-linear function S_E; value of this function at two points of the saturation curve, usually at 100% and 75% of the exciter ceiling voltage, are used to represent the saturation function for computer simulations. Stabilization to the exciter is provided by a derivative feedback compensation [32] of gain K_F and time constant T_F. Exciter data have been chosen based on sample data provided in [32].

2.2.3 Turbine-Governor

Simplified turbine-governor model as available with the simulation package has been used. Speed error signal is amplified via steady-state gain, $1/r$, where r represents droop or speed regulation. Summation of power and amplified speed error signal, being limited by maximum power output T_{max}, goes through dynamic blocks representing speed governing and turbine systems. The reheater time constant is typically high, which causes the slow response of the governor [34].
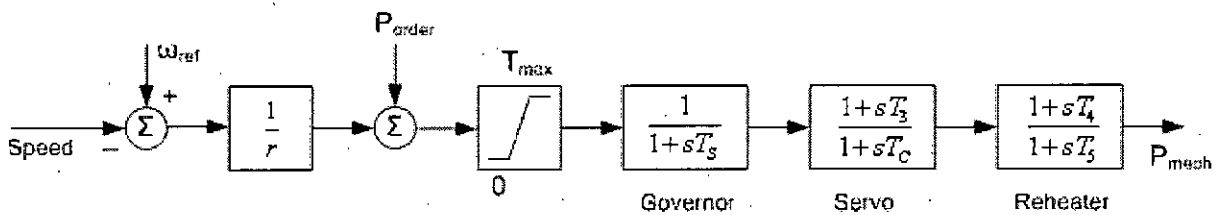
Fig. 2.5: Simplified Turbine Governor Model

2.2.4 Transmission Line

Medium length transmission lines are typically modeled using Nominal Pi-Circuit, which represents the shunt capacitance of the line as two lumped capacitances placed at both ends of the line, each having a value equal to half of the total capacitance [1]. Though T-model is also applicable for medium length lines, the EWIs have been modeled using nominal Pi-

17

Model in this work. Based on the design data, the nominal-pi model of the 1st interconnector.
line is shown below.
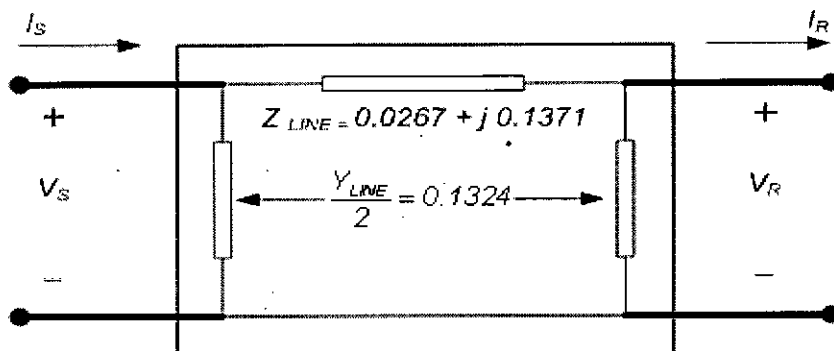
Figure 2.6: Nominal-Pi Model 1st of East-West Interconnector

The nominal-pi model above has been used for the generic two-port network representation of the line. Sending and receiving end quantities of a two-port network are related to each other by general network constants ABCD in the following way. Detailed derivation is available in textbooks e.g. [1, 35].

$$\begin{bmatrix} V_S \\ I_S \end{bmatrix} = \begin{bmatrix} A & B \\ C & D \end{bmatrix} \begin{bmatrix} V_R \\ I_R \end{bmatrix}$$ [Eqn. 2.4]

Where,

$$A = D = 1 + \frac{Y_{LINE}}{2} Z_{LINE}$$

$$B = Z_{LINE}$$

$$C = Y_{LINE} \left(1 + \frac{Y_{LINE}}{4} Z_{LINE} \right)$$

Z_{LINE} and Y_{LINE} represent the line impedance and susceptance respectively. Besides the tie-lines, all other lines in the network are also represented with pi model.

2.2.5 Load

Load has been applied to 132 kV buses in the western grid. Active load data at these buses have been collected from PGCB. Constant active and reactive power load, usually defined as "Constant PQ" load has been used. As PGCB does not keep record of reactive demand at substation end, power factor from operational data was not available. During Power System Master Plan (PSMP) [36] update in 2005, collected data on grid substations showed that power factor varied from 0.85 to 0.95 during peak periods. Based on collected data and discussions with PGCB and BPDB, PSMP assumed an improved power factor scenario of

18

"0.90 or more" by 2010. In this work, power factor at all of the load buses has been assumed as 0.928 lagging, which corresponds to the Ishurdi end power factor in the Scenario-1 base case during approx. 200 MW injection. Variation of load is accomplished by multiplying each of the loads by Loading Factor (LF) – this provides a common platform for finding the loading margins in terms of LF from two different simulation tools.

2.2.6 Capacitive Shunt

BPS network contains capacitive shunt compensation at 33 kV sides of the grid substations. As loads are applied in aggregate manner at 132 kV bus, capacitive shunts are also modeled in the same way for the respective buses.

2.2.7 Series Compensation

This is essentially a capacitive element in series with the inductive reactance of the transmission line to be compensated as shown in Fig. 2.7 and introduces a negative reactance [6], which in turn reduces the net transfer reactance of the transmission system. Series capacitive reactance has been represented by a variable reactance to model the controllability of series compensation.
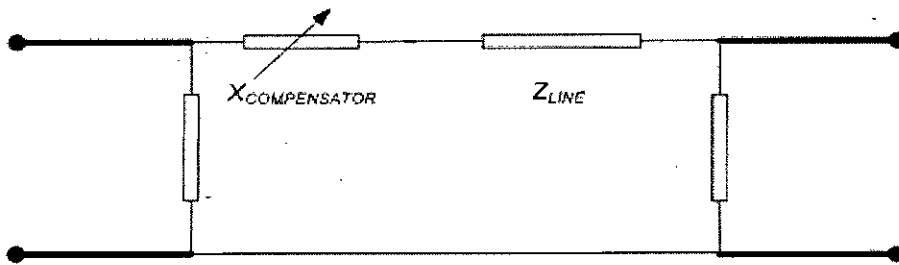
Figure 2.7: Variable Reactance Model of Series Compensation

In this work, controlled series compensation has been applied by TCSC. Typically, a TCSC consists of a TCR module and a fixed capacitor connected in parallel. This combination is connected in series with the line to be compensated, as shown in Fig. 2.8.
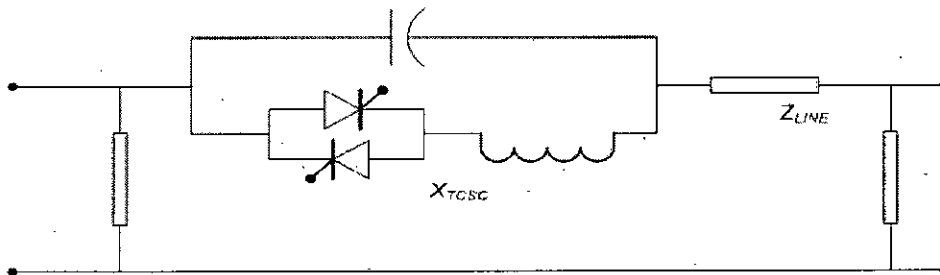
Figure 2.8: Basic Schematic of a TCSC

Equivalent reactance produced by the TCSC depends on the firing angle of the TCR branch. For the analyses performed in this work, "Phase Controlled" mode of TCSC operation has been used [37]. Mathematical relation of thyristor firing angle with the fundamental frequency equivalent reactance of TCSC used for the simulations of this work has been presented in several papers, e.g. [18-19, 21, 28] as:

$$X_e = -X_C \left[1 - \frac{k_x^2}{k_x^2 - 1} \frac{\sigma + \sin \sigma}{\pi} + \frac{4k_x^2 \cos^2\left(\sigma/2\right)}{\pi\left(k_x^2 - 1\right)^2} \left(k_x \tan \frac{k_x \sigma}{2} - \tan \frac{\sigma}{2} \right) \right] \qquad \text{[Eqn. 2.5]}$$

Where, $\sigma = 2(\pi-\alpha)$ and $k_x = \sqrt{\dfrac{X_C}{X_L}}$

α = thyristor firing angle

X_e = equivalent reactance produced by TCSC

X_C = fundamental frequency reactance of the capacitor of TCSC

X_L = fundamental frequency reactance of inductor of TCSC
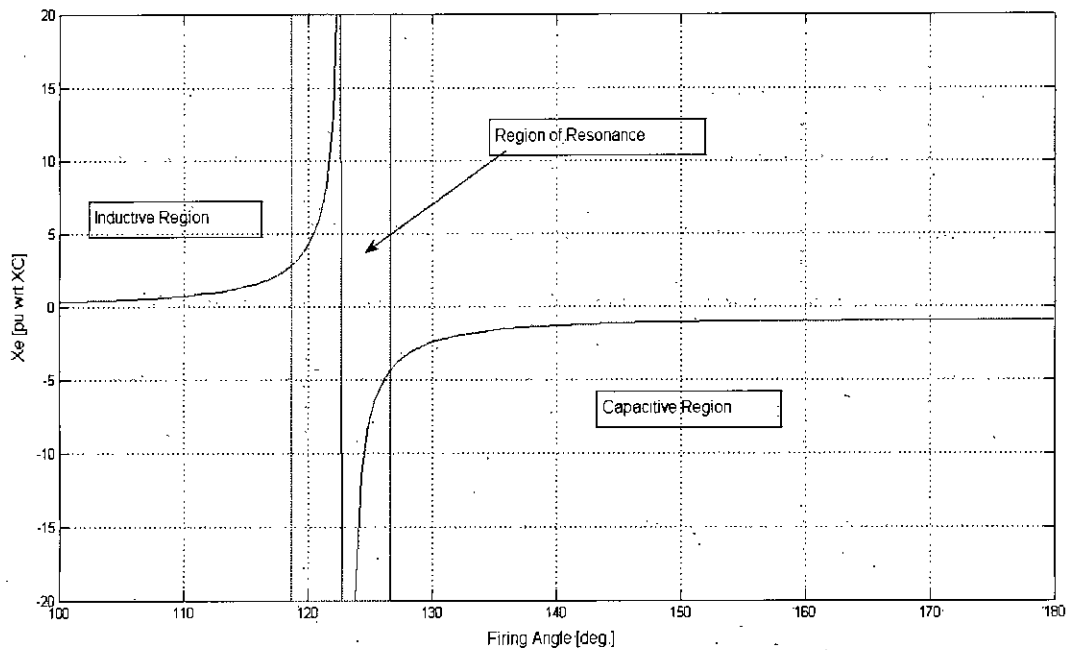
Figure 2.9: Variation of TCSC Reactance with Thyristor Firing Angle

By variation of the firing angle, the device can be operated both in inductive and capacitive region. As typical application of TCSC is in providing series capacitive compensation, limit of the firing angle is set up as [24]:

$\alpha_{min} < \alpha < 180°$, where $\alpha_{min} > \alpha_r$.

α_{min} = minimum thyristor firing angle

α_r = firing angle which produces resonance in the system and must be avoided

20

For steady state analyses at a given level of compensation, the effect of series compensation can be modeled either by directly inserting a negative reactance or can be obtained from the relation of TCSC equivalent reactance with firing angle. Both the approaches have been used in this work based on the requirements of the simulation tools used. Detailed modeling data is provided in Appendix B.

In [25], the authors described typical control schemes used for a TCSC controller – namely the "internal control" and "external control". External control guides the TCSC to provide the required compensation based on specified objective and measured system variables whereas, the internal control provides the required gate firing signals for thyristors to produce desired output reactance. In addition to providing steady-state series reactive compensation for power flow control, oscillation damping controller is usually included in the external control, which provides with improved transient performance for a given level of power transfer.

External control function for steady state power flow control is usually implemented by PI controller or direct operator intervention [25]. In this work, steady-state level of compensation, i.e., the set point is varied manually for achieving different degrees of compensation. For oscillation damping purpose, the reactance is varied by dynamic action of a stabilizing or Damping Controller, which is discussed in Section 2.2.8 below.

2.2.8   TCSC Damping Controller

A fixed level of series compensation can improve transient performance of a transmission system than that without compensation; but for achieving even better transient performance, a damping controller can be added for modulating the TCSC reactance [18, 24-25].

The first step in addition of a damping controller is identification of the critical mode of oscillation by performing modal analysis of the system; then appropriate controller is added to provide additional damping to that mode. Controller structure and parameter calculation methods used in reference [23, 38] have been applied in this work.
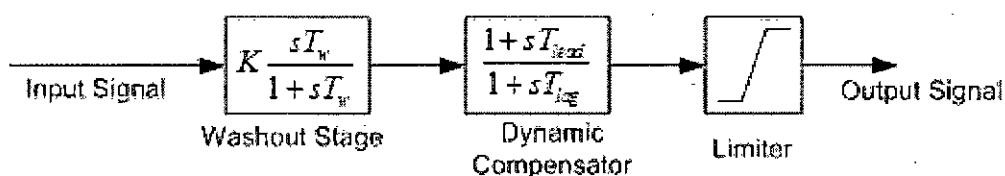
Figure 2.10: Block Diagram of TCSC Damping Controller

The controller contains three blocks as shown in Fig. 2.9; the first one is a wash-out block used to make the controller non-responsive to the DC offset of the input signal [24]. Then

21

comes the lead-lag block, which provide dynamic compensation and finally a limiter is placed to limit the level of compensation within practical ranges.

For an oscillation mode to be damped by the stabilizing action of a controller, the mode must be visible in the input signal to, and must be excited by the output of that controller [38]. These properties are defined as "observability" and "controllability" of that mode respectively and determined from eigenvectors, input and output matrix of the linear representation of power system. Details on this subject matter are discussed in several references e.g., [26, 34, 38]. Line active power flow has been used as input signal for TCSC controller in several references, e.g., [23-25, 38] and also in this work.

2.3   Analytical Techniques

Considering the scope of this work, i.e., demonstrating the enhancement of transmission capability of tie-line by applying series compensation, the analytical framework has been structured based on methods that are typically used for analyzing static and dynamic performance of transmission systems. Bifurcation based techniques have been used in this work to identify system loading limits based on stability considerations [39].

2.3.1   Steady State Analysis

For demonstrating steady state performance of series compensation, ABCD parameter based analysis and load flow studies have been performed.

A.   Two-Port Network based Analysis

Application of generic two-port representation of a transmission system is widely used in analyzing basic steady state performance. General network constants of two-port network, conventionally termed as ABCD constants, have been determined from the Pi-Model of the transmission line and have been applied to demonstrate the improvement of line performance.

Amount of real power delivered to the receiving end by a line can be expressed in terms of ABCD parameters as the Equation 2.5 below [1]:

$$P_R = \frac{V_R V_S}{|B|} cos(\theta_B - \delta) - \frac{|A|V_R^2}{|B|} cos(\theta_B - \theta_A) \qquad \text{[Eqn. 2.6]}$$

Where, P_R is Receiving End Power, V_S and V_R represent Sending and Receiving End Voltage respectively and δ is the Transmission Angle

22

From this expression it is apparent that modification of the ABCD parameters can change the level of power transferred for a fixed sending, receiving end voltage and transmission angle. With the application of series compensation, ABCD parameters of the line can be changed in the direction which enhances the level of power transferred through the line.

B.   Load Flow Analysis

As known for years, this is a basic study which provides the platform to perform further studies by providing the steady state operating conditions of the network. ABCD constant based analysis reveals the improvement in performance of an isolated single line from a circuit point of view; to demonstrate the improvement with the line in an actual network, load flow analysis is applied. Newton-Raphson based power flow routine, as available with the simulation tools, has been used for this work. Transmission angle and voltage at the receiving end was observed in the load flow results to compare the steady state performance with and without series compensation.

Transmission Angle

Fundamental requirements of bulk electric power transmission is that the major synchronous machines must remain in synchronism and voltages must be kept near the rated values [40]. For a given transmission line, there is a maximum level of power which can be transferred stably through the line and this is called the steady state stability limit. Angular displacement has always been used as a convenient criterion for assessing stability of power system [41]. For a given level of steady state power transfer, a system operating with lower angular displacement is said to have a better stability. Approximate expression of a power system consisting of a source, load and a series compensated transmission line connecting them can be stated as follows [40]:

$$P = \frac{V_S V_R}{X_L (1 - k_{se})} \sin\delta \qquad \text{[Eqn. 2.7]}$$

Where, P = power transferred through the line

V_S, V_R = sending and receiving end voltage respectively

X_L = inductive reactance of line

k_{se} = percentage of series compensation
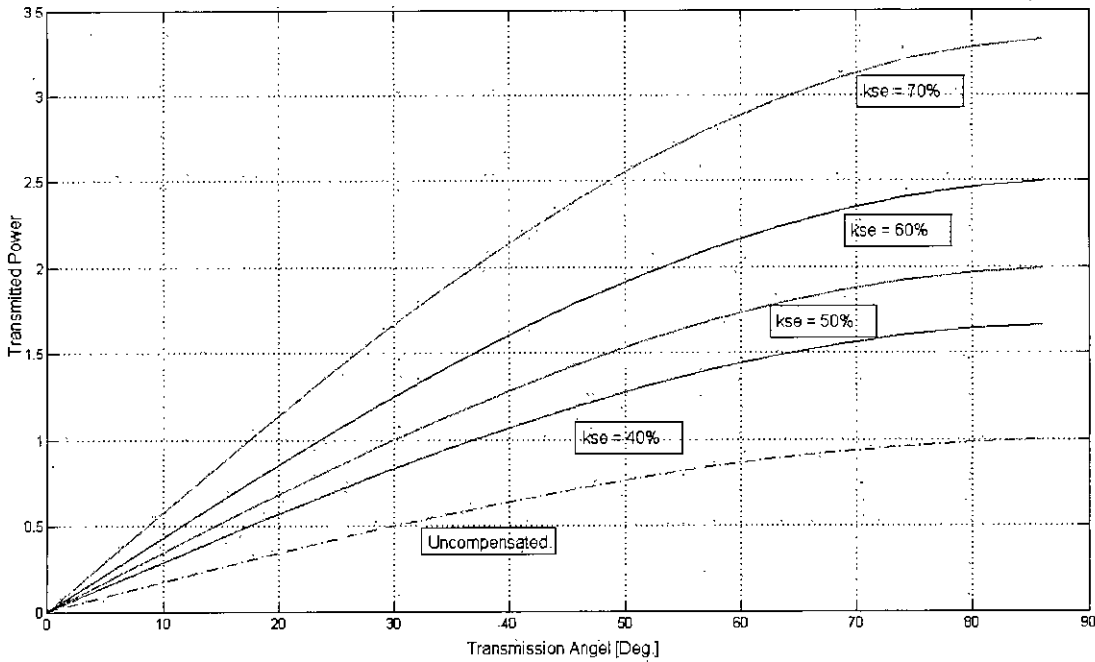
Figure 2.11: Variation of Transferred Power with Degree of Compensation

When $k_{se} = 0$, the line behaves like a natural or uncompensated line. The curves shown in Figure 2.11 depicts that with increasing level of series compensation, same amount of power can be transferred with lower angular displacement, i.e., with better steady state stability.

Voltage Drop

Bus voltage lower than the specified range indicates that line loading is approaching the steady state stability limit. Though, due to lumped characteristic, natural application of series compensation is to increase limit of stable power transmission by compensating for line electrical length, it has been observed that improvement in voltage drop scenario can also be achieved as a by-product of applying series compensation, when installed in a radial system. Series compensation decreases the voltage drop along the line by decreasing the net series reactance [1].

Improvement in voltage drop scenario can also be explained based on Characteristic Impedance of the line, which for a lossless approximation, is defined as Surge Impedance and expressed as,

$$Z_o = \sqrt{\frac{L}{C}} \qquad \text{[Eqn. 2.8]}$$

where L is the series inductance of line and C is line shunt capacitance per unit length of line

24

Surge Impedance Loading (SIL) is the power delivered by a lossless line to a load whose ohmic value is equal to the surge impedance of the transmission line and mathematically expressed as,

$$SIL = \frac{(kV_{rated})^2}{Z_c}$$ [Eqn. 2.9]

where kV_{rated} = rated system voltage and Z_c = Surge Impedance

If a line is terminated by its surge impedance, it produces a flat voltage profile and reactive power flow through the line is zero. In real world cases, transmission lines are not terminated exactly by surge impedances, rather loading vary from fraction to multiples of the SIL depending on the natural behavior of a power system. If the SIL of the line can be modified such a way that the actual required loading of the line is near the SIL, a substantial improvement in the voltage profile can be achieved at that particular load level.

Effect of series compensation is to decrease the series reactance of the line, which eventually decreases the surge impedance and increases SIL; surge impendence varies in the following way as the degree of compensation is changed [40]:

$$Z_o^{'} = Z_o\left(\sqrt{1-k_{se}}\right)$$ [Eqn. 2.10]

Where $Z_o^{'}$ and Z_o are the modified and natural surge impedance respectively and k_{se} is the degree of series compensation.

2.3.2   Bifurcation Analysis

Bifurcation Analysis is a mathematical tool used to study the non-linear behavior of a dynamic system, as any specific parameter of the system changes. Bifurcation occurs when an incremental change made to that parameter causes a sudden change in the system behavior. Mainly two types of bifurcation are of interest to the power system community – Saddle-Node Bifurcation (SNB) and Hopf Bifurcation (HB). Determination of bifurcation points of a system by mathematical techniques requires appropriate representation of the system in mathematical terms.

An electric power system, being a highly non-linear and dynamic physical system, can be represented by the following "general mathematical description" [2, 28] as in Eqn. 2.11:

$$\dot{x} = f(x, y, \lambda, p)$$
$$0 = g(x, y, \lambda, p)$$ [Eqn. 2.11]

25

Where, $x \in \Re^n$ is a vector of power system state variables related to dynamic states of generator and its associated controls such as exciter, governor etc, FACTS state variables and so on; $y \in \Re^m$ represents system algebraic variables such as bus voltage, $\lambda \in \Re^l$ is a set of non-controllable parameters, typically represents system loading factor which is varied to drive the system into bifurcation and $p \in \Re^k$ corresponds to a set of directly controllable system parameters, such as series or shunt compensation levels, $f(\cdot)$ and $g(\cdot)$ represents vector function of right hand side of the system differential equations and algebraic constrains respectively. Determination of bifurcation points involves monitoring the eigenvalues of system Jacobian at the operating point [42, 43].

To detect bifurcation points, system loading is increased in the following manner:

$$P = P_0(1 + \lambda)$$
$$Q = Q_0(1 + \lambda)$$

[Eqn. 2.12]

P_0 and Q_0 represent Base Case Loading and λ is the Loading Factor

A.   Detection of Saddle Node Bifurcation – Continuation Power Flow

Combined effects of constraints associated with constructing new transmission facilities and contractual bindings compel utilities to operate the system in stressed condition which may lead to the situation of static voltage instability, more often termed as "voltage collapse" [2, 28, 42-44].

The following two-bus radial system shown in Figure 2.12 can be used to describe the voltage collapse phenomenon in quite fundamental manner, where the constant PQ load in region-2 receives power from the source in region-1 through the tie line with impedance jX.
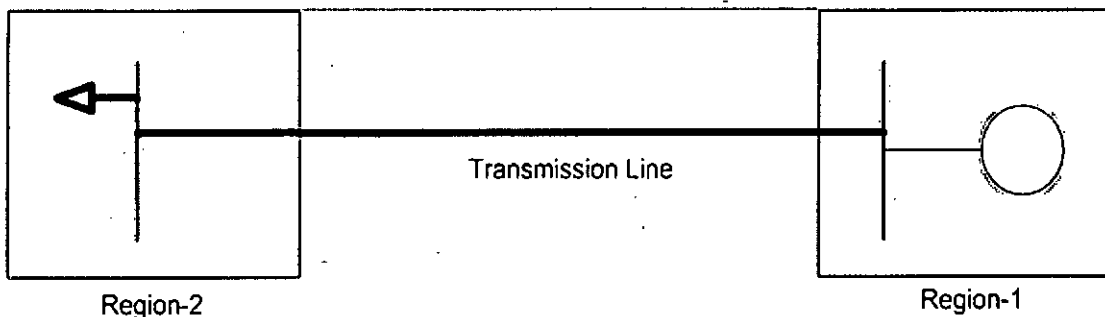
Figure 2.12: Two Bus Radial System

For a base-case transfer scenario, it is assumed that Region-2 is receiving P_0 amount of active power from Region-1 and in this scenario, V_0 is the voltage of the receiving end bus. Now, if P_0 is increased with all other network conditions fixed, V_0 will decrease and at some point, a

further increase in transfer may lead to a situation of sharp and rapid decrease in voltage magnitude, i.e., the voltage "collapses". The following PV curve Fig. 2.13, commonly known as "Nose" curve, depicts the voltage collapse phenomenon. This is also called "Bifurcation Diagram".
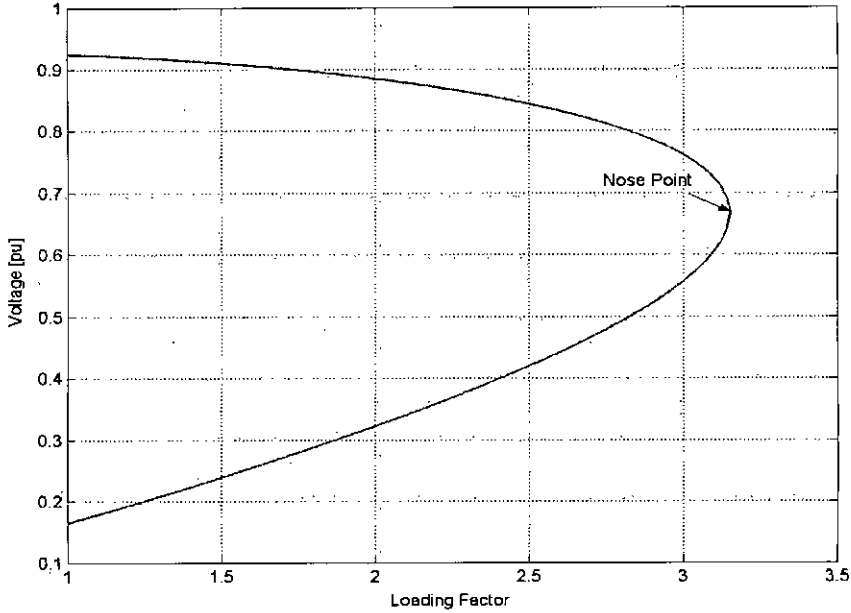
Figure 2.13: Nose Curve or, PV Curve or, Bifurcation Diagram

Physically, voltage collapse is an issue related to reactive power imbalance in the system. Availability of reactive power for any specific node of the system limits the loading margin at that node. With the course of increasing the loading of that bus, a point – usually called as "Nose" point, is reached – beyond which an incremental change in loading cannot any more be supported by the system reactive supply and the voltage declines very sharply. Large amount of voltage drop is observed before reaching the nose point due to huge reactive loss [44-45]. By applying series compensation, reactive loss of the system is reduced resulting in a better reactive reserve and thus loading margin of the system can be improved.

In mathematical terms, the static voltage collapse phenomenon is typically associated with Saddle Node Bifurcation [2, 28, 43] and is "characterized" as an equilibrium point where the system Jacobian is singular and has a simple and unique "zero" eigenvalue with non-zero left and right eigenvectors [46], under the assumption that the Jacobian of algebraic constraints is non-singular along the system trajectories of interest [42, 47]. For a power system Differential Algebraic (DAE) model, as shown in Eqn. 2.11, SNB corresponds to the equilibrium point $(x_o, y_o, \lambda_o, p_o)$ where:

$$\begin{bmatrix} f(x_o, y_o, \lambda_o, p_o) \\ g(x_o, y_o, \lambda_o, p_o) \end{bmatrix} = F(z_o, \lambda_o, p_o) = 0 \quad \text{[Eqn.2.13]; and } D_z F|_o \text{ has a simple zero eigenvalue [2].}$$

These criteria are based on a "local reduction" [47] by elimination of algebraic variables y by applying Implicit Function Theorem [47]: $y = y^{-1}(x, \lambda)$ [Eqn. 2.14],

if, $D_y g(\cdot)$, i.e., Jacobian of the algebraic constraints $g(\cdot)$ can be assumed non-singular along the system trajectories of interest. Detailed mathematical representations and conditions for Saddle Node Bifurcation can be found in several references, e.g., [42-43, 46-48]. It is to be noted that all of the voltage collapse phenomena are not related to SNB [43, 47-48], rather may be caused by "fast dynamic events", such as "large disturbances" [47] or by voltage control devices [42-43].

Voltage collapse point corresponding to SNB has been used in several papers to identify the loadability limit of a system based on static voltage stability [28, 44, 49]. Gradually increasing the system load and performing conventional power flow analysis in each step until the solution fails to converge may be thought as a "simple alternative" to find out loadability margins [46]. This approach has drawbacks like intervention between two consecutive steps to change the system loads manually and numerical problems related to ill-conditioned Jacobians near singularity points [46, 48]. Solutions obtained by this approach also depend on the specifications of the power flow routine and may vary depending on the simulation tools used [48].

More convenient and precise detection of the proximity to SNB is typically performed by Continuation Power Flow technique. In [46], the technique for tracing bifurcation diagrams by continuation method has been described in details. The three step process is initiated with predicting a new equilibrium point from the previous one by choosing arbitrary steps of loading parameter and state variables; this is called the Predictor Step. For finding actual position of the new equilibrium, Corrector Step is used which finds the intersection point between the plane perpendicular to the tangent vector at previous equilibrium and the bifurcation diagram itself. If the solution fails to converge, step sizes are reduced. As the system approaches bifurcation in the course of varying the loading parameter, system Jacobian becomes ill-conditioned. Parameterization step is then used to replace the loading parameter with one of the system variables which possesses the highest change and makes the Jaccobian non-singular at bifurcation point; bus voltage has been used as the swap variable in the simulation tool used. Bifurcation point is detected as sign change in the determinant of power flow Jacobian for the case of loading parameter itself or sign change in the change in loading parameter step for the case of replacing loading parameter with system variable.

B. Detection of Hopf Bifurcation – Modal Analysis

Physical appearance of this type of local bifurcations in the system is characterized by oscillatory behavior of system variables and probable "instabilities" [50]. Linearized model of power systems about an operating point is widely used to extract oscillatory stability related information of the system and aids to reveal the feasibility of a desired operating point based on a given set of dynamic data. Modal analysis involves computation of eigenvalues, eigenvectors and system modes from state-space representation of power system model. These analyses are also collectively termed as "Small Signal Stability Analysis" or "Eigenvalue Analysis".

Reference [50] reviews the approach for determining Hopf Bifurcation point that starts with linearization of nonlinear dynamic system model about an operating point. Linearization of the DAE model in Eqn. 2.11 at an operating point (x_o, y_o) for given values of (λ, p) gives:

$$\begin{bmatrix} \Delta \dot{x} \\ 0 \end{bmatrix} = \begin{bmatrix} \left.\frac{\partial f}{\partial x}\right|_0 & \left.\frac{\partial f}{\partial y}\right|_0 \\ \left.\frac{\partial g}{\partial x}\right|_0 & \left.\frac{\partial g}{\partial y}\right|_0 \end{bmatrix} \begin{bmatrix} \Delta x \\ \Delta y \end{bmatrix} \quad \text{[Eqn. 2.15]}$$

Eliminating the vector of algebraic variables y in Eqn. 2.15, based on non-singularity assumption of $\left.\frac{\partial g}{\partial y}\right|_0$ as before, it is found,

$$\Delta \dot{x} = \left(\left.\frac{\partial f}{\partial x}\right|_0 - \left.\frac{\partial f}{\partial y}\right|_0 \left(\left.\frac{\partial g}{\partial y}\right|_0\right)^{-1} \left.\frac{\partial g}{\partial x}\right|_0 \right) \Delta x = A \Delta x \quad \text{[Eqn. 2.16]}$$

Where, A is System State Matrix.

HB is identified as an equilibrium point when a pair of complex conjugate eigenvalues of the system state matrix crosses the imaginary axis with "non-zero speed", i.e., at the HB point, derivative of real part of the purely imaginary eigenvalue with respect to system loading parameter is non-zero and all other eigenvalues have non-zero real parts [42, 50-51].

For a given set of dynamic data of the system, such as parameters for synchronous machine, exciter, governor and TCSC, modal analysis routine of the simulation tool used constructs the state matrix and computes eigenvalues, left and right eigenvectors and system modes. Position of an eigenvalue in the s-plane gives an idea of system's dynamic stability. Eigenvalues closer to the imaginary axis indicates lower system damping and higher degree of oscillatory behavior.

With series compensation applied, critical eigenvalues have been observed to move more into the left half region of the s-plane which indicates the system is achieving better dynamic stability [49, 51]. Position of critical eigenvalues with and without series compensation has been compared in this work to show the effect of series compensation on dynamic stability of the system.

2.3.3 Transient Stability Analysis

The concept of transient stability is based on the ability of the system to recover normal operation upon occurrence of a major disturbance. For testing the improvement in transient performance by applying series compensation, a severe disturbance has been applied to a specific load bus in the test networks. System variables such as Voltage at faulted bus, machine angle of the nearest unit from the fault and tie-line active power flow has been plotted in a 20 sec. snap-shot. Profiles of these variables with and without series compensation are presented on the same plot to compare the transient performance.

2.3.4 Analytical Framework

For the Two Area System, the analysis has been started with finding the steady state operating conditions of the uncompensated system at the base case loading and loading factor was increased up to the point where transmission angle across the tie lines exceed safe limit Though theoretical steady state limit of a system is calculated assuming the transmission angle as 90°, in practice, for safe operation of the system transmission angle is not allowed to exceed 30° across the line, even it is tried to keep smaller for ensuring better stability [52]. Series compensation was then applied and improvement achieved was observed. Bifurcation analyses have been performed to find Static Loading Margin (SLM) by CPF technique and Dynamic Loading Margin (DLM) by Modal analysis [49] of the uncompensated system and compared with the results of the compensated one. Finally time domain simulations have been performed to assess the system's transient behavior with and without compensation.

For the EWIS, two-port network based analysis was the starting point. Before working with the detailed model, static bifurcation analysis has been performed with a three-bus approximation of EWIS by keeping the voltages at rated level and providing with a higher reactive supply. This has been performed due to the fact that positive effects of series compensation on transmission capability enhancement is not fully understood due to low voltage and lack of reactive supply in BPS network. After this, all the other similar analyses as in Two Area System have been performed.

2.4 Simulation Tools

Two software tools have been used for the simulations in this thesis. UWPFLOW has been used for performing continuation based analysis; modal and transient simulations have been performed with PST. Load flow results presented in the thesis are also performed with PST. A brief narrative on the packages is presented below.

2.4.1 UWPFLOW

This is a research tool designed and developed by Prof. Claudio A. Canizares and Shu Zhang from University of Waterloo, Ontario, Canada and Prof. Fernando L. Alvarado from University of Wisconsin-Madison, Wisconsin, USA, for calculating local bifurcations related to system limits or singularities in the system Jacobian. The program codes are written in C / C++ and run both under WINDOWS and UNIX environments.

The program reads basic power flow data in WSCC / BPA / EPRI format and IEEE common format and FACTS devices data in a special format exclusive to this package. Power flow equations are solved using Newton-Raphson algorithm. Static bifurcations can be determined both by Direct Method and Continuation Method.

Solutions form this tool are provided in ASCII format; additional data can be obtained with specified options for post processing analyses such as bifurcation diagrams, tangent vectors, left and right eigenvectors at a singular bifurcation point, jacobians, voltage stability indices etc. The program and associated information is available in [53].

2.4.2 PST

This is a MATLAB based tool for initially designed and developed by Prof. Joe Chow of Rensselaer Polytechnic Institute. Since 1993, it has been marketed and further developed by Graham Rogers from Cherry Tree Scientific Software, Ontario, Canada. The version of PST which has been used for this work is based on the version that Graham Rogers has used for [34].

PST can be used for dynamic analysis of AC/DC/FACTS power systems. The most attractive feature of PST is that it can integrate user-defined models into simulation environment; and as the program codes are open, users can modify or extend the computational capabilities to tailor for specific simulation requirements. The program and associated information is available in [54].

Analysis and Results

This chapter presents the results of analyses performed on the Two Area test system and the proposed approximate model of the EWIS based on the analytical framework developed in the Chapter-2.

3.1 Two Area System

The Two Area system has a base case load of 967 MW in Area-1 and 1767 MW in Area-2; reactive load is 100 MVAR in both areas.

3.1.1 Steady State and Bifurcation Analysis

Power flow analysis has been performed on the base case and then loading in Area-2 is increased up to the level where transmission angle exceeds safe operating limit; power flow results are provided Table 3.1

Table 3.1: Steady State Conditions of the Uncompensated Two Area System

Increase in Area-2 Loading	Export from Area-1 [MW+ j MVAR]	Voltage at Area-2 Load Bus [pu]	Transmission Angle [deg.]
0.0 %	400.44 + j 12.30	0.9712	27.48
1.5 %	430.76 + j 26.72	0.9642	30.21

It is observed that transmission angle limit exceeds at 430 MW transfer level, which is 1.5% higher than the base case loading. If series compensation is applied at this loading level, transmission angle is reduced and further loading becomes possible.

Table 3.2: Steady State Conditions of the Compensated Two Area System

Increase in Area-2 Loading	Export from Area-1 [MW + j MVAR]	Voltage at Area-2 Load Bus [pu]	Transmission Angle [deg.]
1.5 %	429.04 – j 43.30	0.9734	17.39
12 %	651.70 + j 21.38	0.9227	30.06
20.3 % [70% Comp.]	842.26 – j 14.32	0.8889	21.34

Table 3.2 shows that with 40% steady state series compensation, at approx. 12% higher loading than the base case, the transmission angle limit exceeds. As the level of series compensation is increased at this condition, transmission angle is further reduced and system

loading can be further increased. Analysis has been performed up to 70% series compensation, which is considered as the practical maximum [48].

Maximum loadability of the system has been determined by performing bifurcation analysis based on the given set of static data. CPF analysis shows that in the system without compensation, voltage collapse occurs at LF of 0.07747 whereas in the 40% compensated system, the collapse point corresponds to LF = 0.13524 which is more than 74% higher than the natural system. For 70% compensation, voltage collapse appears at LF = 0.203; power flow analysis at this level shows transmission angle is satisfactorily below the safe limit, as shown previously in Table 3.2.

Modal analysis reveals that the oscillatory instability related to HB is triggered at LF = 0.045 in the uncompensated system, whereas, no such phenomenon was observed in the compensated system in the entire operating range up to the collapse point.
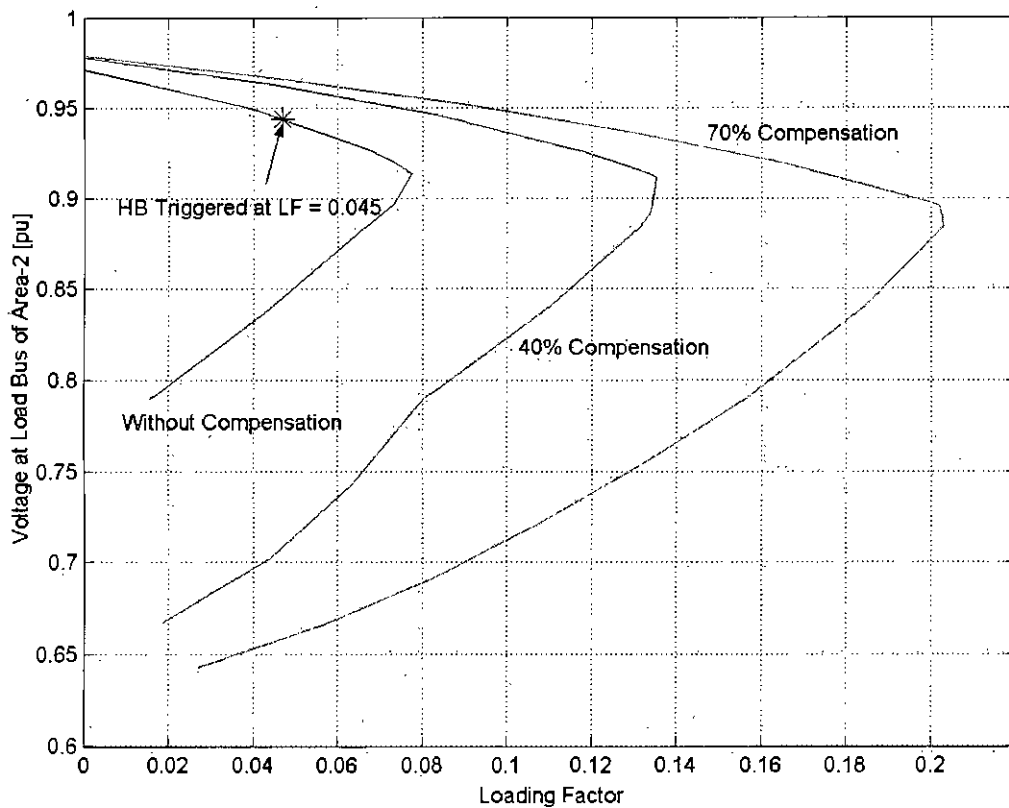
Fig. 3.1: Bifurcation Diagram of Two Area System

Eigenvalues of the system with and without compensation have been plotted in Fig. 3.2, which shows that the critical eigenvalue moves deeper into the left half region of the complex plane for the system with series compensation – indicating better dynamic stability.

Table 3.3: Critical Eigenvalue with Series Compensation in Two Area System

Level of Compensation	LF = 0.015	LF = 0.12
Uncompensated	-0.0197 + j 3.3537	-
40%	-0.0740 + j 4.1362	-0.0219 + 3.5176

Dynamic response is further improved by deploying of a damping controller, as shown in Chapter 2. For using active power flow though the line as input signal to the controller, controllability and observability analysis has been performed. Finally controller parameters are calculated from residue of the critical mode.

Table 3.4: Indices for using Line Active Power Flow as Input Signal

Controllability	Observability	Residue
0.0272 – j 0.0456	-0.7215 + j 0.5789	0.0068 + j 0.0487

Phase compensation required to shift the critical eigenvalue more into the left half plane along the –ve real axis is equal to the supplement of residue phase angle, which in association with frequency of the critical mode is used to calculate the time constants of the lead-lag controller, as shown in Eqn. 3.1 [23, 38].

$$\frac{T_{lead}}{T_{lag}} = \frac{1 - \sin\left(\frac{\phi_{comp}}{n}\right)}{1 + \sin\left(\frac{\phi_{comp}}{n}\right)} = \alpha \qquad \text{Eqn. 3.1 (a)}$$

Here, ϕ_{comp} = Amount of Phase Compensation

n = Number of Controller or Compensator Stage

$$T_{lag} = \frac{1}{\omega_{mode\ to\ be\ damped}\sqrt{\alpha}} \qquad \text{Eqn. 3.1 (b)}$$

Table 3.5: Controller Parameters for TCSC in Two-Area System

Gain (K)	Washout Time Constant [sec.]	T_{lag} [sec.]	T_{lead} [sec.]
30	10	0.6460	0.0905

Root locus of the critical eigenvalue with the damping controller deployed is shown in Figure 3.2, which depicts the shift of the critical eigenvalue with controller action. Selection of gain is performed so that damping is more than 3% - and no other eigenvalue is shifts to the unstable region with the selected value of gain.
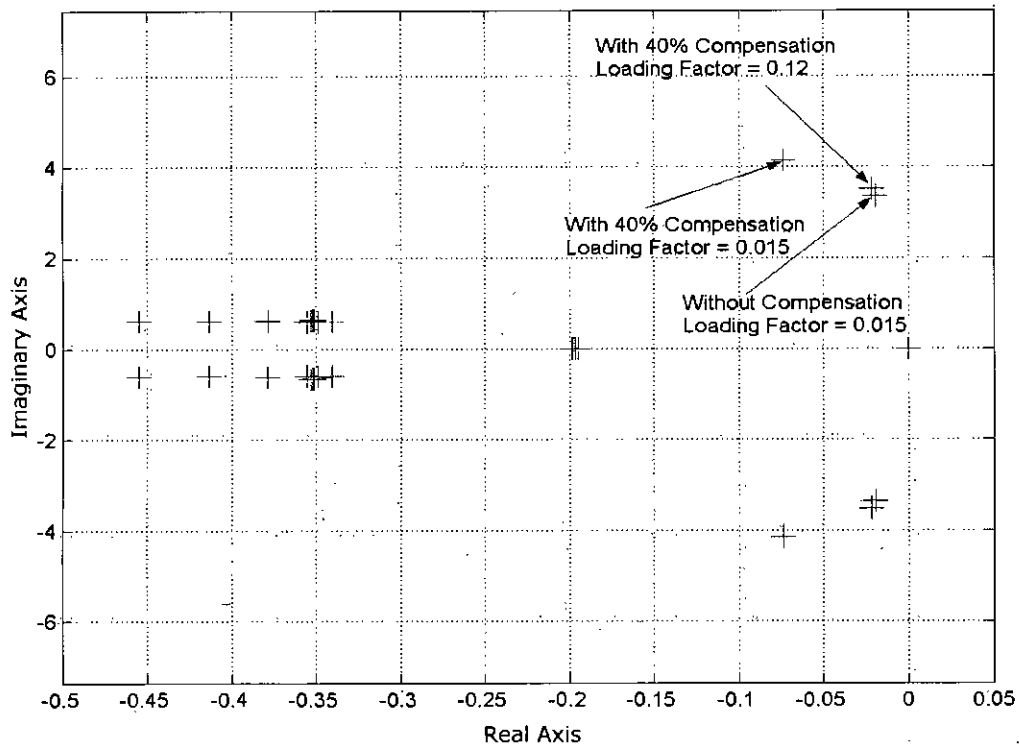
Fig. 3.2: Critical Eigenvalue of Two Area System
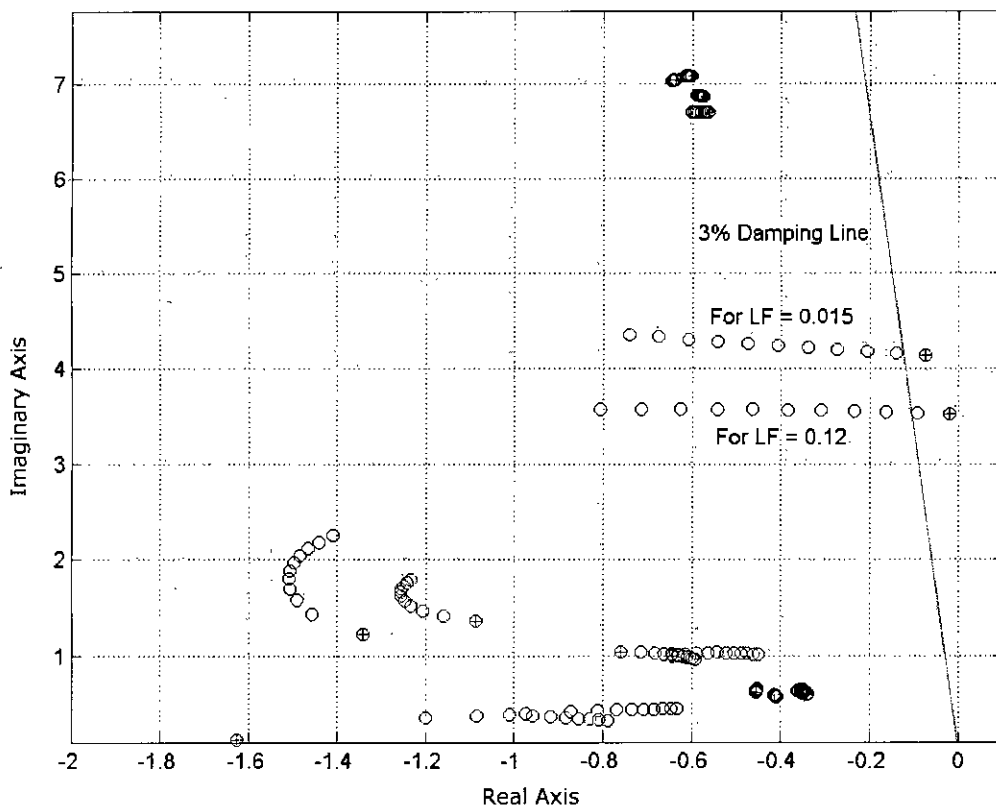
Fig. 3.3: Root Locus of Critical Eigenvalue for Two Area System

The plotted root locus of the system shows that for the same range of gain, shift of critical eigenvalue from initial position is greater in the system with higher loading; this is due to the fact that the magnitude of residue, i.e, sensitivity of the critical eigenvalue is higher than the previous loading (LF = 0.015).

3.1.2 Transient Stability Analysis

Now, transient performance of the system with and without compensation is compared. A three phase fault is applied at t = 0.3 sec at a load bus [Bus 12] in Area 2 with subsequent tripping of the line. Time domain simulation profiles obtained show the improvement in transient stability of the series-compensated system with a tuned damping controller. Transient performance at the highest possible loading level with 40% series compensation, i.e., LF = 0.12 has also been presented on the same plots.
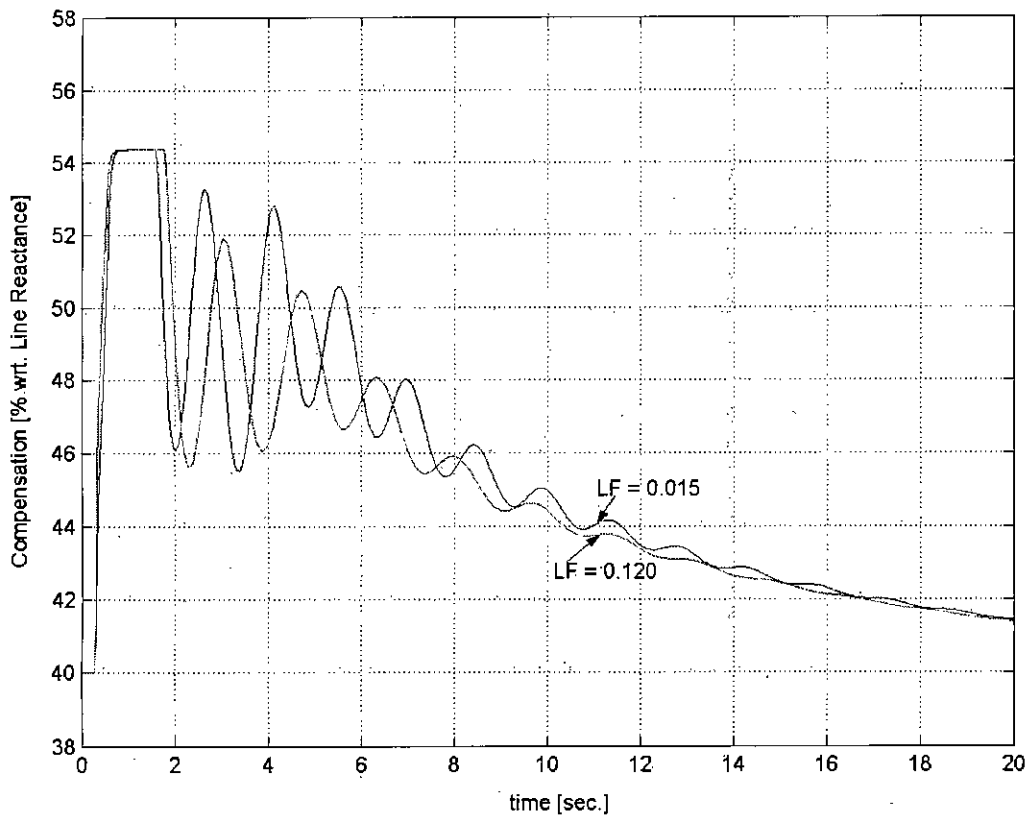
Fig. 3.4.: Dynamic Compensation by TCSC in Two Area System
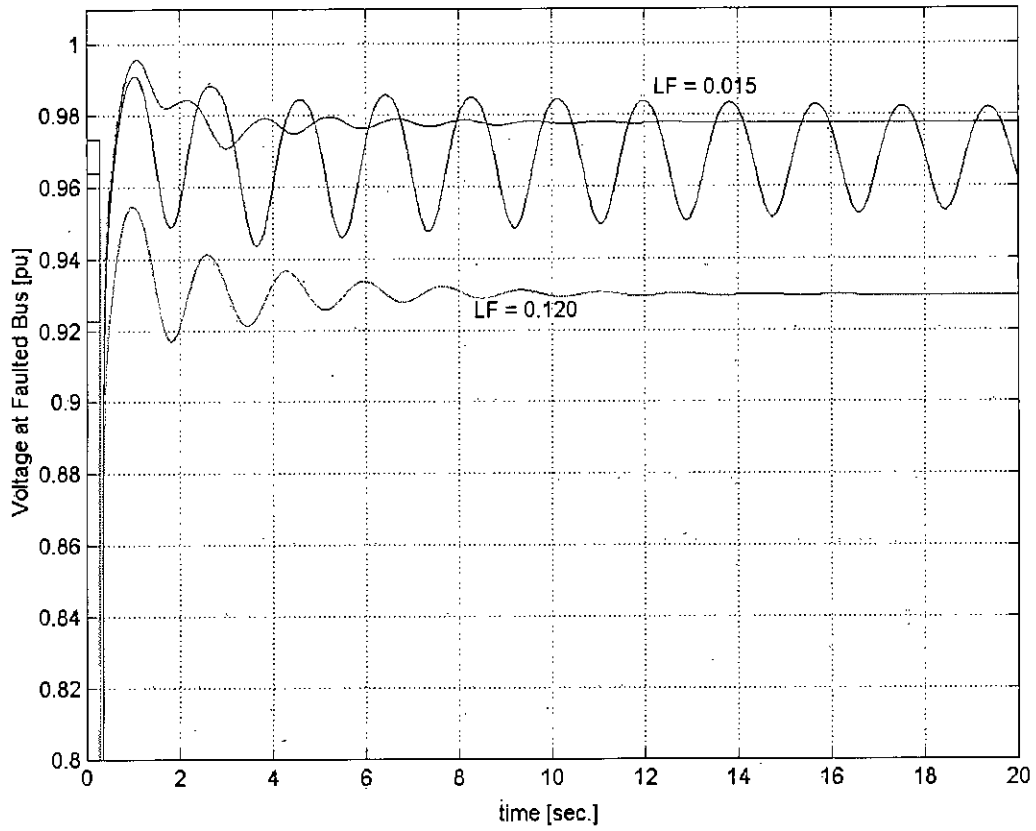
Fig. 3.5: Voltage Profile at the Faulted Bus in the Two Area System
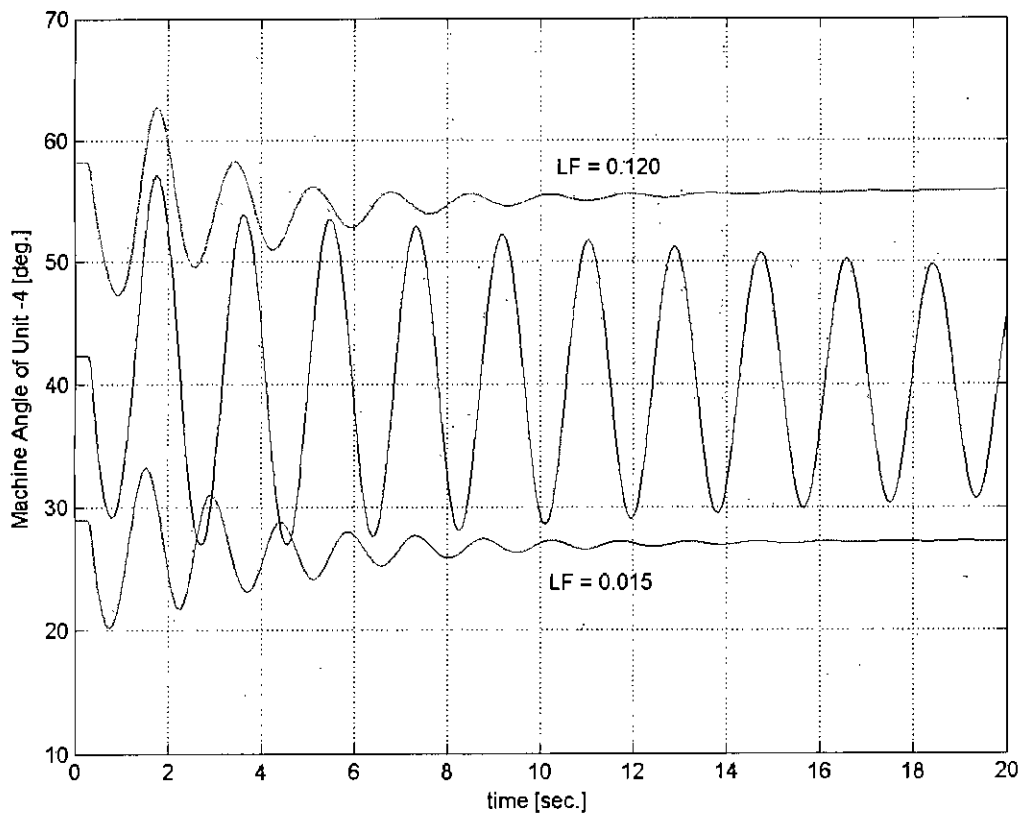
Fig. 3.6: Machine Angle in the Two Area System

37
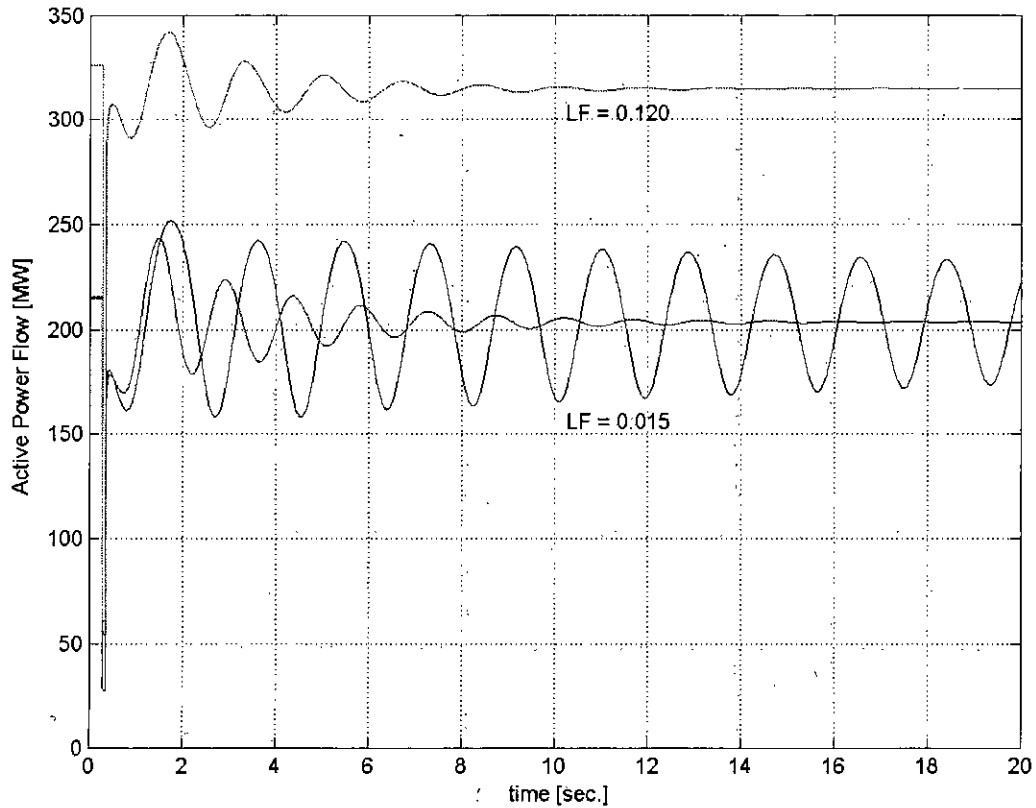
Fig. 3.7: Tie Line Power Flow in the Two Area System

Fig. 3.4 depicts the dynamic action of the TCSC controller, fed back by input signal as the active power through the tie-line. Controller provides the highest compensation in the post fault scenario. Voltage profile at the faulted bus, angle of the machine nearest to the faulted bus and tie line active power flow variables have been plotted in Fig. 3.5 to Fig. 3.6 respectively to compare the improvement in transient performance by applying controlled series compensation.

3.2 East-West Interconnected System

3.2.1 Two-Port Network Based Analysis

General Two-Port Network Constants or "ABCD" Constants of a transmission can be used to show mathematically the improvement of line performance by applying series compensation. From the Equation 2.5 in Chapter 2, it is apparent that modifying "B" can contribute to the increase of power transferred through the transmission line for a fixed sending and receiving end voltage and transmission angle. For this work, a Simulink model has been created that takes these parameters and transmission line constants as input and calculates the ABCD parameters of the uncompensated line. An input is provided in the model for varying percentage of series compensation. Based on the compensation provided, the model then calculates the modified ABCD parameters and displays the power delivered with and without series compensation.

Though the nominal operating voltage for EWI is 230 kV, practical operating data before commissioning the 2nd EWI shows that the voltage level rarely crossed 200 kV at Ghorasal end; most of the cases it has been found to be around 190 kV. Based on this observation, sending and receiving end voltage in the Simulink Model has been kept 190 kV and 175 kV respectively and the transmission angle has been assumed 25 degree, slightly below the safe operating limit.

Variation of ABCD parameters resulted from variation of level of series compensation and corresponding amount of real power transferred is shown in Table 3.6. Analysis has performed on the 1st EWI only.

Table 3.6: Received Real Power with Different Level of Series Compensation

Compensation Level	A	B	Real Power [MW]
0 % (Natural Line)	0.981 + j 0.00353	14.12 + j 72.53	185.4
30 %	0.992 + j 0.00355	14.20 + j 51.16	253.4
40 %	0.996 + j 0.00356	14.23 + j 44.04	287.1
50 %	0.999 + j 0.00357	14.25 + j 36.92	329.3

It is observed, the natural or uncompensated line is unable to carry more than 185 MW of real power into the receiving end for the specified voltage and angle conditions; at this operating point, theoretically about 210 MVA flows from the sending end which is about 70% of the thermal rating of the line. Applying series compensation can increase the level of power transferred for fixed sending and receiving end voltage and transmission angle. In other

words, for a fixed amount of power transfer, transmission angle is reduced if series compensation is applied – which indicates better steady-state stability of the system. At 50% series compensation, the apparent power flowing from sending end is beyond the thermal rating and hence results beyond this are not tabulated.

Typical surge impedance of a 230 kV overhead line is in the range of 365 to 395 Ohm and SIL varies usually from 134 to 145 MW [1]. Table 3.7 shows the enhancement of SIL by applying different level of series compensation. As the SIL is increased with series compensation, higher loading with less voltage drop becomes possible.

Table 3.7: Variation of SIL with Different Level of Series Compensation

Compensation Level	Surge Impedance (Ohm)	SIL [MW]
0 % (Natural Line)	380.86	138.89
30 %	318.43	166.01
40 %	295.01	179.31
50 %	269.31	196.43

3.2.2 Analysis on 3-Bus Approximation of EWIS

A 3-bus approximation of the East-West interconnected system has been shown in Figure 3.8.
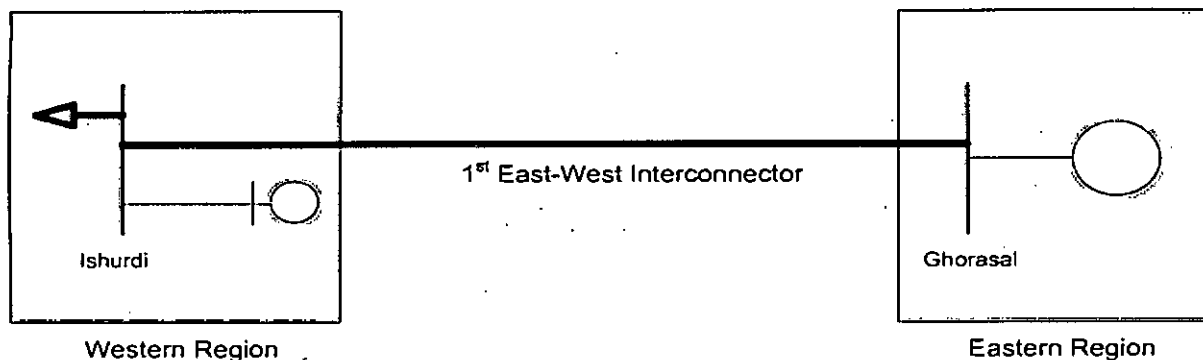
Fig. 3.8: 3-Bus Approximation of EWIS

The system consists of two regions, representing eastern and western grid of BPS and a transmission line interconnecting them with its Pi-model parameters same as the first EWI. The western region has a generation deficiency of 200 MW, which is being met by the eastern grid. Before entering into analysis with a more detailed system model, improvement in line performance by applying series compensation has been examined by this three bus approximation.

CPF analysis has been performed on this model, without enforcing the practical limitations of voltage and reactive power generation at the PV node representing generators in the western grid. The load is applied at 230 kV, the rated operating voltage of EWI. The plot in Figure 3.9 shows nose curves for the system. In the uncompensated system, voltage collapse occurs at LF slightly above 0.206 whereas in the 70% compensated system it occurs at about 0.816.
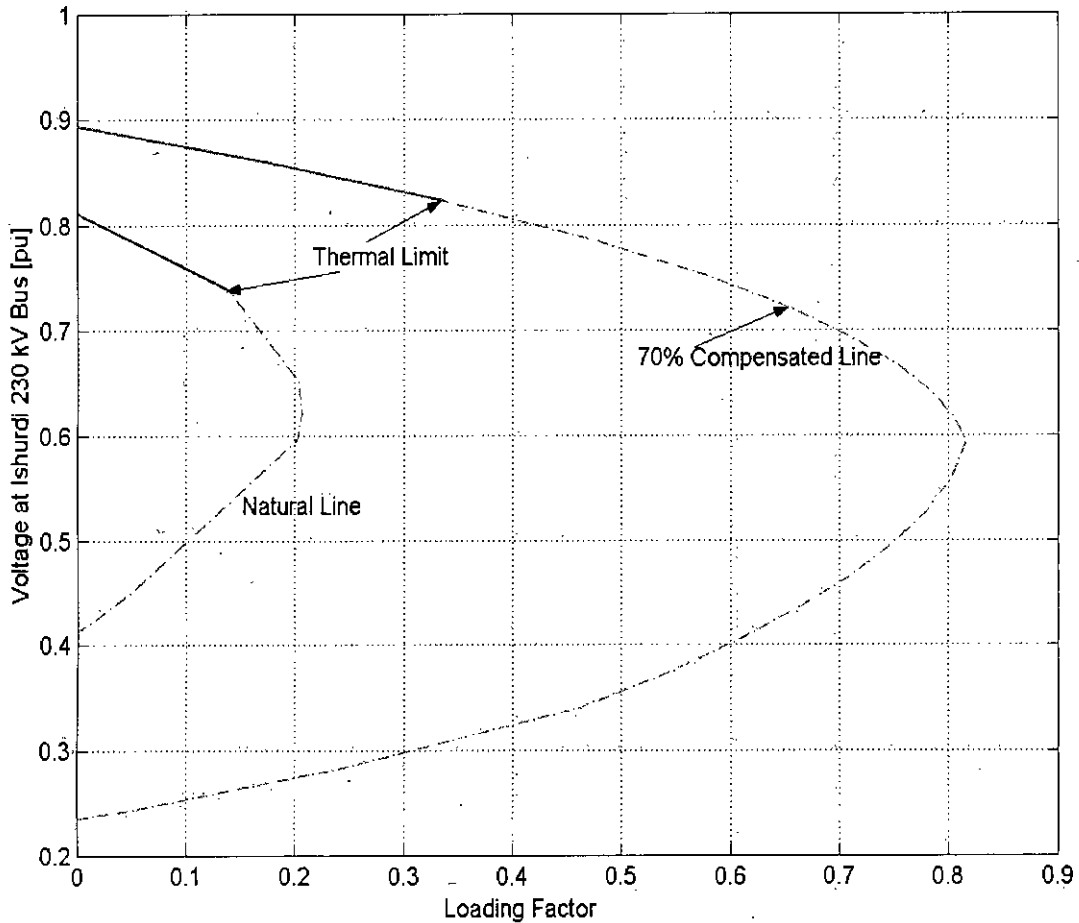
Fig. 3.9: Bifurcation Diagram of the 3-Bus Approximation of EWIS

Thick lines in the bifurcation traces of Figure 3.9 shows that thermal limit of EWI exceeds at LF = 0.140 in the uncompensated system, whereas in the compensated system it is 0.337, which is more than double of the uncompensated limit.

Now, analyses have been performed on the approximate model shown in Chapter 2. Here two scenarios have been considered – the first one is with single interconnection but without the new 230 kV transmission lines in west region (Scenario-1) and the second one is with two interconnections and with those new lines (Scenario-2).

3.2.3 Analysis on the Approximate Model (Scenario-1)

Though Scenario-1 does not correspond the prevailing topology of the actual BPS network at present (i.e., with two interconnections), it is has been considered due to the fact that the main motivation of this thesis originated the transfer capacity limitation with single interconnection and base case of the test network in this thesis has also been set up on this scenario.

Available data from PGCB show that during the maximum transfer, i.e., 200 MW, the power factor at Ishurdi end is around 0.983 and approx. 15 to 20 kV voltage drop occurs across the line. In this work, the base case network set up gives nearly similar results – power factor at Ishurdi 230 kV node is found as 0.9826 and 15.27 kV drop occurs across the interconnection.

With this base case set-up, several modal simulations have been performed, changing the loading factor in each run. It has been observed, the system can transfer 244.86 MVA from Ghorasal to Ishurdi before HB is triggered in the system; an incremental addition of load in the western grid beyond this level triggers the oscillatory instability.
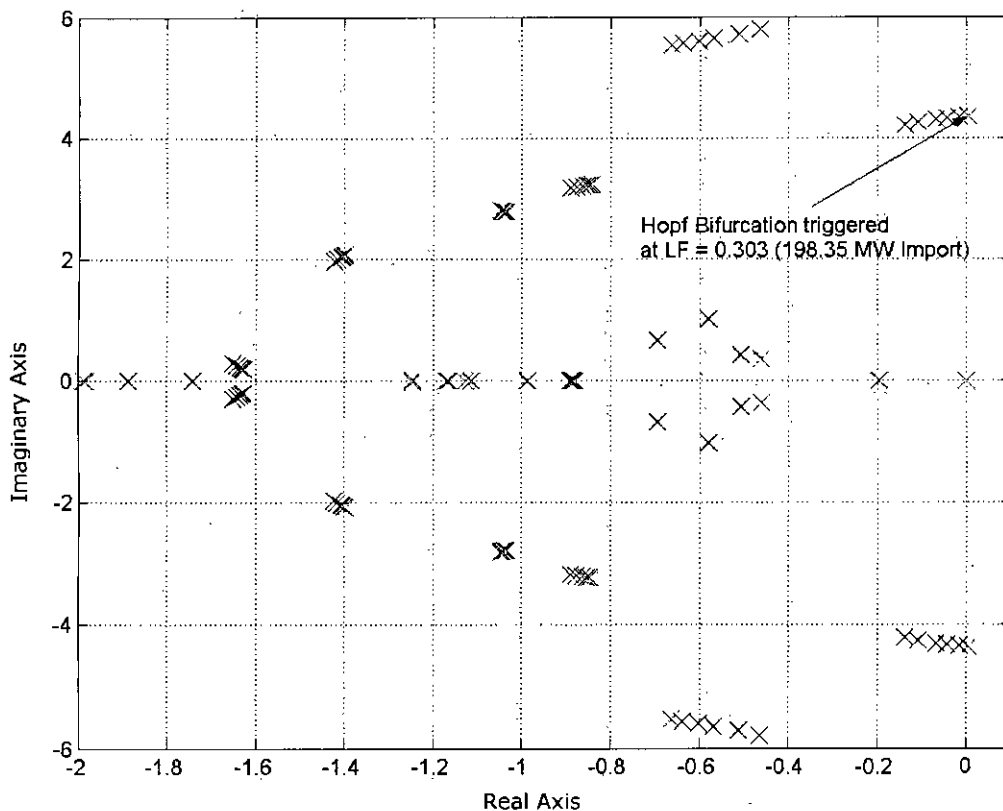
Fig.3.10: Occurrence of Hopf Bifurcation in Scenraio – 1

Results found with modal analyses stated above are plotted in Figure 3.10, which eventually forms a root locus of eigenvalues of the uncompensated system with the loading factor

variation; it is observed that at approx. loading factor of 0.303, i.e., at equivalent import level of 198.35 MW the system encounters the Hopf bifurcation.

Performing load flow study at the maximum loading level prior to the occurrence of HB, i.e., at LF = 0.3 provides the following steady state results, as shown in Table 3.8, for the uncompensated system.

Table: 3.8 Steady State Conditions without Compensation (Scenario-1)

Import Required to West Grid [MW]	Export to West Grid [MW + j MVAR]	Voltage at Ishurdi Bus [pu]	Transmission Angle [deg.]
197.00	240.35 + j 46.83	0.7932	27.12

It is observed that beyond 77% of the total MVA transfer capacity of the line can not be used due to dynamic stability limitation. Transmission angle is also near the safe operating limit.

Static bifurcation analysis performed on Scenario-1 system, reveals that the voltage collapse occurs at LF = 0.33124, which corresponds to an import of 211 MW to west grid. For analyses with EWIS, "import" is defined as the difference in own active power generation and active power demand in the west grid.

Now if series compensation is applied to the line, electrical length is reduced and system loadability is enhanced. Figure 3.11 depicts that distance to the collapse point is increased with the application of series compensation. The plots also show the points of HB as the loading factor is varied and similarly demonstrates that the compensated system possesses a higher dynamic stability limit. Analyses have been performed up to maximum 70% compensation, as with the Two Area System.
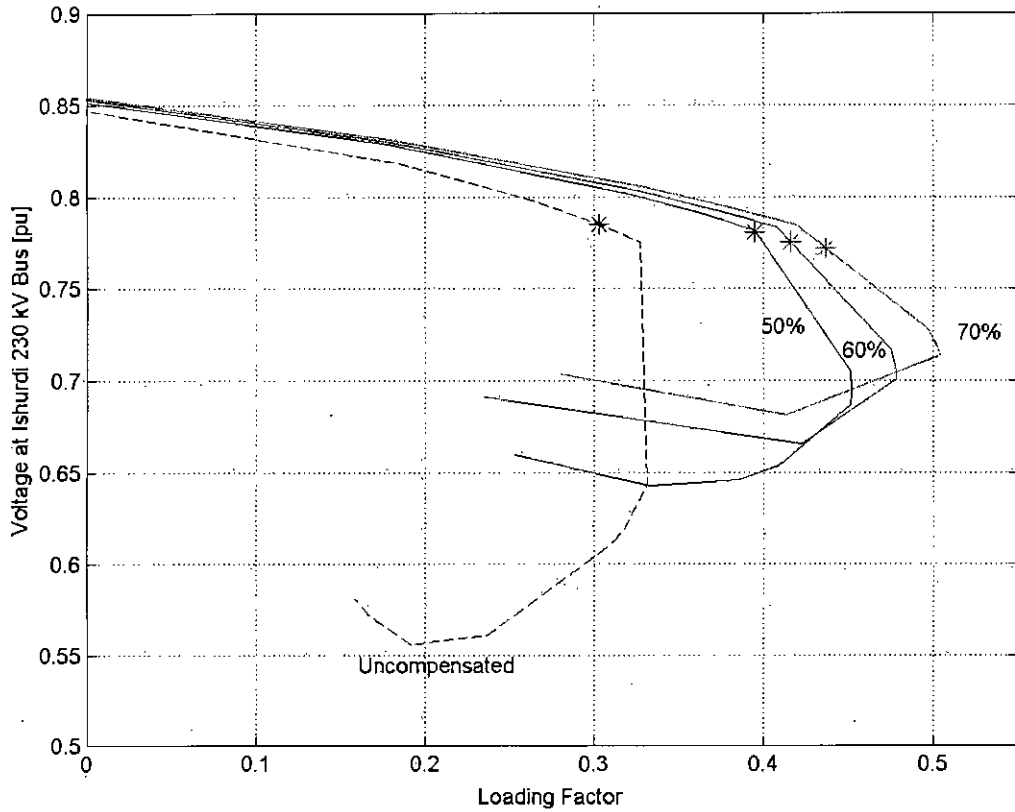
Fig. 3.11: Bifurcation Diagram for Scenario – 1

It is evident from the plot of Figure 3.11 that system loadability is enhanced with series compensation – and further enhances as the level of series compensation is increased. With highest level of series compensation, the SLM is approx. 37% higher and the DLM is approx. 29.7% higher than the uncompensated system. Table 3.9 shows a comparison of DLM and SLM of the system with and without compensation and aids to understand the enhancements achieved by applying different level of series compensation.

Table 3.9: Loading Margins with and without Compensation (Scenario-1)

Level of Compensation	Static Loading Margin (SLM)	Dynamic Loading Margin (DLM)
Uncompensated	0.331 (210.95 MW)	0.300 (197.0 MW)
50%	0.452 (265.4 MW)	0.390 (237.5 MW)
60%	0.478 (277.1 MW)	0.412 (247.4 MW)
70%	0.504 (288.8 MW)	0.430 (255.5 MW)

Steady state conditions of the compensated network at LF = 0.300, which is the highest possible transfer of the uncompensated network due to oscillatory instability, have also been investigated and it has been observed that transmission angle and voltage at Ishurdi end improves as the level of compensation increases [Table 3.10].

44

Table3.10: Steady State Conditions with Series Compensation (Scenario-1)

Level of Series Compensation	Export to West Grid [MW]]	Voltage at Ishurdi Bus [pu]	Transmission Angle [deg.]
50%	237.31 + j 7.830	0.8113	13.17
60%	237.02 − j 0.040	0.8135	10.65
70%	236.84 − j 8.340	0.8150	8.159

With 70% compensation the transmission angle reduces by 69.9% and creates a significant amount of safe margin before the steady state stability limit. As found in the bifurcation studies, the both the SLM and DLM are higher than the thermal limit, which is found to be 0.420. At this loading, the system attains the steady state conditions shown in Table 3.11.

Table 3.11: Steady State Conditions at Thermal Limit (Scenario − 1)

Import Required to West Grid [MW]	Export to West Grid [MW + j MVAR]	Voltage at Ishurdi Bus [pu]	Transmission Angle [deg.]
251.00	315.86 + j 7.060	0.7888	10.98

Modal analysis reveals that in the uncompensated system with LF of 0.300 the critical mode has a damping co-efficient of 0.0036, which is much lower than typical minimum level of 0.03 [55]. By applying series compensation position of the critical eigenvalue moves into the left direction on the s-plane and damping is improved. Fig. 3.10 depicts position of some of the eigenvalues of the system with and without compensation.
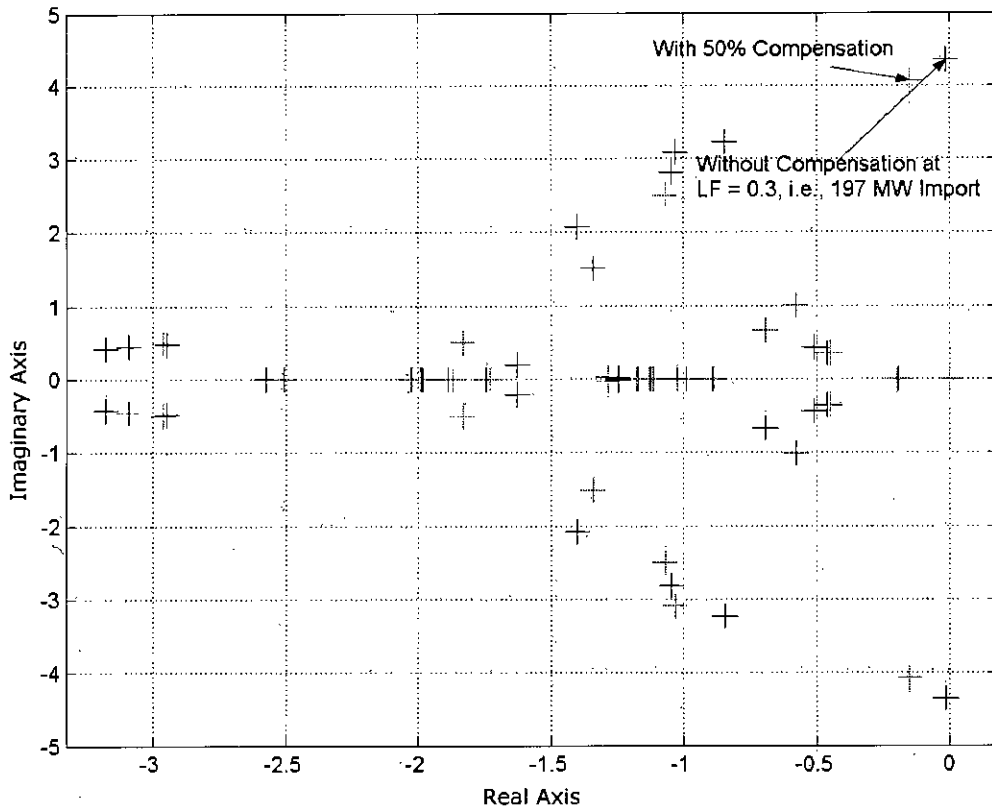
Fig. 3.12: Critical Eigenvalue without and with Compensation (Scenario-1)

Table 3.12 pin-points the position of critical eigenvalue as the level of compensation is varied; the loading factors correspond to the highest possible transfer with and without series compensation.

Table 3.12: Critical Eigenvalue with Different Level of Compensation (Scenario-1)

Level of Compensation	LF = 0.300 (197 MW)	LF = 0.420 (251 MW)
Uncompensated	-0.0154 + j 4.3459	-
50%	-0.1536 + j 4.0672	0.1044 + 4.3616
60%	-0.1582 + j 4.0412	0.0144 + j 4.2761
70%	-0.1615 + j 4.0196	-0.0369 + j 4.2093

It is observed that at LF = 0.42, even with 70% compensation, damping of the critical mode is 0.0088, i.e., much lower than 0.03. This is improved by deploying the dynamic controller. Root locus of the critical eigenvalue with variation of controller gain is shown in Figure 3.13. Controller parameters are given in Power System Data in Appendix B.
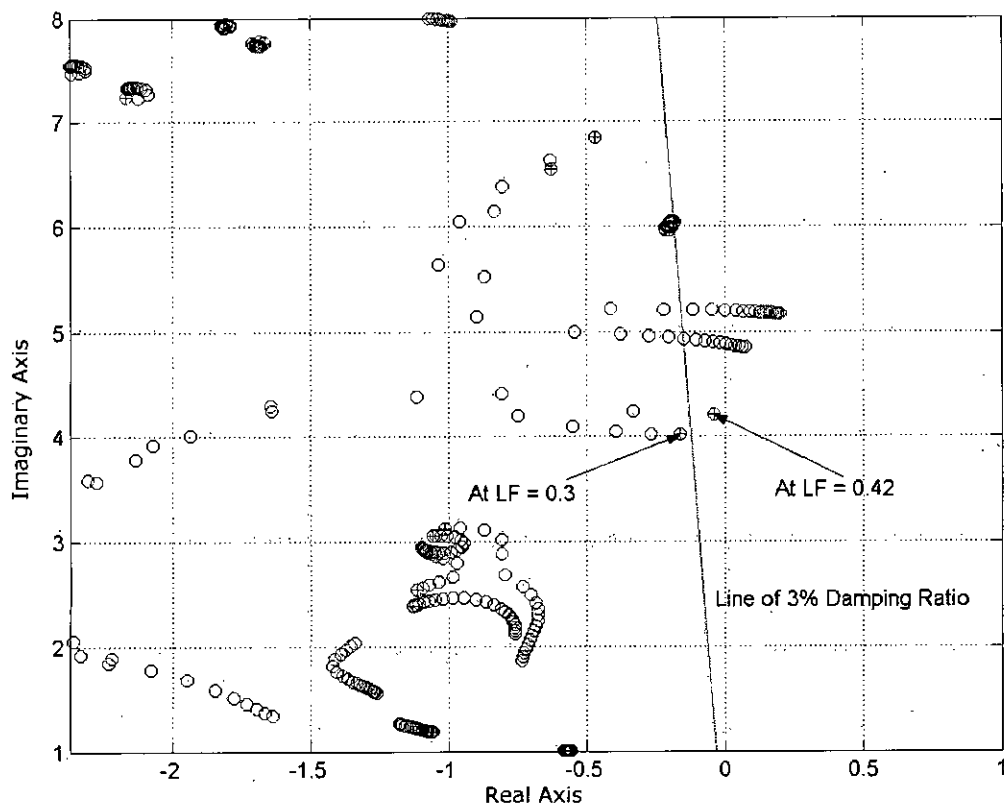
Fig. 3.13: Root Locus of Critical Eigenvalue of EWIS for Scenario-1

Root locus plot depicts, when system loading is 0.42, as the gain is varied beyond 40, one of the modes enters into the right half plane; magnitude of gain has been selected carefully to avoid this kind of difficulties.

Now a severe disturbance has been applied to test the system's transient stability. Two pre-fault operating conditions are simulated; one is with LF = 0.3 which corresponds to the highest possible transfer based on the dynamic stability limit of the uncompensated system and the other one is with LF = 0.42, which corresponds to the thermal limit of the line with highest degree of compensation.

The disturbance applied is a three phase fault at Ishurdi 132 kV bus with a subsequent tripping of small line serving an active load of 10 MW, modeled for the simulation purpose only. As observed before with the Two Area System, the dynamic compensator functions to provide highest level of compensation immediately upon the occurrence of the fault. Figure 3.14 shows the variations in level of compensation in the post fault period. The steady state compensation in the pre-fault system was 70% - it jumps steeply up to 80% immediately upon clearing the fault – and then varies dynamically to minimize the oscillation and aids the system state variables to the new equilibrium point. Voltage at Ishurdi bus, machine angle at

47

Banghabari and active power flow through the tie line have been plotted to show the systems transient performance [Figure 3.15 to 3.17].
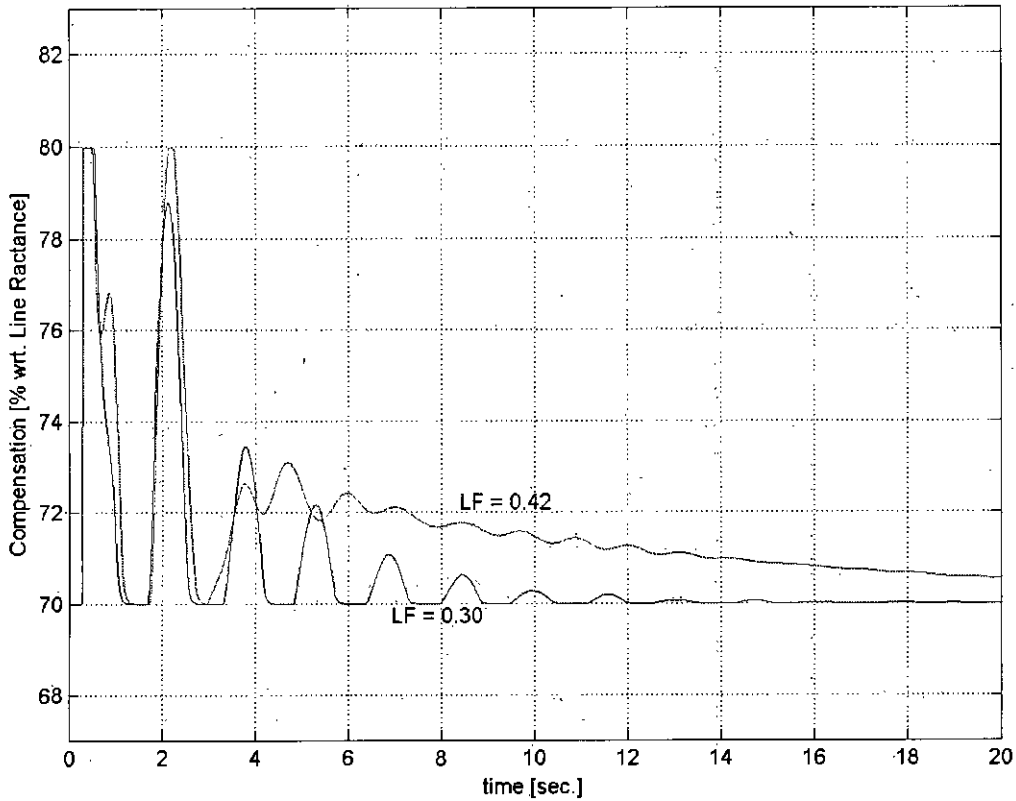
Fig. 3.14: Compensation with TCSC Controller in EWIS (Scenario-1)

Each of the plots contains transient simulation results for two loading levels; LF = 0.300 represents the maximum loading without series compensation. Improvement in transient performance with series compensation at this loading level is quite visual.. LF = 0.420 represents the maximum loading with 70% series compensation. The machine angle profiles in Fig. 3.16 shows the angle excursions in Bahgabari unit, as this is the largest machine near the faulted bus (Ishurdi 132 kV) and showed largest angle excursion.
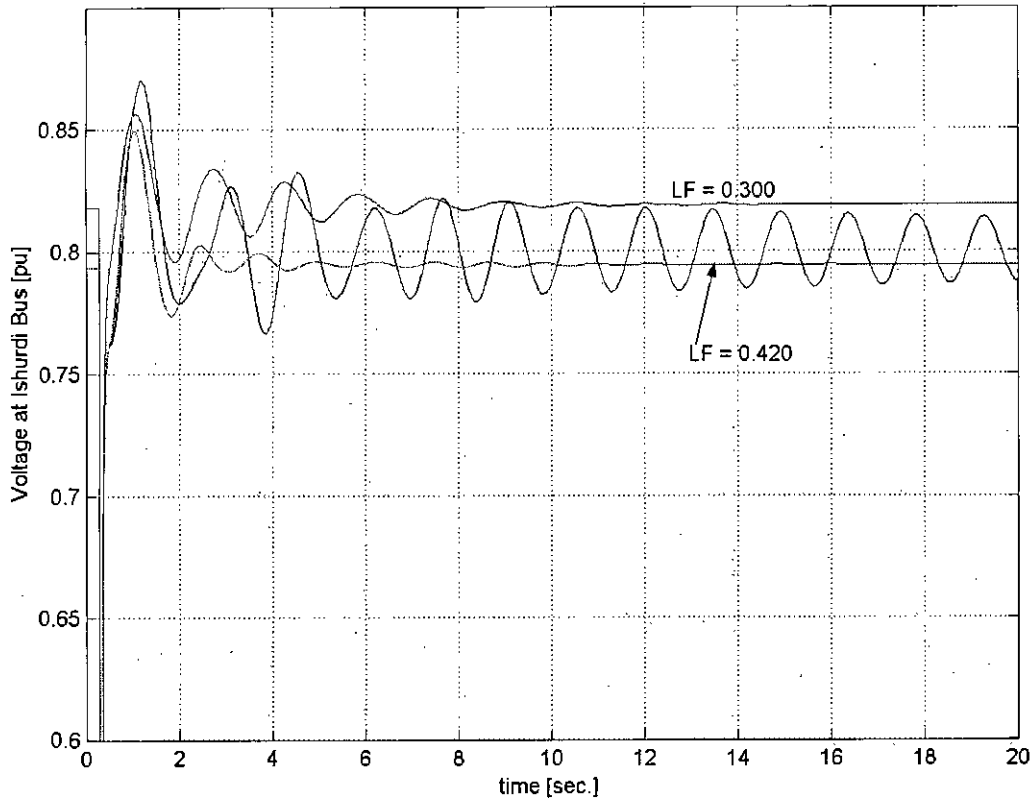
Fig. 3.15: Voltage Profile at Ishurdi Bus (Scenario – 1)
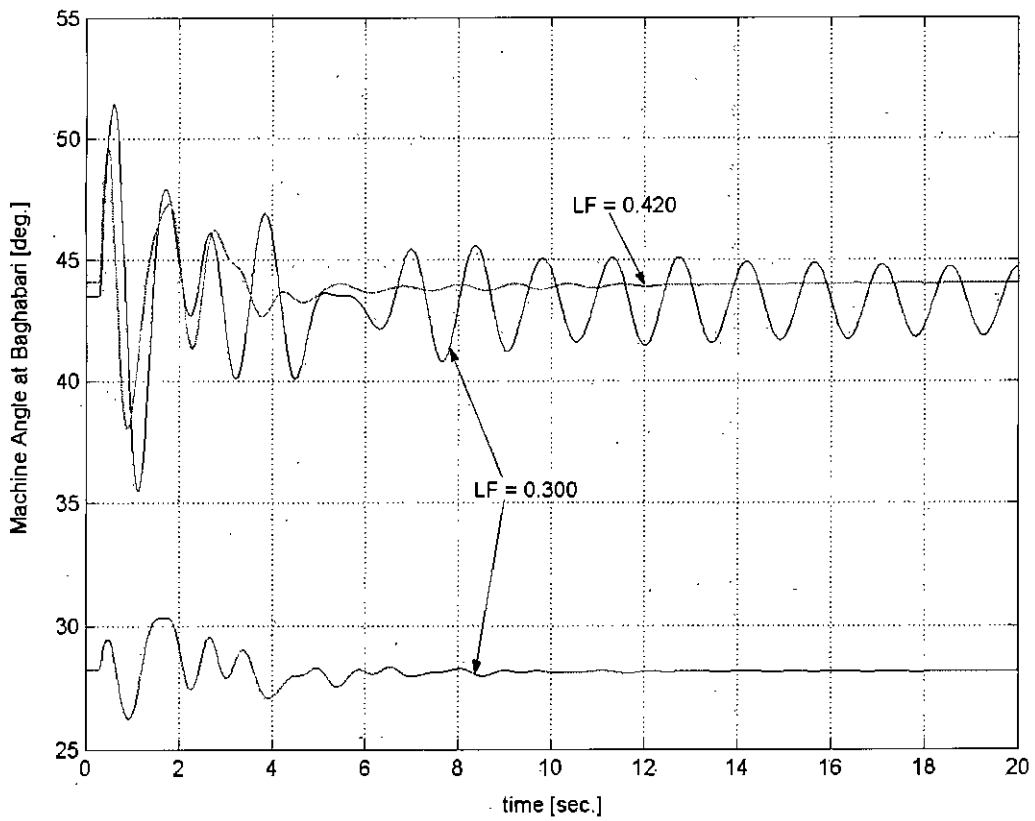
Fig. 3.16: Machine Angle at Baghabari (Scenario – 1)
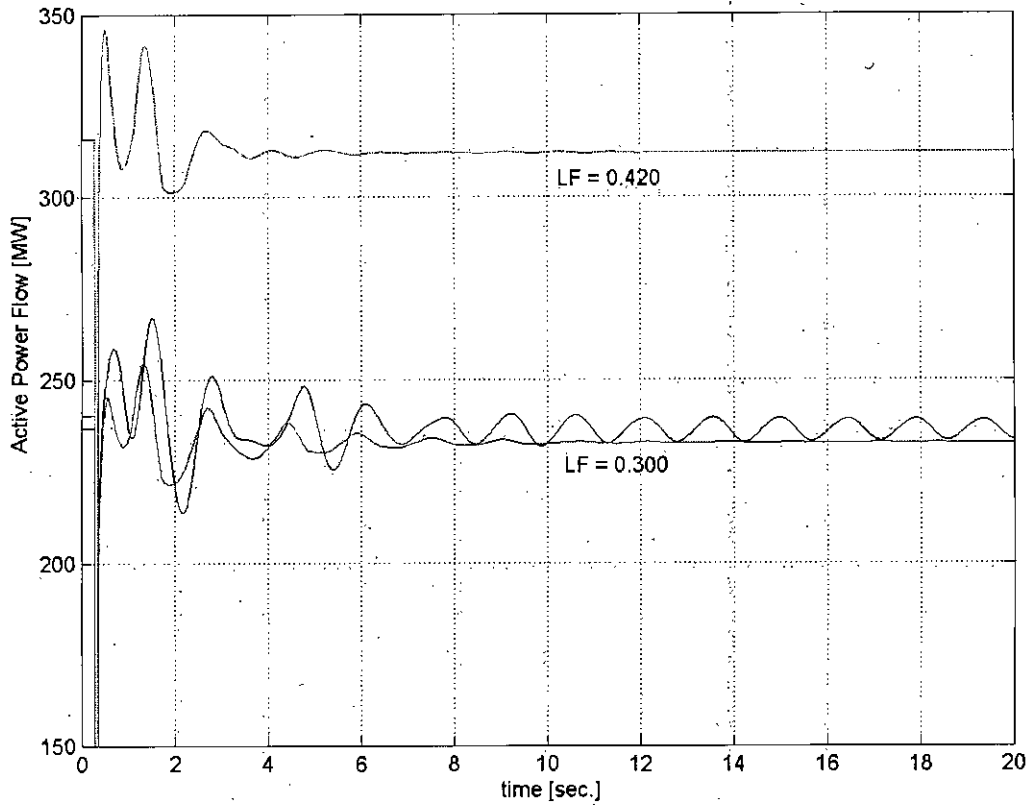
Fig. 3.17: Active Power Flow through EWI (Scenario – 1)

3.2.4 Analysis on the Approximate Model (Scenario-2)

For the system with two EWIs and with the new 230 kV lines, loading in west-grid has been increased gradually as before with Scenario-1 to reach the safe steady-state transmission angle limit and modal analysis has been performed in each case. It has been observed that at loading level of 386 MW [LF. 0.720], Hopf Bifurcation is triggered in the system, as shown in Fig. 3.18. Dynamic Loading Margin is hence considered to be limited at LF = 0.700, i.e., equivalent to 377 MW, where damping of the critical mode is 0.0018.
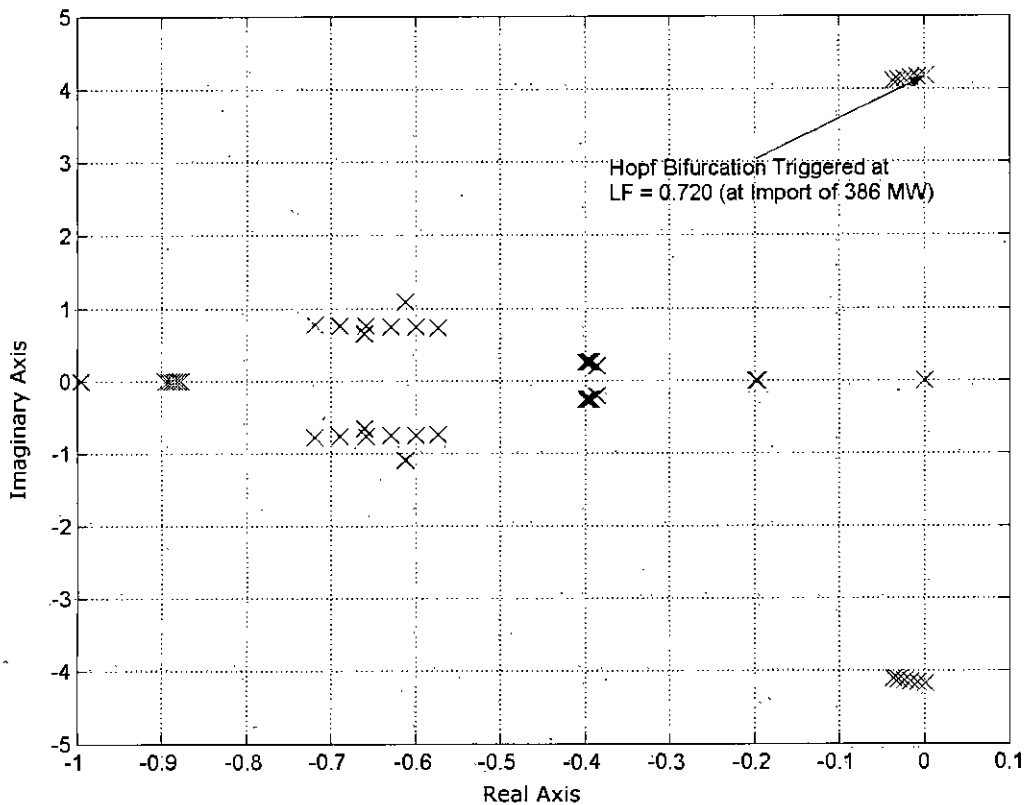
Fig. 3.18: Occurrence of Hopf Bifurcation in Scenraio – 2

At this transfer level, steady state results shown in Table 3.13 reveal that about 47% of thermal capacity in the first EWI and about 60% of the 2nd EWI is left unexploited if dynamic stability limit is to be considered.

Table 3.13: Steady State Conditions of EWIS without Compensation (Scenario-2)

Import Required to West Grid [MW]	Export to West Grid [MW + j MVAR]		Voltage at Ishurdi Bus [pu]		Transmission Angle [deg.]	
	*G-I	**A-S	I	S	G-I	A-S
377.00	165.32 + j 4.200	256.89 + j 4.090	0.8370	0.8542	17.82	15.30

*Ghorasal-Ishurdi
**Ashuganj-Sirajganj
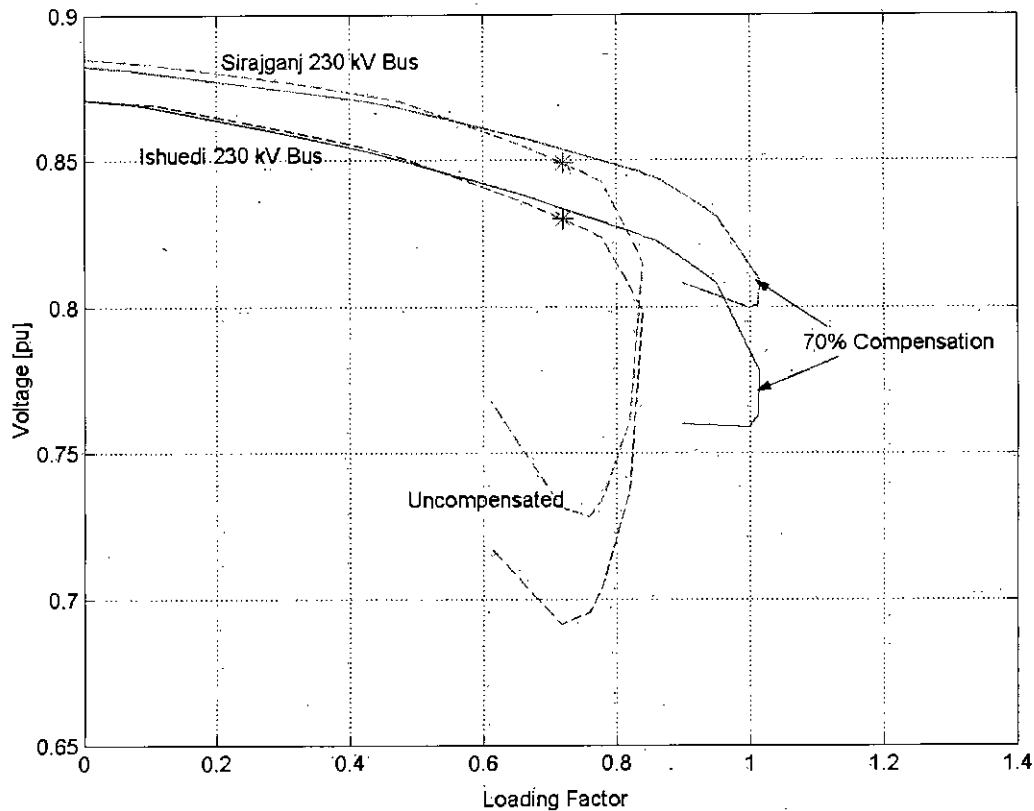
Fig. 3.19: Bifurcation Diagram for Scenario – 2

Transmission angle and receiving end voltage is satisfactorily within the safe operating limits. As before, bifurcation analyses have been performed on the system. For this scenario, results shown are only for 70% compensation. Table 3.14 provides a summary of the loading margins.

Table 3.14: Loading Margins of EWIS with and without Compensation (Scenario-2)

Level of Compensation	Static Loading Margin (SLM)	Dynamic Loading Margin (DLM)
Uncompensated	0.838 (439 MW)	0.700 (377.0 MW)
70%	1.0134 (518 MW)	–

In the 70% compensated system, no Hopf Bifurcation occurs in the entire operating range – transfer is only limited by SNB or voltage collapse point. Though the modal and transient analyses for Scenario-2 have been performed by operating the compensated system at LF = 1.0134, in actual practice this would not be "safe" as an incremental increase in the loading will drive the network into voltage collapse and hence, it would be necessary to keep a margin before this limit.

Table 3.15: Steady State Conditions of EWIS with 70% Compensation (Scenario – 2)

Import Required to West Grid [MW]	Export to West Grid [MW + j MVAR]		Voltage at Receiving Bus [pu]		Transmission Angle [deg.]	
	G-I	A-S	I	S	G-I	A-S
377.00	184.31 – j 28.10	238.61 – j 37.11	0.8386	0.8567	6.60	9.85
518.00	266.98 + j11.72	343.94 + j 46.69	0.7970	0.8213	9.01	6.05

Position of critical eigenvalue is exactly shown in Table 3.16 which reveals that for 70% compensation, the shift into the left half plane along real axis is about 6.5 times of the initial position and the damping ratio increases from 0.18% to 1.25%.

Table 3.16: Critical Eigenvalue of EWIS with 70% Compensation (Scenario-2)

Level of Compensation	LF = 0.700 (377 MW)	LF = 1.0134 (518 MW)
Uncompensated	-0.0077 + j 4.1558	-
70%	-0.0505 + j 4.0398	0.1044 + 4.3616
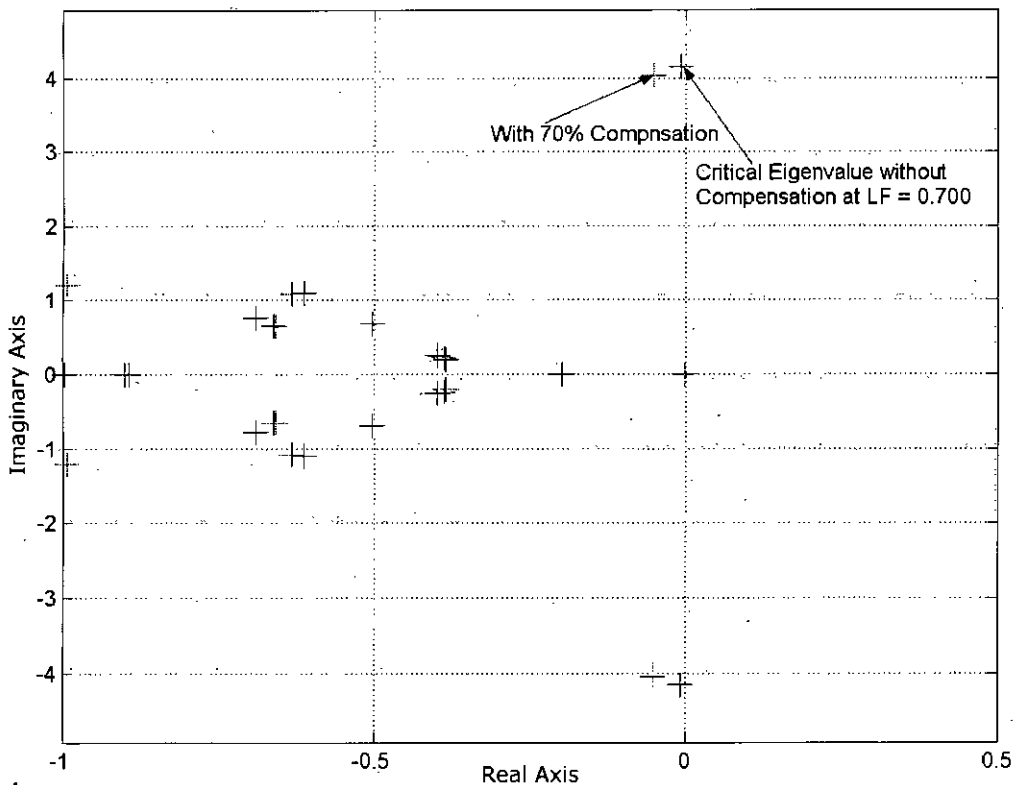
Fig. 3.20: Position of Critical Eigenvalue in Scenario - 2

Action of the damping controller associated with TCSC shifts the critical eigenvalue more into the left half plane and aids to exceed the threshold of 3%.

Root locus of the critical eigenvalue with the controller gain variation is presented in Figure 3.21 for LF = 0.700 and LF = 1.0134, which are the highest possible loading without and without TCSC, respectively. Shift of eigenvalue has been observed to be more with higher loading for the same range of gain and is attributed to higher controllability of the TCSC to the critical mode, similar to the Two Area System.
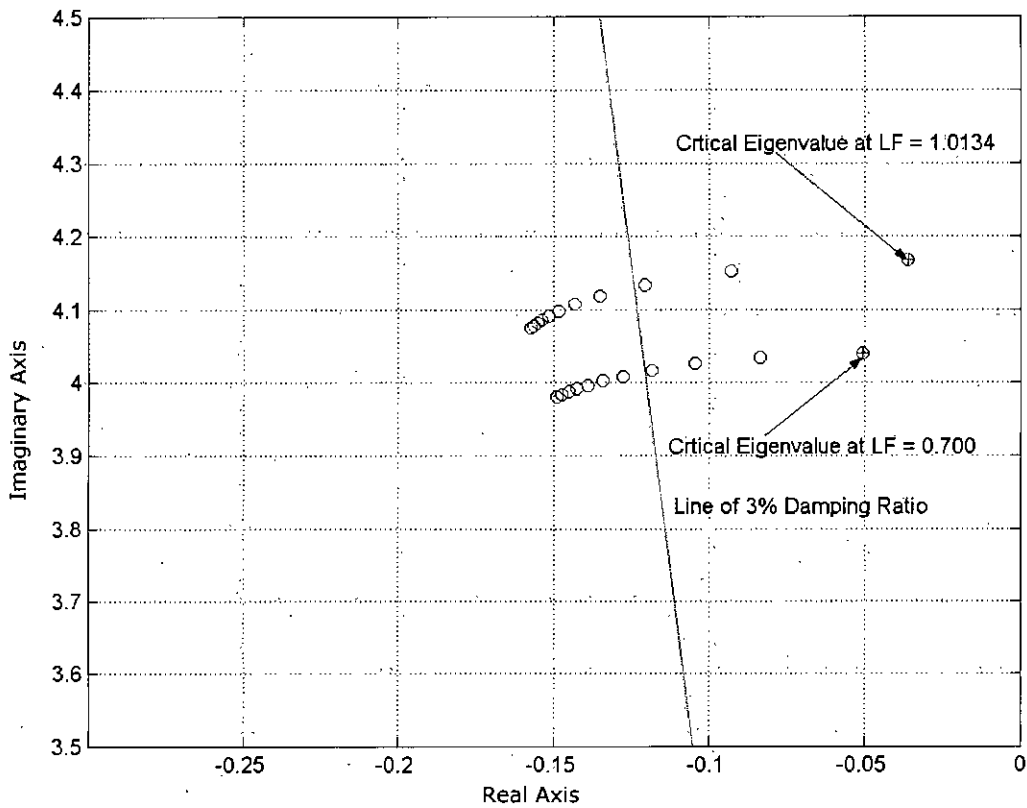
Fig. 3.21: Rootlocus of Critical Eigenvalue with TCSC Controller Gain (Scenario – 2)

Time-domain simulation profiles in the Figures 3.22 to 3.25 reveal the improvement in transient performance. Similar to Scenario-1, simulation results for maximum loading without (LF = 0.700) and with (LF = 1.0134) compensation has been presented. Active power flow through both of the interconnections has been presented.
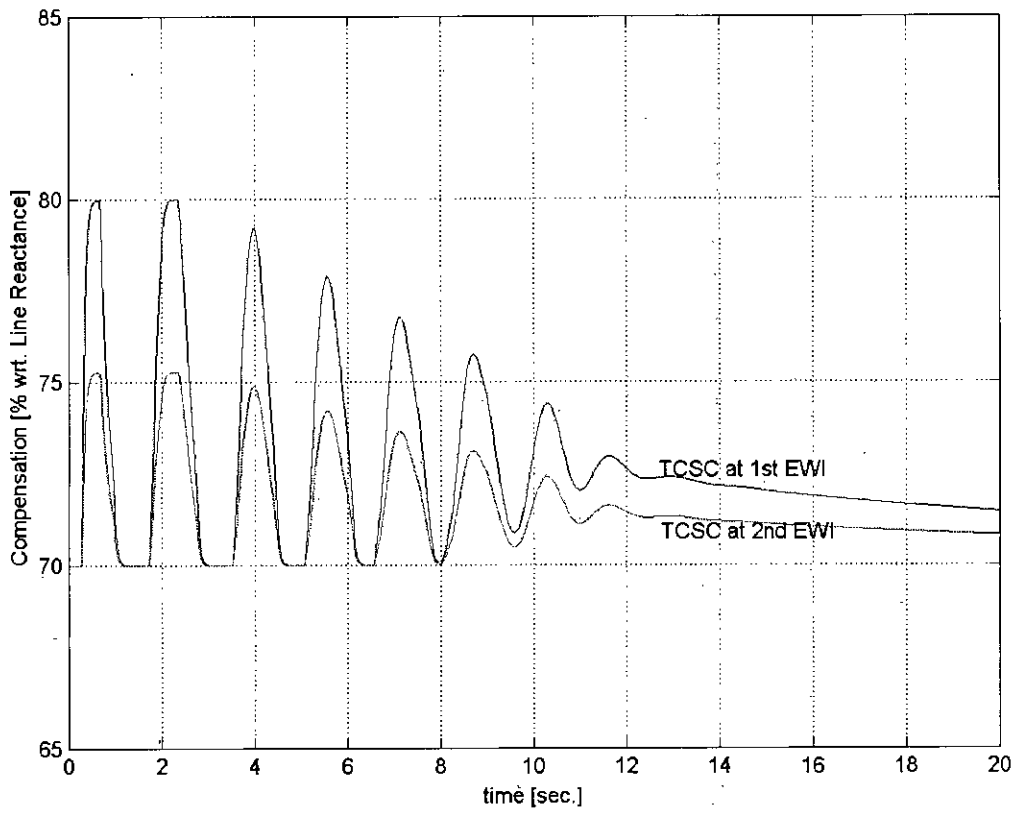
Fig. 3.22: Compensation with TCSC Controller (Scenario-2)
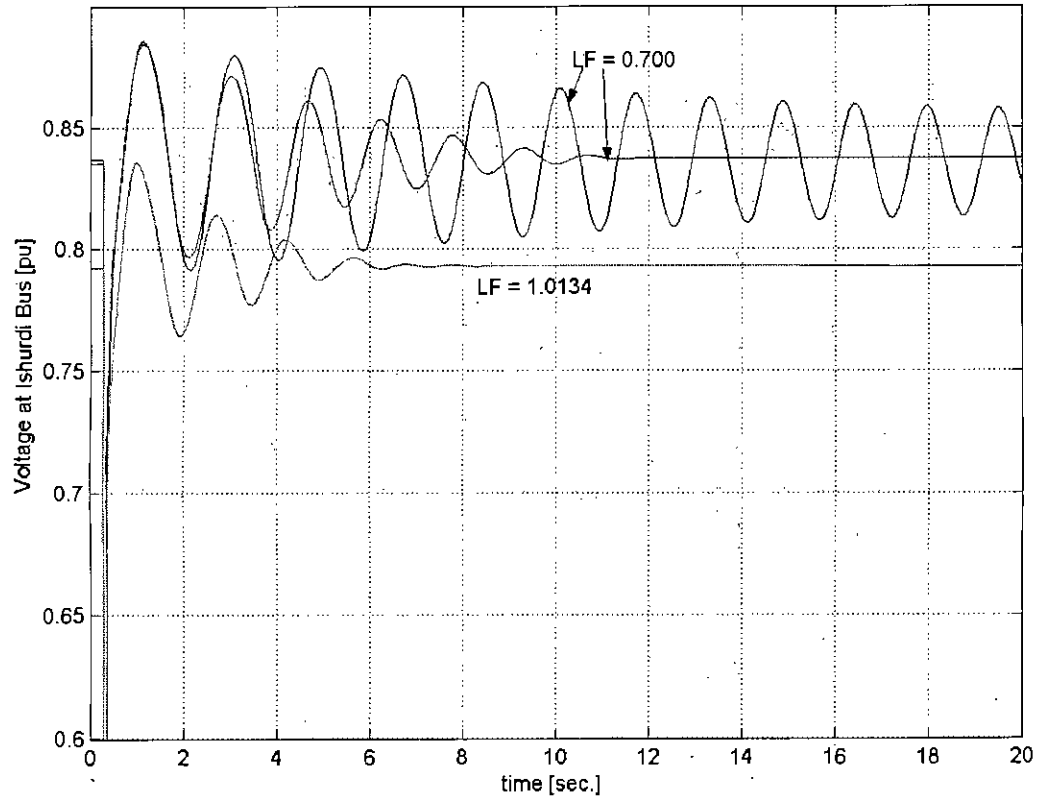
Fig. 3.23: Voltage Profile at Ishurdi Bus (Scenario – 2)
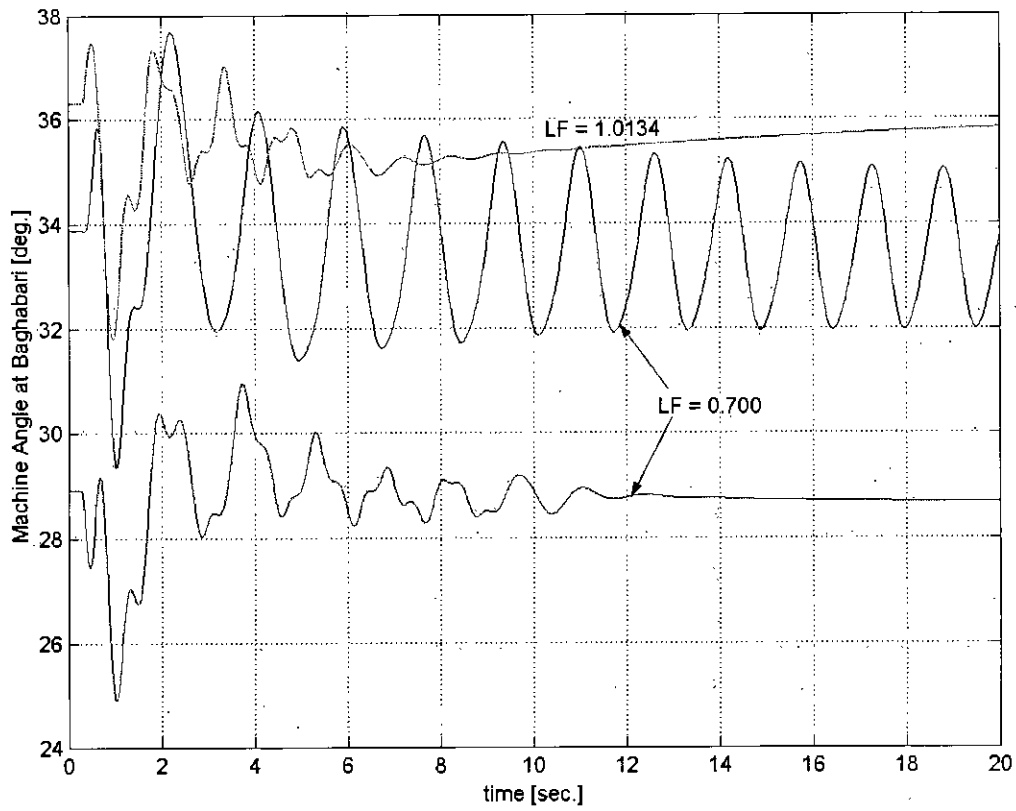
Fig. 3.24: Machine Angle at Baghabari (Scenario – 2)
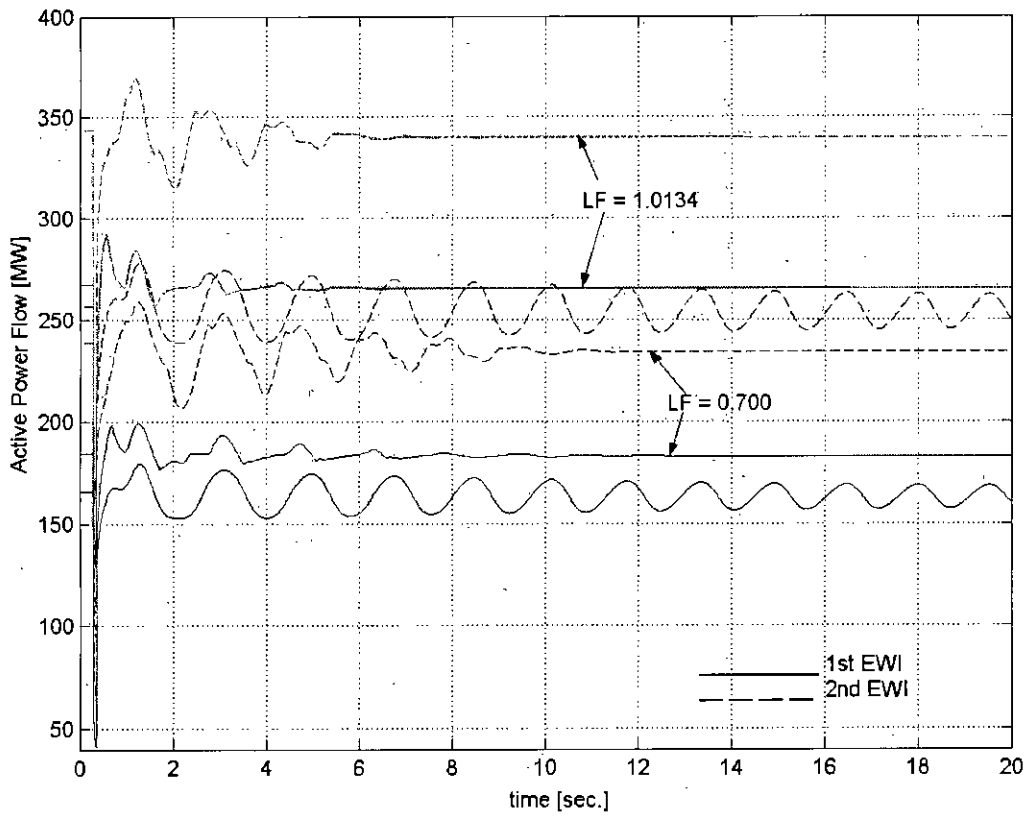
Fig. 3.25: Active Power Flow through EWIs (Scenario – 2)

56

3.2.5 Summary of Capacity Enhancement (Scenario-2)

From the static, dynamic and transient analyses performed above it is understood that introducing series compensation enhances the power transmission capability of EWI, though full thermal capacity is yet to be exploited due to limitations resulting from adequate reactive power reserve and low voltage.

Based on the sending end voltage used in this work (200 kV) and ampacity of the conductor [1], thermal rating of the 1st and 2nd EWI is approx. 315 MVA and 630 MVA respectively. Based on the steady state data presented in Table 3.15, even with the highest level of series compensation, 15% capacity of the 1st EWI and 45% capacity of the 2nd EWI are left unused; beyond this loading limit the system encounters voltage collapse. Though in Table 3.17, SLM of the 70% compensated system has been shown as LF = 1.0134, the actual limit for safe operation is kept slightly lower with 1% margin, i.e., LF =1.00, i.e., equivalent to 512 MW import.

Table 3.17 provides a summary of transmission capability improvement by applying series compensation. The MW values shown are in terms of double circuit operation.

Table 3.17: Capacity Enhancement of EWIS by Series Compensation (Scenario-2)

Cause of Limitation	Uncompensated System [MW]	70% Compensated System [MW]	Enhancement [%]
Voltage Collapse (SNB)	878	1024	16.62
Oscillatory Instability (HB)	754	1024	35.80

It is to be noted that system enhancement at 132 kV, 33 kV or at distribution level might be required to deliver this additional amount of power to the load centers, in order to keep bus voltage and line currents below the operational constraints and thermal limits.

Simple Financial Analysis

This Chapter provides a financial appraisal of series compensation project for East-West Interconnectors of Bangladesh Power System network in a simplistic manner. Adequacy of transfer capacity of the compensated lines in context with the existing Power system Master Plan has also been studied.

4.1 Sufficiency of Transfer Capacity

To study the sufficiency of transfer capability of the series compensated transmission corridor to serve peak import requirement from Eastern to Western Grid of BPS, load and generation forecast data available from [36] was compared with Table 3.17, which shows the maximum possible active power import to west grid through the series compensated lines.

Table 4.1: Generation and Load Forecast Data in West Grid

Year	Total Generation in West Grid [GWh]	Capacity in West Grid [MW]*	Peak Load [MW]	Peak Import [MW]
2010	8,129	1237	1588	351
2011	8,801	1340	1718	378
2012	9,528	1450	1858	408
2013	10,315	1570	2010	440
2014	11,167	1700	2174	474
2015	12,089	1840	2352	512
2016	12,996	1978	2527	549
2017	13,971	2126	2714	588
2018	15,019	2286	2914	628
2019	16,145	2457	3131	674
2020	17,356	2642	3362	720
2021	18,526	2820	3587	767
2022	19,776	3010	3825	815
2023	21,109	3213	4080	867
2024	22,532	3430	4351	921
2025	24,052	3661	4641	980

Based on 75% average plant factor

As per 2007-2008 Annual Report of BPDB [56], many of the larger units in Western Region have been found to run at more than 70% plant factor, except Barapukuria, for which plant factor was found 60.83%. Provided the units are maintained with prudent utility practices and

operation is not hindered due to unavailability fuel, plant factor higher than the existing should be achievable. In this work, calculation of Peak Import in Table 4.1 has been performed assuming 75% annual average plant factor.

As seen from Table 4.1, thermal capacity of the corridor is more than sufficient for serving peak load up to 2025. But due to the dynamic stability limitation presented in Table 3.17, the uncompensated system is not able to transfer beyond 754 MW, i.e., which is below the peak import required in Year 2021, whereas the transfer limit of 70% series compensated lines is higher than peak import of Year 2025.

4.2 Financial Feasibility

Benefit-Cost Ratio approach, as defined in [57], has been used for determining financial feasibility of the project. Further, a Simple Payback Period [57] method has been used for finding the time required for the financial benefit to be equal to the investment.

$$\text{Benefit - Cost Ratio} = \frac{\text{Present Worth of Benefits}}{\text{Present Worth of Cost}}$$

$$= \frac{EAB\left[\dfrac{(1+i)^n - 1}{i(1+i)^n}\right]}{PC} \qquad \text{[Eqn. 4.1]}$$

EAB = Estimated Annual Benefit

i = Interest Rate (%)

n = Project Life (Years)

PC = Project Cost

$$\text{Simple Payback Period} = \frac{\text{Investment}}{\text{Annual Benefit}} \qquad \text{[Eqn. 4.2]}$$

4.2.1 Project Cost Estimation

For determination of indicative cost for installing controlled series compensation in both of the interconnections, cost data provided in [45] has been used. The following assumptions have been made for financial modeling of the project.

- Total amount of series compensation for each line has been split into fixed and variable part.

- Fixed part has been estimated as 78.5% of the total compensation, i.e., 55 % compensation has been assumed to be implemented with fixed series capacitor and

rest 12.5 % has been assumed to come from the controlled portion. These proportions have been assumed from guidelines provided by equipment manufacturers [58]. With a boost factor of 1.2 at nominal operation [3], this will provide 15% compensation and hence will produce a total steady state compensation of 70%.

- Thermal rating for the capacitors for 1st EWI has been assumed equal to the amapcity the conductors whereas for the 2nd EWI it has been assumed lower (1.2 kA), as load flow studies indicated that even at with highest possible transfer with series compensation, current through the line is about 1.03 kA, about 56.7% of the ampacity. Hence, estimating the series compensation for full thermal capacity seems not be an economic choice at this moment. However, as per practical project experience, provisions can be kept to expand the thermal capability without considerable modification in control and protective scheme [12].

- TCSC will be installed at the receiving end substations, i.e., at Ishurdi substation for 1st EWI and at Sirajganj substation for the 2nd EWI to save additional substation and infrastructural costs.

Table 4.2: Series Compensation Project Cost

Line Reactance Ghorashal-Ishurdi (Ohm)	72.5259
Rated Current (Amps)	910
Line Reactance Ashuganj-Sirajganj (Ohm)	40.733
Assumed Rated Current (Amps) [actual rating: 1800 A]	1200
Fixed Compensation	55%
Variable Compensation	15%
Physical Capacitance Required with 1.2 Boost Factor	12.5%
Cost of FC (USD/MVAR)	20000
Cost of VC (USD/MVAR)	40000
Fixed Compensation in Ghoralshal-Ishurdi Line (MVAR)	198
Variable Compensation in Ghoralshal-Ishurdi Line (MVAR)	45
Fixed Compensation in Ashuganj-Sirajganj Line (MVAR)	194
Variable Compensation in Ashuganj-Sirajganj Line (MVAR)	44
Total Compensation in Ghorasal-Ishurdi Line (MVAR)	243
Total Compensation in Ashuganj-Sirajganj Line (MVAR)	238
Total (MVAR)	481
Cost of Compensation (USD)	11,396,565
Cost of Compensation (BDT)	790,921,605

4.2.2 Operating Cost

Operation and maintenance cost for this project is negligible as no additional workforce will be required – manpower at the existing substations can be used to operate and maintain the equipment. Yet, for the purpose of modeling, an annual O&M budget of BDT 10 million has been considered.

4.2.3 Financial Benefit and Feasibility Analysis

Determination of financial benefit from a series compensation project depends highly on the prevailing scenario of electricity industry, where the project is being installed. For instance, if such a project can enhance transmission capability of a system to carry additional hydro power to the load center and hence avoid thermal generation costs, the financial benefit may be highly attractive in comparison to the cost – a practical experience from Venezuelan EHV grid shows a benefit-cost ratio of 17 for such a project [5]. For BPS, generation is mostly thermal all over the grid and can not be justified by such comparison. However, the following three sources of financial benefit, common for a FACTS project [59], match with the BPS context.

A.   Profit from Additional Energy Sales

Studying some recent power generation project financial models, it is apparent that a net profit of BDT 0.3 or more can be achieved from per unit sale of electricity. As a conservative approach, it has been assumed as 0.25 BDT.

B.   Revenue from Additional Wheeling Charge

Per unit wheeling charge is assumed as 0.23 BDT at 230. In order to be conservative in estimating financial benefits, calculation of additional units wheeled and sold has been performed based on 50% utilization of maximum transfer capacity of the compensated lines.

C.   Delaying of Investment for New Transmission Line

From Table 4.1, it is observed that by installing series compensation project, investment for new line can be delayed for about 5 years. At 12% interest rate, the cost of compensation is recovered in 2.71 years solely from the money available from the interest.

Table 4.3: Simple Financial Analysis

Profit from Electrical Energy Sales (BDT/kWh)	0.25
Charge for per unit wheeling (BDT)	0.23
Cost of 230 kV Line (BDT)	2,429,000,000
Annual Avg. Additional Units Transferred (kWh)	1182600000
Profit from Additional Sales (BDT)	295,650,000
Revenue from Additional Energy Wheeling (BDT)	271,998,000
Annual Interest from Cost of Additional 230 kV Line @ 12% Interest	291,480,000
Total Financial Benefit from Additional Units and Investment Delay	859,128,000
Annual Avg. O&M Cost (BDT)	10,000,000
Annual. Operating Benefit (BDT)	849,128,000
Interest Rate	12%
Project Life Cycle (Years)	5
Benefit-Cost Ratio	3.87
Years for Payback (without considering Time Value)	0.931

As seen from Table 4.3, the series compensation project has a benefit-cost ratio of 3.87 and simple payback period of less than one year.

Conclusion

Though operation of transmission system in Bangladesh is still a state owned monopoly and the stringent commercial competition existing in typical deregulated environment is yet to be experienced in this region, the importance of installing series compensation is still justifiable due to the benefits achieved from exploitation of the unused thermal capacity, improvement in steady state, dynamic and transient stability and above all the operational flexibility. This thesis investigates the effect of applying controlled series compensation on both 1st and 2nd EWIs and also analyzes the economic feasibility of the project in a very basic manner.

5.1 Conclusion

5.1.1 Observations

Reducing electrical length of a line by applying series compensation has considerable positive effect on power transmission capability of interconnections among utilities or regions of a power system. A standard Two Area test system has been chosen as a test bed before entering into the approximate model of BPS network. For finding out the maximum transmission capability of the compensated system, 70% series compensation has been applied, which is considered as the highest level. The improvement in loading margin is about 20% than the uncompensated system. Steady state transmission angle limit has also been considered for this system and found to be lower in the compensated system.

Unavailability of required modeling and operational data has been the basic limitation in working with EWIS. Approximate model has been created based on available data from PGCB and the base case has been set up principally based on the network behavior during approx. 200 MW real power injection into the Ishurdi node. Dynamic data has been chosen / set up so that the system behaves in a typical manner.

The analyses have been performed by setting up two scenarios – one with single interconnection and the other with both the old and the new one; the newly commissioned 230 kV lines in western grid have also been included in the latter scenario. Transmission angle has not been found as a limitation for the EWIS; oscillatory stability related issues

appeared before reaching the transmission angle limit. SLM and DLM of the system without compensation have been compared with the ones with compensation. For the system with single tie line, analyses have been performed with the level of compensation starting from 50% to 70% step-by-step, whereas for system with two tie lines, 70% compensation level has been applied initially as the intension is to determine maximum possible transfer with highest compensation. In the system with old and new interconnection, 16% improvement in SLM and 35% improvement in DLM have been observed as a result of applying 70% series compensation.

Load and generation forecast provided in Power System Master Plan [36] has been studied to observe the sufficiency of compensated tie lines' capacity in the planning horizon. As per the "base case" forecast in [36] and Table 3.17 in Chapter 3, DLM of the uncompensated system is lower than the peak import requirement of Year 2021, whereas the loadability of 70% compensated system is higher than peak import level of 2025.

Economic feasibility of the series compensation project has been studied based on typical cost data. Total amount of compensation has been split into fixed and variable parts – proportions have been determined based on typical design recommendations from the manufacturers. Pay back period has been found less than one year and benefit-cost ratio has been found more than 3.8, based on a 5 years project life and 12% interest rate, and identifies the project as a feasible one.

It is noteworthy that, as stated before, all of the analyses on EWIS in this work have been performed with limitations in availability of system data, the results may deviate from that with accurate and actual data. Yet, based on the conservative approach in assumptions, the basic finding, i.e., the possibility of transmission capacity enhancement and higher utilization of thermal capacity by series compensation, is supposed to remain unaffected.

5.1.2   Contribution of the Work

Commercial electric utilities world wide conduct extensive studies to ensure maximum utilization of the installed infrastructures to sustain the profitability and future growth. Application of advanced analytical techniques has not been in wide use in the planning and operation of BPS network. As a consequence, system planners and operators are not always equipped with the required information to plan and operate the system with prudent utility practices and standards.

Though this work principally aims to study the possibility of transmission capacity enhancement by applying controlled series compensation on the tie lines between East and West region of BPS and hence to propose a way for exploiting the unused thermal capacity of the corridor, additionally this work will serve as a sample study in assessing static and dynamic status of the network at different operating points and also to have an idea of the maximum loadabilty of the system, which provides with valuable information for expansion planning.

5.2 Future Research Suggestions

- This work has been performed with limitation on the availability of adequate system modeling data and operational records of BPS network. Further research may be conducted to tune the dynamic models to capture more accurate dynamic behavior of the BPS network. The model can also be extended into a detailed one by splitting the aggregated loads and generations according to actual distribution, incorporating the tapped areas etc.

- Several shunt compensation devices are in the process of installation at different 132 kV nodes in the western grid, which have not been considered in this work. These will eventually increase the loadability of the system. Studies may be conducted to find out the ultimate maximum transfer capability with both series compensation and shunt compensation. Co-ordination of the control schemes for series and shunt compensation in power system stabilization is another important scope of further research.

- Appearance of Sub-Synchronous Resonance (SSR) is a phenomenon experienced in systems with series compensation; and TCSC schemes are used to mitigate this. Study of SSR in the context of BPS network presents an option for future research.

Bibliography

[1] J. Duncan Glover, Muluktla S. Sarma and Thomas J. Overbye, *Power Systems Analysis and Design (4th Edition)*, Thomson Learning Inc. Chapter-5, pp. 227-279

[2] C. A.Canizares, A. Berizzi and P. Marannio, *Using FACTS Controllers to Maximize Available Transfer Capability*, Bulk Power Systems Dynamics and Control IV – Restructuring, August 24-28, 1998, Santorini, Greece, pp. 633-641

[3] Matt Matelle, ABB Power Systems AB, *Enhancing of Transmission Capability of Power Corridors by means of Series Compensation*, IEEE PES PowerTech Conference, October 1999, Mumbai, India, available at: library.abb.com

[4] R. Grünbaum, J. Ulleryd, *Grid Flexibility, FACTS: Novel Means for Enhancing Power Flow*, available at library.abb.com

[5] N. Sandoval, A. Molina, A. Petersson, G. Stroemberg, J. Samuelsson, *Introduction of Series Capacitors in the Venezuelan EHV-grid*, IEEE PES Transmission and Distribution Conference and Exposition Latin America, Venezuela, 2006

[6] R. E. Marbury, J. B. Owens, *New Series Capacitor Protective Device*, AIEE Transactions Vol. 65, March 1946, pp. 142-145

[7] J. W. Butler, C. Concordia, *Analysis of Series Capacitor Application Problems*, AIEE Transactions, June 1937, pp. 975-988

[8] E. C. Starr, R. D. Evans, *Series Capacitors for Transmission Circuits*, AIEE Transactions Vol. 61, May 1942, pp. 963-973

[9] A. A. Johnson, *Application of Capacitors to Power Systems*, Electrical Transmission and Distribution Reference Book (4th Edition), Westinghouse Electric Corporation, 1950 (Indian Edition), pp. 256-257

[10] S. B. Crary, L. E. Saline, *Location of Series Capacitors in High Voltage Transmission Systems*, AIEE Transactions, December 1953, pp. 1140-1151

[11] B. S. A. Kumar, K. Parthasarathy, F. S. Prabhakara, H. P. Khincha, *Effectiveness of Series Capacitors in Long Distance Transmission Lines*, IEEE Transactions on Power Apparatus and Systems, Vol. PAS-89, No. 5/6, May/June. 1970, pp. 941-951

[12] J. A. Maneatis, E. J. Hubacher, W. N. Rothenbuhler, J. Sabath, *500 kV Series Capacitor Installations in California*, IEEE Summer Power Meeting and EHV Conference, Los Angeles, July 12-17, 1970; pp. 1138-1149

[13] E. W. Kimbark, *Improvement of System Stability by Switched Series Capacitor*, IEEE Transactions on Power Apparatus and Systems, Vol. PAS-85, Feb. 1966, pp. 180-188

[14] N. G. Hingorani, *High Power Electronics and Flexible AC Transmission System*, IEEE Power Engineering Review, July 1988, pp. 3-4

[15]   N. G. Hingorani, L. Gyugyi, *Understanding FACTS: Concepts and Technology of Flexible AC Transmission Systems,* IEEE Press, 2000, Chapter-1, pp. 3

[16]   R. L. Hauth, *Reactive Power Compensation and the Dynamic Performance of Transmission Systems,* Reactive Power Control in Electric Systems, John Wiley & Sons, Inc., 1982, Chapter-3, pp. 129-180

[17]   T. J. E Miller, R. W. Lye, *Principles of Static Compensators,* Reactive Power Control in Electric Systems, John Wiley & Sons, Inc., 1982, Chapter-4, pp. 181-220

[18]   N. Christl, R. Hedin, R. Johnson, P. Krause, A. Montoya, *Power System Studies and Modeling for Kayenta 230 kV Substation Advanced Series Compensation,* International Conference on AC and DC Power Transmission, September 1991, pp. 33-37

[19]   J. J. Paserba, N. W. Miller, E. V. Larsen, R. J. Piwko, *A Thyristor Controlled Series Compensation Model for Power System Stability Studies,* IEEE Transactions on Power Delivery, Vol. 10 No. 3 July 1995, pp. 1471-1478

[20]   S. G. Jalali, R. Hedin, R. Johnson, M. Pereira, K. Sadek, *A Stability Model for the Advanced Series Compensator,* IEEE Transactions on Power Delivery, Vol. 11 No. 2 April 1996, pp. 1128-1137

[21]   Z. Xu, G. Zhang, H. Liu, *Controllable Impedance Range of TCSC and Its TCR Reactance Constraints,* Power Engineering Society Summer Meeting, 2001, Vol. 2, pp. 939 – 943

[22]   J. F. Gronquist, W. A. Sethares, F. L. Alvarado, R. H. Lasseter, *Power Oscillation Damping Control Strategies for FACTS Devices Using Locally Measurable Quantities,* IEEE Transactions on Power Systems, Vol. 10 No. 3 August 1995, pp. 1598-1605

[23]   M. E. Aboul-Ela, A. A. Salam, J. D. McCalley, A. A. Fouad, *Damping Controller Design for Power System Oscillations Using Global Signals,* IEEE Transactions on Power System, Vol. 11 No. 2 May 1996, pp. 767-773

[24]   A. D. Rosso, C. A. Cañizares, V. Quintana, and V. M Doña., *Stability Improvement Using TCSC in Radial Power Systems,* Proceedings of the North American Power Symposium *(NAPS),* Waterloo, ON, October 2000, pp. 12-32 - 12-39

[25]   A. D. Rosso, C. A. Cañizares, V. M. Doña, *A Study of TCSC Controller Design for Power System Stability Improvement,* IEEE Transactions on Power Systems, Vol. 18, No. 4, November 2003, pp. 1487-1496.

[26]   L. Rouco, F. L. Pagola, *An Eigenvalue Sensitivity Approach to Location and Controller Design of Controllable Series Capacitors for Damping Power System Oscillations,* IEEE Transactions on Power Systems, Volume 12, Issue 4, Nov. 1997, pp. 1660 - 1666

[27] IEEE/CIGRE Joint Task Force on Stability Terms and Definitions, *Definition and Classification of Power System Stability*, IEEE Transactions on Power Systems, Vol. 19, No. 2, May 2004, pp. 1387-1401.

[28] C. A. Canizares, Z. T. Faur, *Analysis of SVC and TCSC Controllers in Voltage Collapse*, IEEE Transactions on Power Systems, Vol. 14, No. 1, February 1999, pp. 158-165.

[29] C. A. Canizares, *On Bifurcations, Voltage Collapse and Load Modeling*, IEEE Transactions on Power Systems, Vol. 10, No. 1, February 1995, pp. 512-522

[30] I. Dobson, S. Green, R. Rajaraman, C. L. DeMarco, F. L. Alvarado, M. Glavic, J. Zhang R. Zimmerman, Electric *Power Transfer Capability: Concepts, Applications, Sensitivity and Uncertainty*, PSERC Publication 01-34, November 2001

[31] P. Kundur, *Power System Stability and Control*, McGraw-Hill, New York, 1994

[32] P. M. Anderson, A. A. Fouad, *Power System Control and Stability*, The Iowa State University Press, Ames, Iowa, USA; Indian English Language Edition, 1984

[33] Energy Development and Power Generation Committee, IEEE Power Engineering Society, *IEEE Recommended Practice for Excitation System Models for Power System Stability Studies*, IEEE Std. 421.5-2005, April 2006

[34] Graham Rogers, *Power System Oscillations*, Kluwer Academic Publishers 2007

[35] Hadi Sadat, *Power System Analysis*, Tata McGraw-Hill Edition 2002

[36] Nexant, *Power System Master Plan Update 2005*, Ministry of Power, Energy & Mineral Resources, Asian Development Bank TA No. 4379–BAN: Power Sector Development Program II, Component B, Section-3

[37] E. Acha, V. G. Agelidis, O. Anaya-Lara, T. J. E. Miller, *Power Electronic Control in Electrical Systems,* Newnes Power Engineering Series 2002

[38] R. Sadikovic, P. Korba, G. Andersson, *Application of FACTS Devices for Damping of Power System Oscillations,* IEEE Power Tech Conference, St. Petersburg, Russia 2005

[39] V. Ajjarapu, *Bifurcation and Manifold Based Approach for Voltage and Oscillatory Stability Assessment and Control*, Applied Mathematics for Restructured Electric Power Systems: Optimization, Control, and Computational Intelligence, Springer Science+Business Media, Inc. pp. 35-62

[40] T. J. E Miller., *The Theory of Steady State Reactive Power Control in Electric Transmission Systems,* Reactive Power Control in Electric Systems, John Wiley & Sons, Inc., 1982, Chapter-2

[41] R. D Evans, H. N. Muller Jr, J. E. Barkle, R. L., Tremaine, *Power System Stability Basic Elements of Theory and Application,* Electrical Transmission and Distribution

Reference Book (4th Edition), Westinghouse Electric Corporation, 1950 (Indian Edition), Chapter 13, pp. 433-495

[42] C. A. Canizares, S. Hranilovic, *Transcritical and Hopf Bifurcation in AC/DC Systems*, Proceedings of the Bulk Power System Voltage Phenomena III Seminar, NSF/ECC Inc., Davos, Switzerland, August 1994, pp. 105-114.

[43] C. A. Canizares, *Conditions for Saddle-Node Bifurcations in AC/DC Power Systems*, International Journal of Electrical Power & Energy Systems, *Vol. 17, No. 1, 1995, pp. 61-68*

[44] A. Sode-Yome, N. Mithulananthan, *Static Voltage Stability Study Using MATLAB Symbolic and Optimization Toolboxes*, International Conference on Energy for Sustainable Development: Issues and Prospects for Asia, March 1-3, 2006, Phuket, Thailand; available at www.energy-based.nrct.go.th

[45] N. Mithulananthan, A. Sode-yome, N. Acharya., S. Phichaisawat, *Application of FACTS Controllers in Thailand Power Systems*, RTG Budget-Joint Research Project, January 2005, pp. 3 available at www.serd.ait.ac.th

[46] C. A. Canizares, F. L. Alvarado, *Point of Collapse and Continuation Methods for Large AC/DC Systems*, IEEE Transactions on Power Systems, Vol. 8, No. 1, February 1993, pp. 1-8

[47] C. A. Canizares, *Calculating Optimal System Parameters to Maximize the Distance to Saddle-Node Bifurcations*, IEEE Transactions on Circuits and Systems-I: Fundamental Theory and Applications, *Vol. 45, No. 3, March 1998, pp. 225-237*

[48] M A Sc. Thesis of Z. T. Faur , *Effects of FACTS Devices on Static Voltage Collapse Phenomena*, University of Waterloo, 1996, available at www.power.uwaterloo.ca

[49] C. A. Canizares, S. K. M. Kodsi, *Modeling and Simulation of IEEE 14 Bus System with FACTS Controllers*, Technical Report 2003-3, University of Waterloo, Canada, March 2003, available at www.power.uwaterloo.ca

[50] C. A. Canizares, N. Mithulananthan,F. Milano, J. Reeve, *Linear Performance Indices to Predict Oscillatory Stability Problems in Power Systems*, IEEE Transactions on Power Systems, Vol. 19, No. 2, May 2004, pp. 1104-1114

[51] Ph. D Thesis of N. Mithulananthan, *Hopf Bifuraction Control and Indicesfor Power System with Interacting Generator and FACTS Controllers*, University of Waterloo, 2002, available at www.power.uwaterloo.ca

[52] C. L. Wadhwa, *Electrical Power Systems*, New Age International Publishers, 4th Edition 2006

[53] C. A. Canizares, S. Zhang, F. L. Alvarado, *UWPFLOW: Continuation and Direct Methods to Locate Fold Bifurcations in AC/DC/FACTS Power Systems*, available at www.power.uwaterloo.ca

[54] J. Chow, G. Rogers, *Power System Toolbox Version 3.0,* available at
www.eagle.ca/~cherry/pst.htm

[55] Leonard L. Grigsby, *Power System Stability and Control,* CRC Press, Tailor &
Francis Group, 2007

[56] Bangladesh Power Development Board, *Annual Report 2007-2008,* available at
www.bpdb.gov.bd

[57] Ramasamy Natarajan, *Power System Capacitors,* CRC Press, Tailor & Francis Group,
2005

[58] ABB Power Technologies AB, Sweden, *Thyristor Controlled Series Compensation,,*
available at library.abb.com

[59] K. Habur, D. O'Leary, *FACTS for Cost Effective and Reliable Transmission of
Electrical Energy,* was available at:
www.worldbank.org/html/fpd/em/transmission/facts_siemens.pdf during this work.

Series Compensation Examples

Examples of Series Compensated Medium Length Lines

Country	Line	Length [km] (approx.)
USA	Miguel – Imperial Valley 500 kV	135.18
	Imperial Valley – North Gilla 500 kV	128.74
	Hassayampa – North Gilla 500 kV	185.07
	Los Banos – Gates 500 kV	135.18
Finland	Petäjäskoski – Pyhänselkä 400 kV	160.00
	Pirttikoski – Pikkarala 400 kV	150.00

Power System Data

B-1. Data Format for UWPFLOW

Bus Data Format:

T |Ow|Name |kV |Z|PL |QL |MW |Mva|PM |P |QM |Qm |Vpu

T – Type
      "B " PQ load bus
      "BQ" PV generator bus with Q limits

Ow – Owner
Name – Bus Name
kV – Bus kV base
Z – Zone
PL – P load in MW
QL – Q load in MVAR

SHUNT – MW and MVars shunts (+ve for Capacitors)
PM – Max. Generator Active Power in MW
P – Generator Active Power in MW
QM – Max. Generator Reactive Power in MVAR
Qm – Min. Generator Reactive Power in MVAR
Vpu – Desired voltage magnitude in p.u. for PV buses

Line Data Format:

T |Ow|Name_1 |kV1||Name_2 |kV2|||In || R | X | G/2 | B/2 |Mil|

T - Type ("L " for Line)
Ow – Owner
Name_1 – Name of Sending Bus
kV1 – kV Base for Sending Bus
M – Metered Bus for Flow Interchange
Name_2 – Name of Receiving Bus
kV2 – kV Base for Receiving Bus
C – Circuit ID
S – Section Number
In – Rated Amps.
N – Circuit Number
R – p.u. Series Resistance of Line PI Equivalent
X – p.u. Series Reactance of Line PI Equivalent
G/2 – Half of p.u. Shunt Conductance of Line PI Equivalent
B/2 – Half of p.u. Shunt Susceptance of Line PI Equivalent
Mil – Length in Miles

Transformer Data Format:

T |Ow|Name_1 |kV1||Name_2 |kV2|||In || R | X | G/2 | B/2 |Mil|

T - Type ("T " for Transformer)

Ow – Owner
Name_1 – Name of Sending Bus
kV1 – kV Base for Sending Bus
M – Metered Bus for Flow Interchange
Name_2 – Name of Receiving Bus
kV2 – kV Base for Receiving Bus
C – Circuit ID
S – Section Number
Sn – Rated MVA
N – Circuit Number
R – p.u. Series Resistance of Equivalent Circuit
X – p.u. Series Reactance of Equivalent Circuit
G – p.u. Shunt Conductance of Equivalent Circuit
B – p.u. Shunt Susceptance of Equivalent Circuit
Tap1 – kV Tap for Sending Bus
Tap2 – kV Tap for Receiving Bus

TCSC Data Format:

T |Bus1 |kV1 |Bus2 |kV2|Xc |Xl |am|aM|cont ||MVA|al |M1 |

Type – "FC" (F for FACTS, C for TCSC).
Bus1 – Name of Sending Bus, where TCSC is Connected
kV1 – kV Base for Sending Bus
Bus2 – Name of Receiving Bus, where TCSC is Connected
kV2 – kV Base for Receiving Bus
X_c – Per unit TCSC capacitive X w.r.t MVA and kV1 base.
X_l – Per unit TCSC inductive X w.r.t MVA and kV1 base.
am – Minimum firing angle alpha in degrees.
aM – Maximum firing angle alpha in degrees.
cont – TCSC control value: % of X; MW for P; KA for I; degrees for D.
Mode – Control Mode: X for reactance; P for power; I for current; D for angle.
MVA – TCSC rating in MVA. Defaults to MVA system base.
al – Initial value of firing angle in degrees (optional).
M1 – Needed for determining series line reactance for % X Control: $M1 = Xline/Xc$

B-2. Data Format for PST

Bus Data Format:

Col 1 Number
Col 2 Voltage Magnitude (pu)
Col 3 Voltage Angle(degree)
Col 4 Generator Active Power (pu)
Col 5 Generator Reactive Power (pu),
Col 6 Active Load (pu)
Col 7 Reactive Load (pu)
Col 8 Shunt Conductance (pu)
Col 9 Shunt Susceptance (pu)
Col 10 Bus_Type
        - 1, Swing Bus
        - 2, Generator Bus (PV bus)
        - 3, Load Bus (PQ bus)
Col 11 Generator Maximum Reactive Power (pu)
Col 12 Generator Minimum Reactive Power (pu)
Col 13 Rated Voltage (kV)
Col 14 Maximum Voltage (pu)
Col 15 Minimum Voltage (pu)

Line Data Format

Col 1 From Bus
Col 2 To Bus
Col 3 Resistance (pu)
Col 4 Reactance (pu)
Col 5 Line Charging (pu)
Col 6 Tap Ratio
Col 7 Tap phase
Col 8 Tap Max
Col 9 Tap Min
Col 10 Tap Size

Machine Data Format

Col 1 Machine Number,
Col 2 Bus Number,
Col 3 Base MVA,
Col 4 Leakage Reactance x_l(pu),
Col 5 Resistance r_a(pu),
Col 6 d-Axis sychronous reactance x_d(pu),
Col 7 d-Axis transient reactance x'_d(pu),
Col 8 d-Axis subtransient reactance x''_d(pu),
Col 9 d-Axis open-circuit time constant T'_do(sec),
Col 10 d-Axis open-circuit subtransient time constant T''_do(sec),
Col 11 q-Axis sychronous reactance x_q(pu),
Col 12 q-Axis transient reactance x'_q(pu),
Col 13 q-Axis subtransient reactance x''_q(pu),
Col 14 q-Axis open-circuit time constant T'_qo(sec),
Col 15 q-Axis open circuit subtransient time constant T''_qo(sec),
Col 16 Inertia Constant H(sec),
Col 17 Damping Coefficient d_o(pu),
Col 18 Dampling Coefficient d_1(pu),
Col 19 Bus Number
Col 20 Saturation Factor S (1.0)
Col 21 Saturation Factor S (1.2)

IEEE DC-1 Exciter Data Format:

Col 1 Type
Col 2 Machine Number
Col 3 T_R
Col 4 K_A
Col 5 T_A
Col 6 T_B
Col 7 T_C
Col 8 V_{RMAX}
Col 9 V_{RMIN}
Col 10 K_E
Col 11 T_E
Col 12 E_1
Col 13 $S_E(E_1)$
Col 14 E_2
Col 15 $S_E(E_2)$
Col 16 K_F
Col 17 T_F
Cols 18 to 20 are required for Type 3 Exciters and are put "zero" in Type-1 Model

Turbine-Governor Data Format:

Col 1   Turbine Model Number (=1)
Col 2   Machine Number
Col 3   Speed Set Point w_f (pu)
Col 4   Steady State Gain $1/r$ (pu)
Col 5   Maximum Power Order Tmax (pu, On Generator Base)
Col 6   Servo Time Constant T_s (sec)
Col 7   Governor Time Constant T_c (sec)
Col 8   Transient Gain Time Constant T_3 (sec)
Col 9   HP Section Time Constant T_4 (sec)
Col 10   Reheater Time Constant T_5 (sec)

Non-Conforming Load Bus Data Format (for defining TCSC):

Col 1   Bus Number
Col 2   Fraction Const Active Power Load
Col 3   Fraction Const Reactive Power Load
Col 4   Fraction Const Active Current Load
Col 5   Fraction Const Reactive Current Load

TCSC Data Format:

Col 1 TCSC Number
Col 2 From Bus Number
Col 3 To Bus Number
Col 4 Control Gain
Col 5 Control Time Constant
Col 6 Maximum Susceptance B - On System Base
Col7 Minimum Susceptance B - On System Base

B-3. Two Area System Data

1. UWPLOW Format

```
HDG

Two Area Interconnected System

BAS
C
C
C   |Ow|Name    |kV |Z|PL   |QL   |MW |Mva|PM |P     |QM   |Qm   |Vpu
BQ     BUS_01   230                    4000700.01000.-10001.03
BQ     BUS_02   230                     800700.0500.0-500.1.01
BQ     BUS_03   230                     800719.0500.0-500.1.03
BQ     BUS_04   230                     800700.0500.0-500.1.01
B      BUS_05   230
B      BUS_06   230
B      BUS_07   230   967.0100.0    200.0
B      BUS_08   230
B      BUS_09   230  1717.100.0     350.0
B      BUS_10   230
B      BUS_11   230
B      BUS_12   230
B      BUS_13   230    50.
C
C
C
C   |Ow|Name_1 |kV1||Name_2 |kV2|||In || R    | X     | G/2  | B/2 |Mil|
L      BUS_01   230 BUS_05   2301              .0167
L      BUS_02   230 BUS_06   2301              .0167
L      BUS_05   230 BUS_06   2301      .0025 .025          .02187
L      BUS_06   230 BUS_07   2301      .001  .01           .00875
L      BUS_07   230 BUS_08   2301      .011  .11           .09625
L      BUS_07   230 BUS_08   2302      .011  .11           .09625
L      BUS_12   230 BUS_09   2301      .011  .11           .09625
L      BUS_12   230 BUS_09   2302      .011  .11           .09625
L      BUS_09   230 BUS_13   2301            .01
L      BUS_09   230 BUS_10   2301      .001  .01           .00875
L      BUS_10   230 BUS_11   2301      .0025 .025          .02187
L      BUS_04   230 BUS_10   2301            .0167
L      BUS_03   230 BUS_11   2301            .0167
C
C
C      |Bus1    |kV1 |Bus2    |kV2|Xc      |Xl      |am|aM|cont    ||MVA|al  |M1 |
FC     BUS_08   230 BUS_12    230.03300 .003300 144175   70.0  X              3.33
CFC    BUS_08   230 BUS_12    230.06600 .006600 144175   40.0  X              3.33
C
SOL                           50  BUS_01   230     20.2
C
C
ZZ
END
```

76

2. PST Format

```
bus = [...
 1  1.0300   20.2000  7.0000  1.8500      0.00      0.00  0.00  0.00  1  10.0 -10.0  230.0  1.1  0.9;
 2  1.0100   10.5000  7.0000  2.3500      0.00      0.00  0.00  0.00  2   5.0  -5.0  230.0  1.1  0.9;
 3  1.0300   -6.8000  7.1900  1.7600      0.00      0.00  0.00  0.00  2   5.0  -5.0  230.0  1.1  0.9;
 4  1.0100  -17.0000  7.0000  2.0200      0.00      0.00  0.00  0.00  2   5.0  -5.0  230.0  1.1  0.9;
 5  1.0074   20.3799  0.0000  0.0000      0.00      0.00  0.00  0.00  3   0.0   0.0  230.0  1.1  0.8;
 6  0.9804   10.3201  0.0000  0.0000      0.00      0.00  0.00  0.00  3   0.0   0.0  230.0  1.1  0.8;
 7  0.9652    1.9560  0.0000  0.0000      9.67      1.00  0.00  2.00  3   0.0   0.0  230.0  1.1  0.8;
 8  1.0000  -11.7915  0.0000  0.0000      0.00      0.00  0.00  0.00  3   0.0   0.0  230.0  1.1  0.8;
 9  0.9763  -25.2580  0.0000  0.0000  1.015*17.17 1.0150*1.00  0.00  3.50  3  0.0  0.0  230.0  1.1  0.8;
10  0.9862  -16.9988  0.0000  0.0000      0.00      0.00  0.00  0.00  3   0.0   0.0  230.0  1.1  0.8;
11  1.0093   -6.6276  0.0000  0.0000      0.00      0.00  0.00  0.00  3   0.0   0.0  230.0  1.1  0.8;
12  1.0000   -6.6276  0.0000  0.0000      0.00      0.00  0.00  0.00  3   0.0   0.0  230.0  1.1  0.8;
13  0.9763  -25.2580  0.0000  0.0000  1.015*0.5      0.00  0.00  0.00  3   0.0   0.0  230.0  1.1  0.8;
   ];

line = [...
 1     5     0.00     0.0167    0.00      1     0     0     0     0;
 5     6    0.0025     0.025   0.04375    1     0     0     0     0;
 2     6     0.00     0.0167    0.00      1     0     0     0     0;
 6     7    0.001      0.01    0.0175     1     0     0     0     0;
 7     8    0.011      0.11    0.1925     1     0     0     0     0;
 7     8    0.011      0.11    0.1925     1     0     0     0     0;
12     9    0.011      0.11    0.1925     1     0     0     0     0;
12     9    0.011      0.11    0.1925     1     0     0     0     0;
 9    10    0.001      0.01    0.0175     1     0     0     0     0;
 9    13     0.00      0.01     0         1     0     0     0     0;
 4    10     0.00     0.0167    0.00      1     0     0     0     0;
10    11    0.0025     0.025   0.04375    1     0     0     0     0;
 3    11     0.00     0.0167    0.00      1     0     0     0     0;
 8    12     0.00    -0.11*0.4  0.00      1     0     0     0     0;
 8    12     0.00    -0.22*0.4  0.00      1     0     0     0     0;
   ];

mac_con = [ ...
1   1 900 0.200  0.0025  1.8  0.30  0.25 8.00  0.03 1.7  0.55  0.25 0.4  0.05   6.5   2  0  1   0.039  0.267;
2   2 900 0.200  0.0025  1.8  0.30  0.25 8.00  0.03 1.7  0.55  0.25 0.4  0.05   6.5   2  0  2   0.039  0.267;
3   3 900 0.200  0.0025  1.8  0.30  0.25 8.00  0.03 1.7  0.55  0.25 0.4  0.05  6.175  2  0  3   0.039  0.267;
4   4 900 0.200  0.0025  1.8  0.30  0.25 8.00  0.03 1.7  0.55  0.25 0.4  0.05  6.175  2  0  4   0.039  0.267;
   ];

exc_con = [...
1 1 0.01 46.0   0.06  0     0   1.0   -0.9   0.0  0.46   3.1   0.33  2.3  0.1   0.07   1.0    0    0   0;
1 2 0.01 46.0   0.06  0     0   1.0   -0.9   0.0  0.46   3.1   0.33  2.3  0.1   0.07   1.0    0    0   0;
1 3 0.01 46.0   0.06  0     0   1.0   -0.9   0.0  0.46   3.1   0.33  2.3  0.1   0.07   1.0    0    0   0;
1 4 0.01 46.0   0.06  0     0   1.0   -0.9   0.0  0.46   3.1   0.33  2.3  0.1   0.07   1.0    0    0   0
];

tg_con = [...
1  1  1  25.0  1.0  0.1  0.5 0.0 1.25 5.0;
1  2  1  25.0  1.0  0.1  0.5 0.0 1.25 5.0;
1  3  1  25.0  1.0  0.1  0.5 0.0 1.25 5.0;
1  4  1  25.0  1.0  0.1  0.5 0.0 1.25 5.0;
];

load_con = [...
 8 0  0   0  0;
12 0  0   0  0;
];

tcsc_con = [
    1 8 12 1.0 0.05 0 -3;
        ];
```

```
%TCSC Damping Control Function
tcsc_dc=[];
tcsc_dc{1,1}=30.*wo_stsp(10).*(ldlg_stsp(1,0.6460,0.0905).^2); %control state-space object
tcsc_dc{1,2}=1; %tcsc number
tcsc_dc{1,3}=8; %bus number
tcsc_dc{1,4}=0; %control max output limit
tcsc_dc{1,5}=-3; %control min output limit
tcsc_dc{1,6}=3; %number of control states


sw_con = [...
0     0    0    0    0    0         0.01; %sets intitial time step
0.3   9    13   0    0    0         0.005; %thee phase fault
0.35  0    0    0    0    0     0.005556; %clear fault at bus 3
0.40  0    0    0    0    0     0.005556; %clear remote end
0.50  0    0    0    0    0        0.005; % increase time step
1.0   0    0    0    0    0    -    0.01;. % increase time step
20.0  0    0    0.   0    0           0;
]; % end simulation


%Monitors All Line Currents
lmon_con = [1:length(line(:,1))]';
```

B-4. East-West Interconnected System Data

1. UWPFLOW Format

```
HDG

East-West Interconnected System

BAS
C
C
BQ    BUS_01    230                                    500.0-500..87
B     BUS_02    230
B     BUS_03    230
B     BUS_04    230
B     BUS_05    132  24.00 9.60        10
B     BUS_06    132  37.0014.80         5
B     BUS_07    132
B     BUS_08    230
B     BUS_09    230
B     BUS_10    132  20.00 8.00
B     BUS_11    132  30.0012.00        10
B     BUS_12    132  20.00 8.00       7.5
B     BUS_13    132  10.00
B     BUS_14    132  20.00 8.00       2.5
B     BUS_15    132  20.00 8.00       2.5
B     BUS_16    132  20.00 8.00
B     BUS_17    132  10.00 4.00
B     BUS_18    132  10.00 4.00       7.5
B     BUS_19    132   5.00 2.00
B     BUS_20    132   5.00 2.00
B     BUS_21    132  10.00 4.00
B     BUS_22    132  20.00 8.00
B     BUS_23    132  25.0010.00
B     BUS_24    132  26.0010.40       7.5
B     BUS_25    132  38.0015.20       7.5
B     BUS_26    132  10.00 4.00
B     BUS_27    132  10.00 4.00        15
B     BUS_28    132  10.00 4.00
B     BUS_29    132  15.00 6.00        35
B     BUS_30    132  35.0014.00
B     BUS_31    132  10.00 4.00        10
B.    BUS_32    132  10.00 4.00
B     BUS_33    230
B     BUS_34    230
B     BUS_35    132  10.00 4.00
B     BUS_36    230
B     BUS_37    230
B     BUS_38     33
BQ    BUS_39     11                          10.00 7.50 -7.5.950
BQ    BUS_40     11                          125.0127.0-127..870
BQ    BUS_41     11                          120.0122.0-122..950
BQ    BUS_42     11                          23.00 20.0 -20..870
BQ    BUS_43     11                          105.0107.0-107..850
BQ    BUS_44     11                          15.0013.00-13.0.850
C
B     BUS_45    230
B     BUS_46    230
C
L     BUS_01    230 BUS_02  2301              .001
L     BUS_01    230 BUS_03  2301              .001
L     BUS_02    230 BUS_45  2301  910 .0267 .1371      .1324
L     BUS_03    230 BUS_46  2301 1820 .0110 .0770      .1477
L     BUS_31    132 BUS_05  1321       .0174 .066      .0078
L     BUS_31    132 BUS_17  1321       .0093 .0352     .0042
L     BUS_17    132 BUS_26  1321       .0232 .088      .0104
L     BUS_07    132 BUS_26  1321       .00462.0135     .00155
L     BUS_26    132 BUS_32  1321       .0197 .0748     .00884
```

```
L     BUS_31  132 BUS_07  1321      .0385 .1125        .0127
L     BUS_04  230 BUS_33  2301      .0044 .03025       .0581
L     BUS_06  132 BUS_25  1321      .0261 .099         .0117
L     BUS_05  132 BUS_06  1321      .0377 .1430        .0169
L     BUS_31  132 BUS_23  1321      .0261 .099         .011
L     BUS_05  132 BUS_23  1321      .0308 .09          .0102
L     BUS_23  132 BUS_24  1321      .0275 .104         .0122
L     BUS_07  132 BUS_32  1321      .0232 .088         .01044
L     BUS_33  230 BUS_08  2301      .0032 .022         .0422
L     BUS_06  132 BUS_32  1321      .0383 .1452        .0172
L     BUS_34  230 BUS_08  2301      .00544.0374        .0717
L     BUS_06  132 BUS_16  1321      .0291 .1104        .0131
L     BUS_16  132 BUS_27  1321      .0304 .11528       .0136
L     BUS_34  230 BUS_09  2301      .008  .0577        .08
L     BUS_27  132 BUS_35  1321      .0222 .0839        .00985
L     BUS_27  132 BUS_28  1321      .0222 .0839        .00985
L     BUS_35  132 BUS_29  1321      .033  .264         .0116
L     BUS_27  132 BUS_29  1321      .02378.0902        .0106
L     BUS_29  132 BUS_30  1321      .01212.0459        .0054
L     BUS_31  132 BUS_10  1321      .0058 .022         .0026
L     BUS_04  230 BUS_36  2301      .0008 .0055        .0105
L     BUS_10  132 BUS_14  1321      .01305.0495        .0058
L     BUS_14  132 BUS_18  1321      .02517.09548       .0113
L     BUS_18  132 BUS_20  1321      .0261 .099         .0117
L     BUS_20  132 BUS_11  1321      .02767.1049        .0124
L     BUS_36  230 BUS_37  2301      .013  .09          .1
L     BUS_10  132 BUS_15  1321      .0805 .2353        .0253
L     BUS_15  132 BUS_22  1321      .0495 .1449        .0165
L     BUS_22  132 BUS_12  1321      .0433 .1267        .0145
L     BUS_11  132 BUS_19  1321      .0251 .09526       .0112
L     BUS_19  132 BUS_21  1321      .0246 .072         .0083
L     BUS_21  132 BUS_12  1321      .0385 .1125        .013
L     BUS_31  132 BUS_13  1321            .0303
C
T     BUS_04  230 BUS_31  1321            .01
T     BUS_33  230 BUS_07  1321            .01
T     BUS_08  230 BUS_32  1321            .01
T     BUS_34  230 BUS_06  1321            .01
T     BUS_36  230 BUS_10  1321            .01
T     BUS_37  230 BUS_11  1321            .01
T     BUS_09  230 BUS_35  1321            .01
T     BUS_06  132 BUS_38  331             .01
T     BUS_38   33 BUS_39  111             .01
T     BUS_07  132 BUS_40  111             .01
T     BUS_09  230 BUS_41  111             .01
T     BUS_10  132 BUS_42  111             .01
T     BUS_11  132 BUS_43  111             .01
T     BUS_12  132 BUS_44  111             .01

FC    BUS_45  230 BUS_04  230.04113  .004113 144180  70.0  X         3.33
FC    BUS_46  230 BUS_08  230.02310  .002310 144180  70.0  X         3.33
C
SOL                       50  BUS_01   230    0.
C
C
ZZ
END
```

2. PST Format

```
bus=[...
 1  0.87   00.0   0.0   0.0       0.0              0.0    0.0     0.0  1   5.0   -5.0   230   1.01  0.50; %System
 2  0.86  -10.0   0.0   0.0      0.00           0.0000   0.0     0.0  3   0.0    0.0   230   1.01  0.50; %Ghorashal
 3  0.86  -10.0   0.0   0.0      0.00           0.0000   0.0     0.0  3   0.0    0.0   230   1.01  0.50; %Ashuganj
 4  0.86  -10.0   0.0   0.0  2.0134*0.00 0.400*2.0134*0.00  0.0  0.0  3   0.0    0.0   230   1.01  0.50; %Ishurdi
 5  0.86  -10.0   0.0   0.0  2.0134*0.24 0.400*2.0134*0.24  0.0  0.1  3   0.0    0.0   132   1.01  0.50; %Natore
 6  0.86  -10.0   0.0   0.0  2.0134*0.37 0.400*2.0134*0.37  0.0  0.05 3   0.00   0.00  132   1.01  0.50; %Bogra
 7  0.86  -10.0   0.0   0.0      0.00           0.00     0.0     0.0  3   0.0    0.00  132   1.01  0.50; %Baghabari
 8  0.86  -10.0   0.0   0.0  2.0134*0.00 0.400*2.0134*0.00  0.0  0.0  3   0.0    0.0   230   1.01  0.50; %Sirajganj
 9  0.86  -10.0   0.0   0.0  2.0134*0.00 0.400*2.0134*0.00  0.0  0.0  3   0.00   0.00  230   1.01  0.50; %Barapukuria
10  0.86  -10.0   0.0   0.0  2.0134*0.20 0.400*2.0134*0.20  0.0  0.0  3   0.0.   0.00  132   1.01  0.50; %Bheramara
11  0.86  -10.0   0.0   0.0  2.0134*0.30 0.400*2.0134*0.30  0.0  0.1  3   0.00   0.00  132   1.01  0.50; %Khulna
12  0.86  -10.0   0.0   0.0  2.0134*0.20 0.400*2.0134*0.20  0.0  0.075 3  0.00   0.00  132   1.01  0.50; %Barisal
13  0.86  -10.0   0.0   0.0      0.10           0.00     0.0     0.0  3   0.0    0.0   132   1.01  0.50; %Remote-Bus for Fa
ult
14  0.86  -10.0   0.0   0.0  2.0134*0.20 0.400*2.0134*0.20  0.0  0.025 3  0.0    0.00  132   1.01  0.50; %Bottail
15  0.86  -10.0   0.0   0.0  2.0134*0.20 0.400*2.0134*0.20  0.0  0.025 3  0.00   0.00  132   1.01  0.50; %Faridpur
16  0.86  -10.0   0.0   0.0  2.0134*0.20 0.400*2.0134*0.20  0.0  0.0  3   0.00   0.00  132   1.01  0.50; %Palashbari
17  0.86  -10.0   0.0   0.0  2.0134*0.10 0.400*2.0134*0.10  0.0  0.0  3   0.00   0.00  132   1.01  0.50; %Pabna
18  0.86  -10.0   0.0   0.0  2.0134*0.10 0.400*2.0134*0.10  0.0  0.075 3  0.00   0.00  132   1.01  0.50; %Jhenida
19  0.86  -10.0   0.0   0.0  2.0134*0.05 0.400*2.0134*0.05  0.0  0.0  3   0.00   0.00  132   1.01  0.50; %Bagherhat
20  0.86  -10.0   0.0   0.0  2.0134*0.05 0.400*2.0134*0.05  0.0  0.0  3   0.00   0.00  132   1.01  0.50; %Jessore
21  0.86  -10.0   0.0   0.0  2.0134*0.10 0.400*2.0134*0.10  0.0  0.0  3   0.00   0.00  132   1.01  0.50; %Bhandaria
22  0.86  -10.0   0.0   0.0  2.0134*0.20 0.400*2.0134*0.20  0.0. 0.0  3   0.00   0.00  132   1.01  0.50; %Madaripur
23  0.86  -10.0   0.0   0.0  2.0134*0.25 0.400*2.0134*0.25  0.0  0.2  3   0.00   0.00  132   1.01  0.50; %Rajshahi
24  0.86  -10.0   0.0   0.0  2.0134*0.26 0.400*2.0134*0.26  0.0  0.075 3  0.00   0.00  132   1.01  0.50; %Chapainawabganj
25  0.86  -10.0   0.0   0.0  2.0134*0.38 0.400*2.0134*0.38  0.0  0.075 3  0.00   0.00  132   1.01  0.50; %Noagaon
26  0.86  -10.0   0.0.  0.0  2.0134*0.10 0.400*2.0134*0.10  0.0  0.0  3   0.00   0.00  132   1.01  0.50; %Shahjadpur
27  0.86  -10.0   0.0   0.0  2.0134*0.10 0.400*2.0134*0.10  0.0  0.15 3   0.00   0.00  132   1.01  0.50; %Rangpur
28  0.86  -10.0   0.0   0.0  2.0134*0.10 0.400*2.0134*0.10  0.0  0.0  3   0.00   0.00  132   1.01  0.50; %Lalmanirhat
29  0.86  -10.0   0.0   0.0  2.0134*0.15 0.400*2.0134*0.15  0.0  0.35 3   0.00   0.00  132   1.01  0.50; %Saidpur
30  0.86  -10.0   0.0   0.0  2.0134*0.35 0.400*2.0134*0.35  0.0  0.0  3   0.00   0.00  132   1.01  0.50; %Purbasadipur
31  0.86  -10.0   0.0   0.0  2.0134*0.10 0.400*2.0134*0.10  0.0  0.1  3   0.0    0.0   132   1.01  0.50; %Ishurdi
32  0.86  -10.0   0.0   0.0  2.0134*0.10 0.400*2.0134*0.10  0.0  0.0  3   0.0    0.0   132   1.01  0.50; %Sirajganj
33  0.86  -10.0   0.0   0.0  2.0134*0.00 0.400*2.0134*0.00  0.0  0.0  3   0.0    0.0   230   1.01  0.50; %Baghabari
34  0.86  -10.0   0.0   0.0  2.0134*0.00 0.400*2.0134*0.00  0.0  0.0  3   0.0    0.0   230   1.01  0.50; %Bogra
35  0.86  -10.0   0.0   0.0  2.0134*0.10 0.400*2.0134*0.10  0.0  0.0  3   0.00   0.00  132   1.01  0.50; %Barapukuria
36  0.86  -10.0   0.0   0.0  2.0134*0.00 0.400*2.0134*0.00  0.0  0.0  3   0.0    0.0   230   1.01  0.50; %Bheramara
37  0.86  -10.0   0.0   0.0  2.0134*0.00 0.400*2.0134*0.00  0.0  0.0  3   0.0    0.0   230   1.01  0.50; %Khulna
38  0.86  -10.0   0.0   0.0  2.0134*0.00 0.400*2.0134*0.00  0.0  0.0  3   0.0    0.0    33   1.01  0.50; %Bogra

39  0.95  -10.0   0.1   0.0  2.0134*0.00 0.400*2.0134*0.00  0.0  0.0  2   0.075 -0.075   11   1.01  0.50; %G-Bogra
40  0.870 -10.0   1.25  0.0      0.00           0.00     0.0     0.0  2   1.27  -1.27    11   1.01  0.50; %G-Baghabari
41  0.950 -10.0   1.20  0.0  2.0134*0.00 0.400*2.0134*0.00  0.0  0.0  2   1.22  -1.22    11   1.01  0.50; %G-Barapukuria
42  0.870 -10.0   0.23  0.0  2.0134*0.00 0.400*2.0134*0.00  0.0  0.0  2   0.2   -0.2     11   1.01  0.50; %G-Bheramara
43  0.850 -10.0   1.05  0.0  2.0134*0.00 0.400*2.0134*0.00  0.0  0.0  2   1.07  -1.07    11   1.01  0.50; %G-Khulna
44  0.850 -10.0   0.15  0.0  2.0134*0.00 0.400*2.0134*0.00  0.0  0.0  2   0.13  -0.13    11   1.01  0.50; %G-Barisal

45  0.86   0.0    0.0   0.0      0.00           0.00     0.0     0.0  3   0.0    0.0    230   1.01  0.50; %TCSC Bus
46  0.86   0.0    0.0   0.0      0.00           0.00     0.0     0.0  3   0.0    0.0    230   1.01  0.50; %TCSC Bus
   ];

line=[...
        1    2        0.000       0.001       0.00    1.0     0.0     0.0    0.0     0.0;
        1    3        0.00        0.001       0.00    1.0     0.0     0.0    0.0     0.0;
        2   45        0.0267      0.1371      0.2647  1.0     0.0     0.0    0.0     0.0;
       45    4        0.0   -0.7*0.1371      0.0     1.0     0.0     0.0    0.0     0.0;
        3   46        0.0110      0.0770      0.2954  1.0     0.0     0.0    0.0     0.0;
       46    8        0.0   -0.7*0.0770      0.0     1.0     0.0     0.0    0.0     0.0;
       31    5        0.0174      0.066      2*0.0078 1.0     0.0     0.0    0.0     0.0;
       31   17        0.0093      0.0352     2*0.0042 1.0     0.0     0.0    0.0     0.0;
       17   26        0.0232      0.088      2*0.0104 1.0     0.0     0.0    0.0     0.0;
        7   26        0.00462     0.0135     2*0.00155 1.0    0.0     0.0    0.0     0.0;
       26   32        0.0197      0.0748     2*0.00684 1.0    0.0     0.0    0.0     0.0;
        4   33        0.0044      0.03025     0.1161  1.0     0.0     0.0    0.0     0.0;
       31    7        0.0385      0.1125     2*0.0127 1.0     0.0     0.0    0.0     0.0;
        6   25        0.0261      0.099      2*0.0117 1.0     0.0     0.0    0.0     0.0;
        5    6        0.0377      0.1430     2*0.0169 1.0     0.0     0.0    0.0     0.0;
       31   23        0.0261      0.099      2*0.0115 1.0     0.0     0.0    0.0     0.0;
        5   23        0.0308      0.09       2*0.0102 1.0     0.0     0.0    0.0     0.0;
       23   24        0.0275      0.104      2*0.0122 1.0     0.0     0.0    0.0     0.0;
       33    8        0.00320     0.022       0.0844  1.0     0.0     0.0    0.0     0.0;
        7   32        0.0232      0.088      2*0.01044 1.0    0.0     0.0    0.0     0.0;
       34    8        0.00544     0.03740     0.1435  1.0     0.0     0.0    0.0     0.0;
        6   32        0.0383      0.1452     2*0.0172 1.0     0.0     0.0    0.0     0.0;
        6   16        0.0291      0.1104     2*0.0131 1.0     0.0     0.0    0.0     0.0;
       16   27        0.0304      0.11528    2*0.0136 1.0     0.0     0.0    0.0     0.0;
       34    9        0.008       0.05775     0.20    1.0     0.0     0.0    0.0     0.0;
       27   35        0.0222      0.0839     2*0.00985 1.0    0.0     0.0    0.0     0.0;
       27   28        0.0222      0.0839     2*0.00985 1.0    0.0     0.0    0.0     0.0;
       35   29        0.033       0.264      2*0.0116 1.0     0.0     0.0    0.0     0.0;
       27   29        0.02378     0.0902     2*0.0106 1.0     0.0     0.0    0.0     0.0;
       29   30        0.01212     0.0459     2*0.0054 1.0     0.0     0.0    0.0     0.0;
```

81

```
   4   36      0.0008       0.0055      0.021   1.0    0.0    0.0    0.0    0.0;
  31   10      0.0058       0.022     2*0.0026  1.0    0.0    0.0    0.0    0.0;
  10   14      0.01305      0.0495    2*0.0058  1.0    0.0    0.0    0.0    0.0;
  14   18      0.02517      0.09548   2*0.0113  1.0    0.0    0.0    0.0    0.0;
  18   20      0.0261       0.099     2*0.0117  1.0    0.0    0.0    0.0    0.0;
  20   11      0.02767      0.1049    2*0.0124  1.0    0.0    0.0    0.0    0.0;
  36   37      0.013        0.09        0.340   1.0    0.0    0.0    0.0    0.0;
  10   15      0.0805       0.2353    2*0.0253  1.0    0.0    0.0    0.0    0.0;
  15   22      0.0495       0.1449    2*0.0165  1.0    0.0    0.0    0.0    0.0;
  22   12      0.0433       0.1267    2*0.0145  1.0    0.0    0.0    0.0    0.0;
  11   19      0.0251       0.09526   2*0.0112  1.0    0.0    0.0    0.0    0.0;
  19   21      0.0246       0.072     2*0.0083  1.0    0.0    0.0    0.0    0.0;
  21   12      0.0385       0.1125     2*0.013  1.0    0.0    0.0    0.0    0.0;

  31   13      0.00         0.0303      0.00    1.0    0.0    0.0    0.0    0.0;

   4   31      0.00         0.01        0.00    1.0    0.0    0.0    0.0    0.0;
  33    7      0.00         0.01        0.00    1.0    0.0    0.0    0.0    0.0;
   8   32      0.00         0.01        0.00    1.0    0.0    0.0    0.0    0.0;
  34    6      0.00         0.01        0.00    1.0    0.0    0.0    0.0    0.0;
  36   10      0.00         0.01        0.00    1.0    0.0    0.0    0.0    0.0;
  37   11      0.00         0.01        0.00    1.0    0.0    0.0    0.0    0.0;
   9   35      0.00         0.01        0.00    1.0    0.0    0.0    0.0    0.0;
  38   39      0.00         0.01        0.00    1.0    0.0    0.0    0.0    0.0;

   6   38      0.00         0.01        0.00    1.0    0.0    0.0    0.0    0.0;
   7   40      0.00         0.01        0.00    1.0    0.0    0.0    0.0    0.0;
   9   41      0.00         0.01        0.00    1.0    0.0    0.0    0.0    0.0;
  10   42      0.00         0.01        0.00    1.0    0.0    0.0    0.0    0.0;
  11   43      0.00         0.01        0.00    1.0    0.0    0.0    0.0    0.0;
  12   44      0.00         0.01        0.00    1.0    0.0    0.0    0.0    0.0;

];


mac_con = [ ...
1   1  768   0.240  0.0012  2.100  0.400   0.250 4.50  0.034 2.050  1.200  0.250   1.50    0.15   2.40  2.0   0    1;
2  39   25   0.134  0.0014  1.250  0.232   0.120 4.75  0.0590 1.220  0.715  0.120  1.500   0.210  5.020 2.0   0   39;
3  40  192   0.102  0.0026  1.651  0.232   0.171 5.90  0.033 1.59   0.380  0.171  0.535   0.078  3.30  2.0   0   40;
4  41  192   0.102  0.0026  1.651  0.232   0.171 5.90  0.033 1.59   0.380  0.171  0.535   0.078  3.30  2.0   0   41;
5  42   35   0.134  0.0014  1.250  0.232   0.120 4.75  0.0590 1.220  0.715  0.120  1.500   0.210  5.020 2.0   0   42;
6  43  160   0.110  0.0031  1.700  0.245   0.185 5.90  0.033 1.64   0.380  0.185  0.540   0.076  3.96  2.0   0   43;
7  44   25   0.134  0.0014  1.250  0.232   0.120 4.75  0.0590 1.220  0.715  0.120  1.500   0.210  5.020 2.0   0   44;
   ];


exc_con=[...
1   1 0.01 46.0   0.06  0    0   1.0   -0.9 0.0  0.4   4.5   0.267  3.4  0.07   0.02  1.0    0    0   0;
1   2 0.01 46.0   0.06  0    0   1.0   -0.9 0.0  0.4   4.5   0.267  3.4  0.07   0.02  1.0    0    0   0;
1   3 0.01 46.0   0.06  0    0   1.0   -0.9 0.0  0.4   4.5   0.267  3.4  0.07   0.02  1.0    0    0   0;
1   4 0.01 46.0   0.06  0    0   1.0   -0.9 0.0  0.4   4.5   0.267  3.4  0.07   0.02  1.0    0    0   0;
1   5 0.01 46.0   0.06  0    0   1.0   -0.9 0.0  0.4   4.5   0.267  3.4  0.07   0.02  1.0    0    0   0;
1   6 0.01 46.0   0.06  0    0   1.0   -0.9 0.0  0.4   4.5   0.267  3.4  0.07   0.02  1.0    0    0   0;
1   7 0.01 46.0   0.06  0    0   1.0   -0.9 0.0  0.4   4.5   0.267  3.4  0.07   0.02  1.0    0    0   0;
];


tg_con = [...
1  1  1  25.0  1.0  0.1  0.5 0.0 1.25 5.0;
1  2  1  25.0  1.0  0.1  0.5 0.0 1.25 5.0;
1  3  1  25.0  1.0  0.1  0.5 0.0 1.25 5.0;
1  4  1  25.0  1.0  0.1  0.5 0.0 1.25 5.0;
1  5  1  25.0  1.0  0.1  0.5 0.0 1.25 5.0;
1  6  1  25.0  1.0  0.1  0.5 0.0 1.25 5.0;
1  7  1  25.0  1.0  0.1  0.5 0.0 1.25 5.0;
];


tcsc_con = [...
        1 45   4 1.0 .05 0 -1.3;
        2 46   8 1.0 .05 0 -1.3;
          ];


load_con = [...
        4 0 0 0 0; % for TCSC
       45 0 0 0 0; % for TCSC
       46 0 0 0 0; % for TCSC
        8 0 0 0 0; % for TCSC
   ];
```

```
tcsc_dc=[];
%tcsc_dc{1,1}=20.*wo_stsp(2).*(1dlg_stsp(1,0.4216,0.1468)).^1; %for Scenario-1
tcsc_dc{1,1}=70.*wo_stsp(10).*(1dlg_stsp(1,0.4227,0.1449)).^1; %for Scenario-2 (TCSC-1)
tcsc_dc{1,2}=1;%tcsc number
tcsc_dc{1,3}=45;%bus number
tcsc_dc{1,4}=0;% control max output limit
tcsc_dc{1,5}=-1.3;% control min output limit
tcsc_dc{1,6}=2;% number of control states


tcsc_dc{2,1}=70.*wo_stsp(10).*(1dlg_stsp(1,0.4227,0.1449)).^1; %for Scenario-2 (TCSC-2)
tcsc_dc{2,2}=2;%tcsc number
tcsc_dc{2,3}=46;%bus number
tcsc_dc{2,4}=0;% control max output limit
tcsc_dc{2,5}=-1.3;% control min output limit
tcsc_dc{2,6}=2;% number of control states



sw_con = [...
0     0    0    0    0    0    0.01;   %sets intitial time step
0.3   31   13   0    0    0    0.005;  %thee phase fault
0.35  0    0    0    0    0    0.005;  %clear fault at bus 3
0.4   0    0    0    0    0    0.01;   %clear remote end
0.50  0    0    0    0    0    0.01;   % increase time step
1.0   0    0    0    0    0    0.01;   % increase time step
10    0    0    0    0    0    0;
]; % end simulation

% Monitor all line flows
lmon_con = [1:length(line(:,1))]';
```